

Award Number 08HQGR0035

Testing And Analysis Of Deep Sediments In Charleston SC

NEHRP Final Report

Richard P. Ray

Department of Civil and Environmental Engineering

University of South Carolina

300 Main St

Columbia, South Carolina 29208

803-777-7086 office; 803-777-3614 department; 803-777-0670 fax

ray@cec.sc.edu

Start: September 1, 2008

End: May 31, 2010

Research supported by the U.S. Geological Survey (USGS), Department of the Interior, under USGS award number 08HQGR0035. The views and conclusions contained in this document are those of the authors and should not be interpreted as necessarily representing the official policies, either expressed or implied, of the U.S. Government.

ABSTRACT

In this project we designed and built a resonant column/torsional simple shear (RC-TOSS) device. It is capable of simulating isotropic confining conditions to about 500 m depth. Maximum design pressure is 5500 kPa, however in the completed system has only been verified to 2800 kPa. Fabrication and equipment delivery delays did not permit high confining stress tests to be performed, however, testing is anticipated to be completed by December 2010. The device will test hollow cylinder specimens 2 cm inside, 3cm outside radius by 14 cm long.

In order to verify other components of the system, a series of 10 low-confining stress tests (100-300 kPa) on Cooper Marl was performed and is reported here. The tests revealed a unique behavior of Cooper Marl where modulus reduction due to shear strain occurs at 3-5 times lower strain levels than those reported for non-plastic silt or fine sand. The data were consistent throughout the tests. A Ramberg-Osgood curve was fit to the plots of G/G_{max} vs. γ/γ_{ref} . In this case, the definition of reference strain, γ_{ref} used by Darendeli and others was not accurate. We went back to the original definition of γ_{ref} and were successful in defining a suitable empirical curve.

One dimension response analysis by method of characteristics was used to study the impact of the shifted modulus reduction curves on surface response. As expected, the reduced stiffness at high strains generated lower accelerations but higher displacements than analyses using reduction curves for fine sand and non-plastic silt.

The report includes detailed test data, a thorough discussion on the development of method of characteristics and its implementation. Analysis of stress states in hollow cylinder specimens were also performed and are discussed as well. The newly generated data will increase the accuracy and reliability of models to predict ground motion in the Charleston SC area

Chapter 1. Introduction, Objectives, and Format

Introduction

Modeling the response of sediments under high-amplitude earthquake loading has been an evolving issue since 1960. Factors influencing behavior have been enumerated by several authors in state-of-the-art papers (Richart 1975, Drnevich et al, 1978; Finn, 2000, Boore, 2004). This study addresses problems particular to deep, (relatively) soft sediments such as those found in the Central and Southeastern U.S. These sites differ from many sites in the Western U.S. due to the fact that the sediment or soil profile is very deep everywhere and there are no rock outcrops. Given the rarity of strong events, scientists and engineers have little data for comparison to predictive models. Performing laboratory studies of the behavior of these soils can be difficult as well. Studies that measured behavior under laboratory conditions have been few (Laird and Stokoe 1993) and confining stresses have typically been less than 500 kPa. Resonant column testing has been shown to be a consistent and reliable method for determining dynamic soil properties. This report will address the use of a high confining pressure resonant column/torsional simple shear device.

Objectives

Primary objectives of this study were

1. Review pertinent literature on dynamic properties of deep soil deposits
2. Design and construct a device to test soil under high confining stresses and dynamic loads
3. Analyze the behavior of test specimens to extend their applicability to other conditions
4. Determine the impact of differences found in soil behavior on the overall response of deep deposits to earthquake strong motion.

These objectives were met by the study. However, in doing so, they raised more questions and possible avenues for further study as well.

Report Format

The first part of this report reviews pertinent literature on the dynamic response of deep sediments as well as influences of confining stress and other influences found in deep sediments. The primary focus is on engineering behavior and strong motion, however, other nuances which may influence behavior, but have not been explicitly addressed are also discussed.

The second chapter is a brief review and discussion of dynamic laboratory testing via resonant column and torsional simple shear. Several developments over the past decade are summarized and critiqued...

The third chapter is a presentation of the laboratory testing program and a discussion on the design of the device. Analysis of stress-strain state in the specimen during testing is also presented. Chapter four discusses the construction of the testing device.

Results from the testing are presented in Chapter 5 and those results are applied to a 1-dimensional response analysis in Chapter 6. The primary purpose is to study the effects of properties measured in Chapter 5 as they may deviate from previous assumptions and studies.

Chapter 7 discusses a 3-D finite element analysis that was undertaken to better evaluate the impact of imperfections and irregularities in a test specimen.

Chapter 8 lists conclusions and suggestions for further study.

Appendices contain detailed but important specific information concerning the design and construction of the testing equipment, detailed laboratory results, and some detail on the response analysis.

Chapter 2. Literature Review

Deep Sediments in the U.S.

The influence of soil behavior on strong-motion response of structures and natural land features has been documented as long as building damage and shaking intensity. However due to the hidden nature of soil deposits and difficulty of subsurface exploration, a rational framework for soil response and earthquake shaking only evolved from perhaps 1950 onward. Given the fact that most active earthquake zones studied by geologists and engineers generally possessed shallow deposits (<30 m) of soil, much of the analyses and observations were based on assumptions of rock outcrop (no soil at all) or a linear elastic layer with somewhat less stiffness than the parent rock. The assumptions were as much analytical and computational expedients as they were representations of actual conditions.

With the increasing capability of computing equipment and the development of numerical codes, there came a number of modeling approaches. Some of them, with their authors are listed in table 1 (Stewart et al, 2006). The table is limited to 1-D response models. It lists the program name, where the soil models can be found in the literature, where the program can be downloaded and whether the program can perform total stress analysis (TSA) or effective stress analysis (ESA). Effective stress analyses are useful in liquefaction studies as well as other earthwork stability analyses. Most strong-motion response models require shear modulus at low strain (G_{\max} or G_0 in the literature) and a curve to describe modulus reduction (G/G_{\max}) with increasing strain. An additional part of the model is to have a corresponding curve of damping ratio (D) increase with increasing strain as well. Two sets of curves, taken from well-known references are shown in figure 1. The x-axis is typically shear strain (or dimensionless shear strain) on a logarithmic scale. The values of G/G_{\max} and D are on separate, arithmetic scales. Values for shear modulus, and its reduction with strain, may represent secant modulus or tangent modulus, depending on the type of analysis at hand. An equivalent linear analysis usually supposes a secant modulus that remains constant throughout the earthquake while a time-stepping nonlinear analysis requires a tangent modulus that will change with each new time step throughout the duration of the event. The differences between such curves are shown graphically in Appendix D where a specific empirical numerical stress-strain model is discussed.

Table 1. Computer codes for 1D nonlinear ground response analysis (Stewart et al, 2008)

Program	Nonlinear Model	Reference for computer code	TSA/ESA
DEEPSOIL	Hashash and Park (2001, 2002)	Hashash and Park (2001, 2002); www.uiuc.edu/~deepsoil	TSA (ESA option available in Fall 2007)
DESRA-2	Konder and Zelasko (1963); Masing (1926)	Lee and Finn (1978)	TSA or ESA
DESRAMOD	same as DESRA-2; with pore-water pressure generation model by Dobry <i>et al.</i> (1985)	Vucetic and Dobry (1986)	TSA or ESA
DESRAMUSC	Same as DESRA-2 + Qiu (1997)	Qiu (1997)	TSA or ESA
D-MOD_2	Matasovic and Vucetic (1993, 1995)	Matasovic (2006)	TSA or ESA
MARDESRA	Martin (1975)	Mok (pers. comm., 1990)	TSA or ESA
OpenSees	Ragheb (1994); Parra (1996); Yang (2000)	McKenna and Fenves (2001); opensees.berkeley.edu	TSA or ESA
SUMDES	Wang (1990)	Li <i>et al.</i> (1992)	TSA or ESA
TESS	Pyke (1979)	Pyke (2000)	TSA or ESA

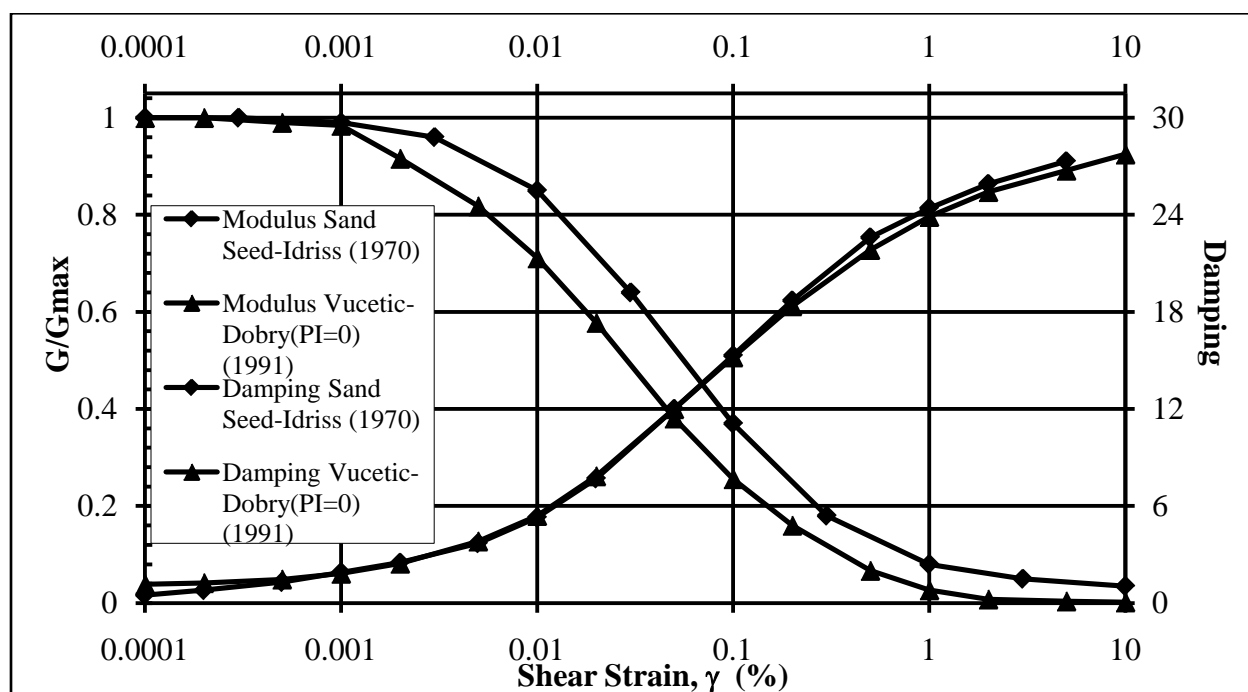


Figure 1. Modulus reduction and damping increase due to increase in shear strain.

The numerical models shown in table 1 represent what is perhaps between state of the practice and state of the art. Certainly SHAKE would be state of the practice since it is the de facto site response program used by consultants. The programs in table 1 have been applied successfully to soft, deep sediments in the Mississippi Embayment as well as around Charleston SC. Recent large construction projects around Charleston SC have led to a quantum increase in field and laboratory dynamic property data. Efforts to integrate this information (Hayati and Andrus, 2007, Chapman et al, 2006; 2003; Martin and Clough, 1990) have fostered a much better understanding of the influence of deep deposits on surface response. However, these efforts suffer from a persistent lack of laboratory data concerning soil modulus degradation at high shear strain amplitudes. This is especially true for soils at depths greater than about 60m.

The study by Laird and Stokoe (1993) presents data that is encouraging but by no means extensive (figure 2). I did not have access to the original publication; the figures are taken.

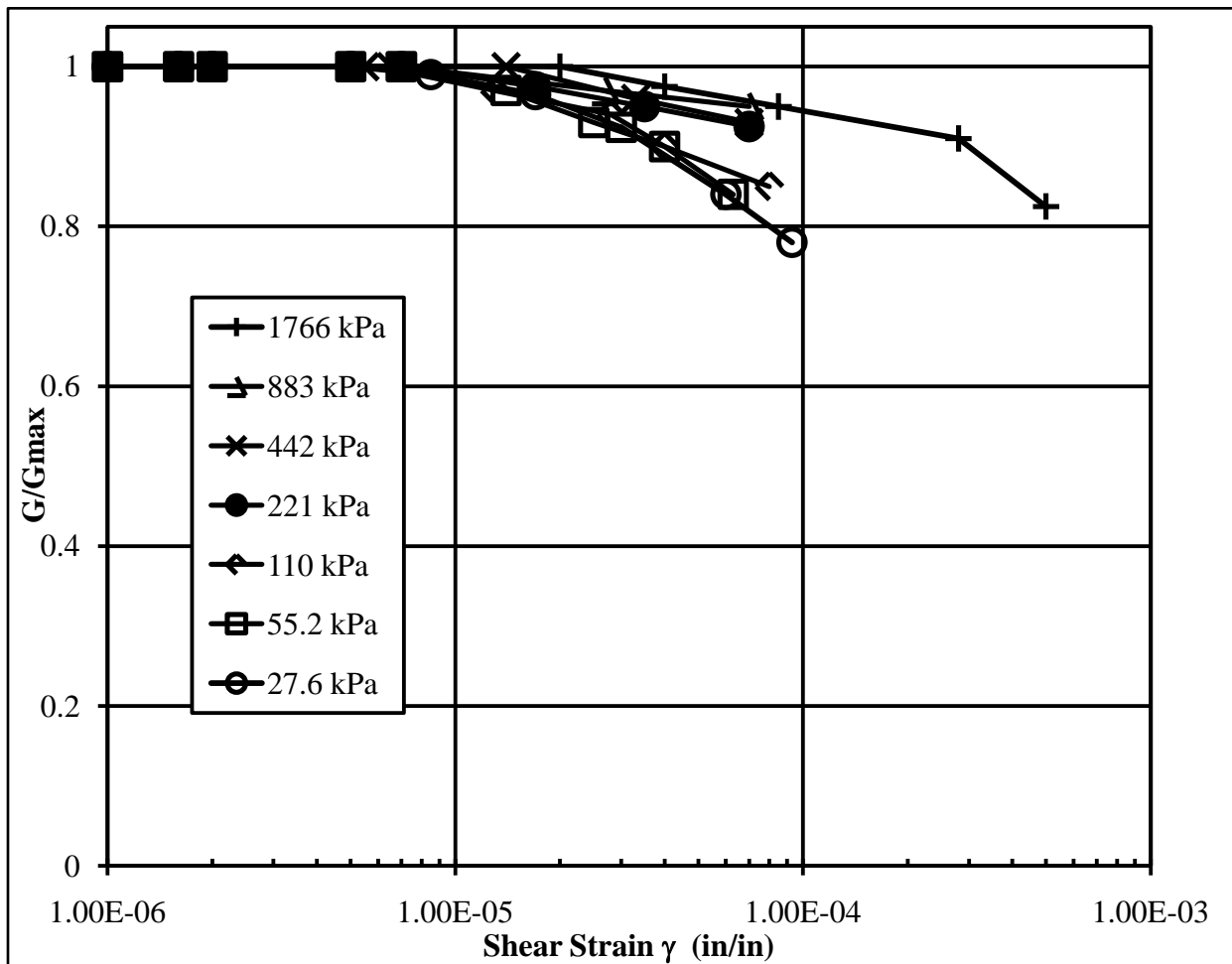


Figure 2. Shear modulus ratio vs. shear strain for seven confining stresses

from Assimaki and Kausel (2006). The general reduction with increasing strain is evident, however the tests were not continued to a high-enough level of excitation to induce a reduction curve that is easily modeled. It is not clear if these are a suite of tests on the same specimen or separate tests on separate specimens. If they are a suite, it would explain the incomplete curves since the researcher would be reluctant to drive the specimen too hard and risk failure (excessive displacement and coil-magnet contact). The highest confining stress may have produced a sample too stiff to resonate any further and the testing device reached its power limit.

By re-plotting the *low-amplitude* data, one can see the general relationship predicted by Hardin and Drnevich (1972b) where G_{max} is a function of confining stress raised to 0.5 power. As shown on the graph (figure 3) one may obtain a better fit with a slightly different power law, but without further study, that would be speculation.

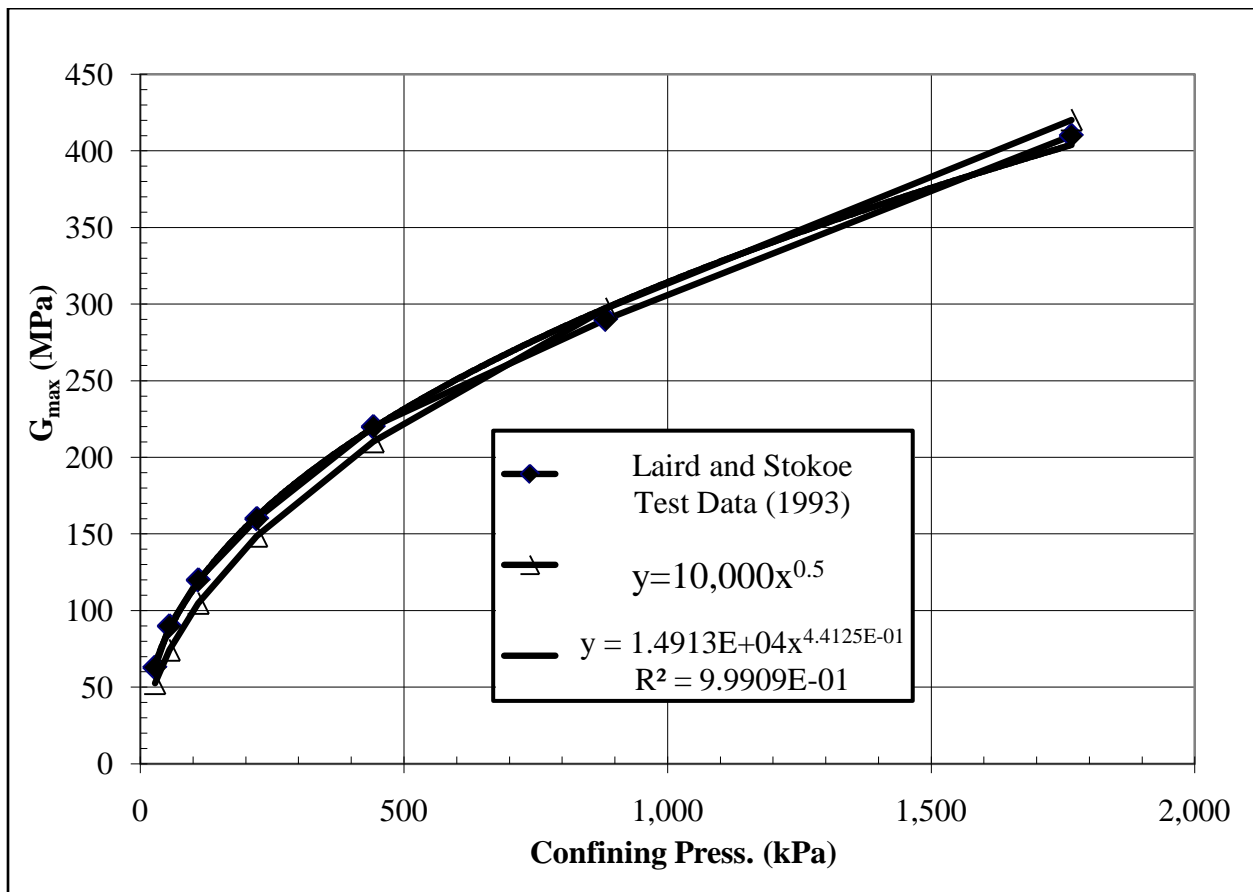


Figure 3. Increase in G_{max} with confining stress Laird and Stokoe data (Assimaki and Kausel, 2006)

Resonant Column-Torsional Shear Testing

Resonant column tests have become a standard method for determining dynamic properties of soils. There is an ASTM standard (D 4015) for performing the test and reducing the data. However, much of it is unnecessarily complicated by outdated computer codes for data processing. The actual test procedure was developed in the mid 1960's and early 1970's and perhaps the most extensive study using resonant column methods was presented by Hardin and Drnevich (1972a,b) Since that time, reviews by Woods (1978), Prashan et al(1988). Hwang (1997) presented a thorough review of device concepts and examined the interaction of counter EMF between coils and magnet drives, effects of imperfect end conditions, or conditions where there are not perfect fixed-free boundaries. Others have examined effects of anisotropic confinement and other unique stress conditions. Effects of loading rate have also been studied for various clays where frequency-dependent viscous damping may occur.

Torsional shear testing for dynamic properties evolved slightly later than resonant column tests. This was due primarily to the difficulty in measuring small amplitude displacements in a testing device. Tatsuoka et al (1981) present a thorough study on Toyura Sand using a torsional device. Other work by Tatsuoka expanded their knowledge of the effect of various parameters on shear modulus and damping. The reliability of very low amplitude stiffness and damping is acknowledged by the authors as being difficult to ascertain. This compounds the problem of modulus reduction ratio since the low-amplitude stiffness is a necessary component to computing the ratios (G/G_{max}). Combining resonant column tests with torsional simple shear were successfully done by Ray (1984) and Ray and Woods (1987). They were able to perform low- and high-amplitude resonant column tests as well as measuring stress strain hysteresis in torsional simple shear during the same test on the same specimen. They concluded that TOSS and RC test measurements for G and D agree when the soil had achieved a sufficient number of loading cycles to account for loading cycle effects, if present. They did not consider clays or soils that may have a high component of viscous damping; therefore frequency effects did not play a role in the study. Additionally they studied irregular load/deformation histories and found the Masing assumption to be adequate.

Modeling Hollow Cylinder Specimen

An additional intent of this study was to examine the state of stress within a hollow cylinder sample in some detail and assess the impact of imperfections on the soil's behavior during testing. Viewed another way, one may ask questions such as:

1. How bad or how large does an inclusion or void have to be before it significantly impacts the test results?
2. Can present computer-based stress-strain models adequately model the behavior of soil in a resonant column or torsional simple shear test?

On first inspection, (2) may seem a trivial question, but it is not. Most finite element models for geotechnical analysis are plasticity-based (with a Mohr-Coulomb failure criterion) or have a small-strain component blended with a plasticity model (Jardine, 1986). The process of modeling is difficult because the built-in soil models do not easily adapt to this sort of behavior at low strains (low with respect to what the models normally analyze). A second option is to supply the computer analysis with your own version of a soil model. This requires coding and “injecting” a subroutine into the finite element software package. While entirely feasible, it was beyond the realm of my students and must wait for further study. A brief discussion of the approach follows in Chapter 7.

Chapter 3. Laboratory Testing Program

Introduction

The laboratory testing program had two general objectives: (1) design, build, and verify the performance of a high confining stress resonant column/torsional simple shear device; and (2) perform laboratory tests at low confining stress and, following construction of (1), high confining stress. All but the final part of (2) have been achieved. We are looking forward to completing the second half of objective (2) by December 2010.

Design and Construction of Device

The only reference to high confining stress testing in the literature was work done by Laird and Stokoe (1993). There are other citations such as Assimaki et al (2000), but the only laboratory test data comes from the Laird and Stokoe study. In that study, they performed tests at various confining pressures from 27 to 1766 kPa. While this does not seem very high, one must consider that these tests use air as a confining fluid rather than water (or oil). This makes safety a much greater concern. The need for air instead of water is due to the nature of the test itself. The top of the specimen is resonated in torsional vibration, requiring a free-end condition. Typically the drive head consists of a magnet and coil arrangement. Due to the required freedom and electrical drive system, a wet confining system becomes impractical.

The system built in this study uses air as the confining medium. However, before testing, the confining system had to undergo hydrostatic testing to prove it was capable of safely handling the confining stresses. So far the device has withstood pressures up to 2800 kPa (400 psi). The confining vessel is designed for 5500 kPa (800 psi), however due to the addition of transducers, pore pressure ports and feed through fittings for instrumentation, testing of the complete, finished system was deemed appropriate. Safety concerns limited the testing pressure. Additional hydrostatic testing to 5500 kPa will be performed at a later date when a suitable surrounding safety chamber is in place.

Confining Stresses

Estimating appropriate target confining stresses required some assumptions regarding unit weights of sediments and influence of groundwater. Shown below is a figure taken from

Chapman et al (2006) (figure 2) delineating estimated shear wave velocities and effective vertical stresses (σ'_v) versus depth for Charleston SC. In their article, Chapman et al do not explain why they chose the values of effective vertical stress that they did, however, one may back calculate such values given typical densities of sediments found there. Figure 3 shows such a calculation with an estimated wet weight of sediment to be 17.28 kN/m^3 . Also shown on the figure are the estimated vertical effective stress (total stress-pore pressure) presented by Chapman et al. for Charleston. A maximum vertical effective stress shown in Chapman's profile is about 4400 kPa. If one assumes a lateral coefficient $K_0=0.7$, then $(\sigma'_x + \sigma'_y + \sigma'_z)/3 \approx 2.4\sigma'_z/3$ and the average effective confining stress for a test would work out to about 3500 kPa. Therefore the chosen upper limit for average effective confining stress value of 5500 kPa in the testing device should be adequate. Even the "proof tested" value of 2800 kPa will be able to replicate confining stresses at about 400-500 m depth ($\sigma'_v = 3000 \text{ kPa}$)

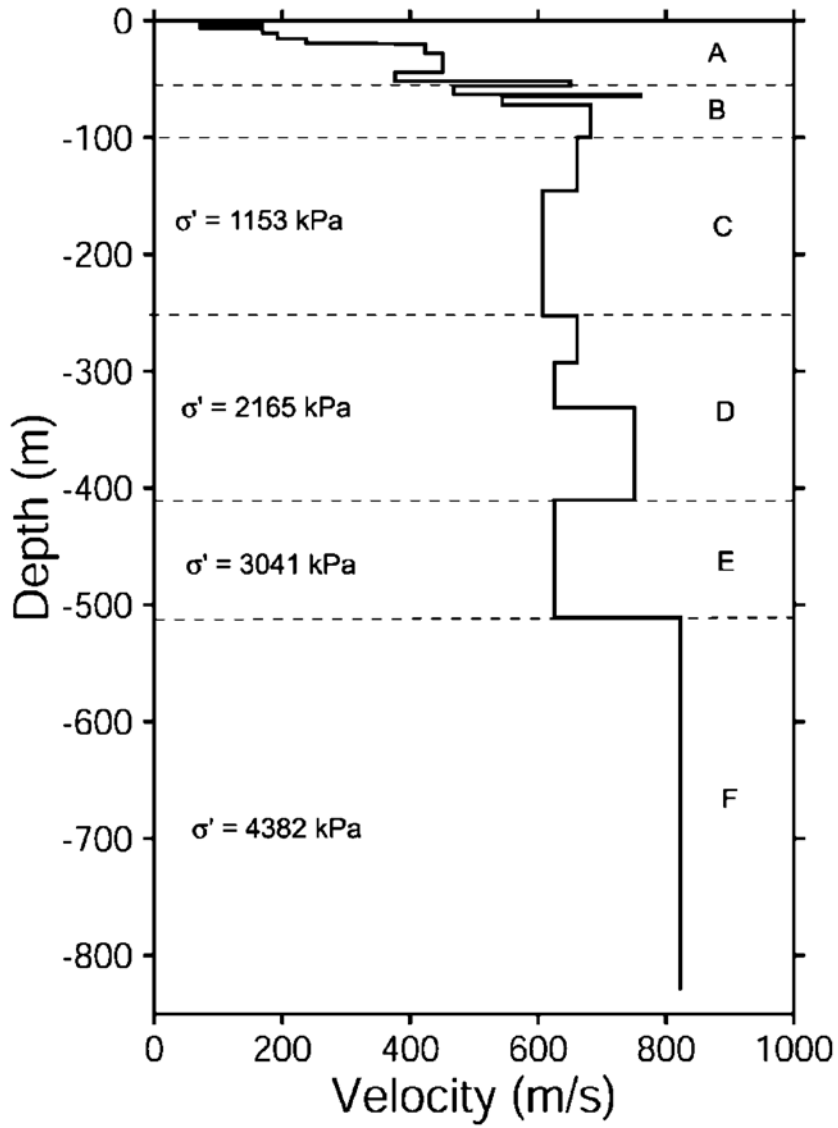


Figure 1. Profile for Charleston (Chapman et al, 2006)

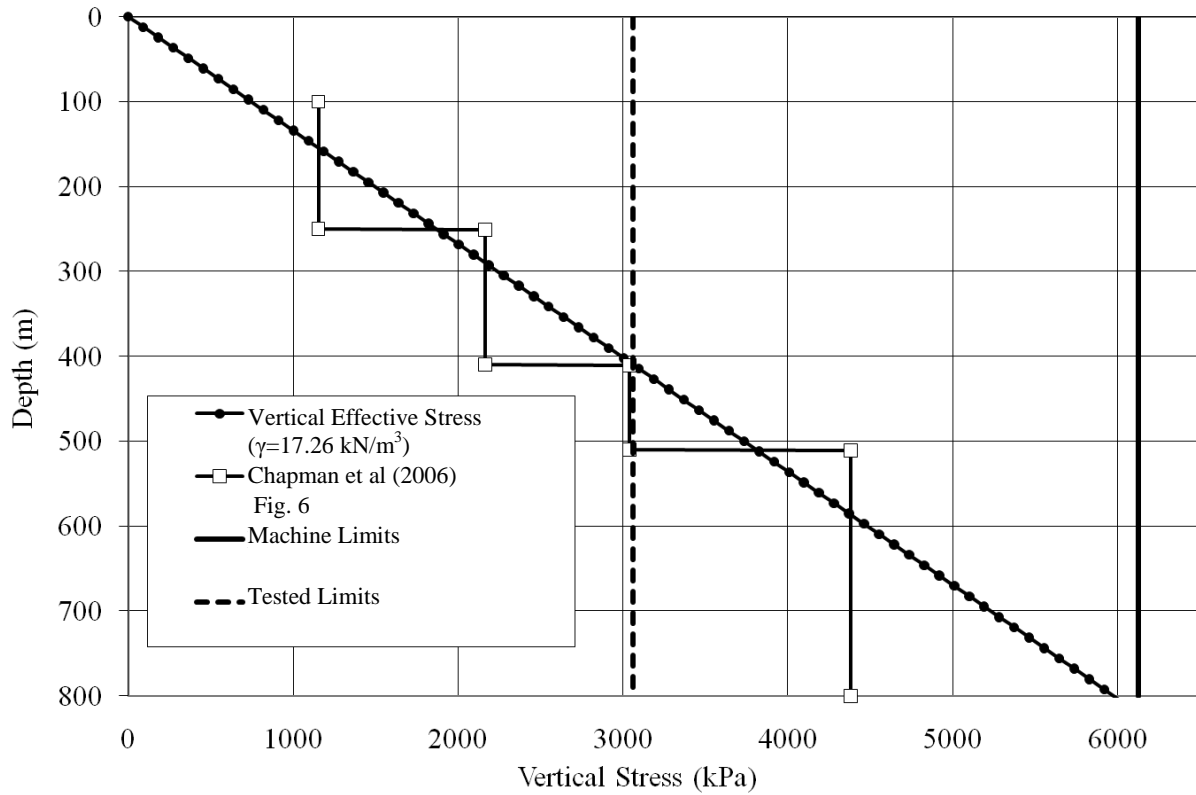


Figure.3-2 Estimated vertical effective stress from Chapman et al and machine limits

Shearing Stress Uniformity and Torque Capacity

Another important consideration in the design of the RC-TOSS test device is the magnitude and distribution of shearing stresses within the specimen. The great advantage of a hollow cylinder specimen is that it reduces the variation of shearing stress (and strain) along its cross-section. In torsional shear tests it is necessary to define shear stress and shear strain, because the distributions of shear stresses and shear strains on a cross section of a hollow cylindrical sample are not uniform when torsionally sheared. Therefore in this study, the torsional shear stress τ , was defined as

$$\tau = \tau_{ave} = \frac{S}{A} \tag{Eq. 3-1}$$

where τ_{ave} = the average shear stress on a cross section

S = the shear force acting on the cross section

A = the area of the cross section = $\pi(r_2^2 - r_1^2)$

The shear stress is usually a function of radial distance in the specimen, therefore to formulate the behavior one must define shear force as an integral

$$S = \int_{r_1}^{r_2} \tau_r 2 \pi r dr \quad \text{Eq. 3-2}$$

where τ_r = shear stress along radius, r

r_1, r_2 = inner and outer radius of the specimen

Computing the torque, T that acts upon the cross section involves a similar integral equation

$$T = \int_{r_1}^{r_2} 2 \pi r \tau_r r dr \quad \text{Eq. 3-3}$$

The additional r term in the equation represents the moment arm that the differential stress element uses to generate torque about the centerline of the specimen.

In order to assess the degree of shear stress uniformity, one can pick two extreme cases: perfectly elastic behavior and perfectly plastic behavior. After those are examined, one may evaluate the more realistic effects of a non-linear soil model. For the linear elastic case, one may envision shearing stress at the outer radius equal to τ_0 and decreasing proportionally as it moves toward the centerline of the specimen (figure 3-3a). The functional relationship for shear stress would be

$$\tau_r = \frac{\tau_0}{r_2} r \quad \text{Eq. 3-4}$$

Substituting into equations 3-2 and 3-3, one may compute intermediate values. While they are not necessary for average stress computations, they are included here for the stress uniformity discussion later.

$$S = \int_{r_1}^{r_2} \frac{\tau_0}{r_2} r 2 \pi r dr = \frac{2\pi \tau_0}{3 r_2} (r_2^3 - r_1^3) \quad \text{Eq. 3-5}$$

$$T = \int_{r_1}^{r_2} \frac{\tau_0}{r_2} r 2 \pi r r dr = \frac{2\pi \tau_0}{4 r_2} (r_2^4 - r_1^4) \quad \text{Eq. 3-6}$$

then using equation 3-1, one can relate torque to average shear stress in the specimen as

$$\tau_{ave\ elastic} = \frac{S_e}{A} = \frac{4}{3\pi} \left\{ \frac{r_2^3 - r_1^3}{(r_2^2 - r_1^2)(r_2^4 - r_1^4)} \right\} T \quad \text{Eq. 3-7}$$

In the case of plastic behavior as illustrated in figure 3-3b, equation 3-4 is merely a constant τ_0 . Applying the same equations with a simpler stress function results in

$$\tau_{ave\ plastic} = \frac{S_p}{A} = \frac{3}{2\pi} \left\{ \frac{1}{(r_2^3 - r_1^3)} \right\} T \quad \text{Eq. 3-8}$$

For the specimen dimensions in this study where $r_1 = 2$ cm and $r_2 = 3$ cm, the average shear stress based on elastic or plastic assumptions (as a function of applied torque) are

$$\begin{aligned} \tau_{ave\ elastic} &= 0.0248 T \\ \tau_{ave\ plastic} &= 0.0251 T \end{aligned} \quad \text{Eq. 3-9}$$

So, for determining average shear stress, elastic or plastic assumptions make little difference.

The *uniformity* of shear stress across the specimen is slightly more complicated. The deviation from average for the plastic case is, of course zero, since the shear stress is uniform throughout. For the elastic case, one may use equation 3-1, 3-4, and 3-5 as a starting point. If the outer shear stress is, say 100 kPa, the average shear stress will be 84.4 kPa and the inner shear stress would be 66.6 kPa. This would imply that the outer stress is 18% higher and the inner stress is 21% lower than the average shear strain.

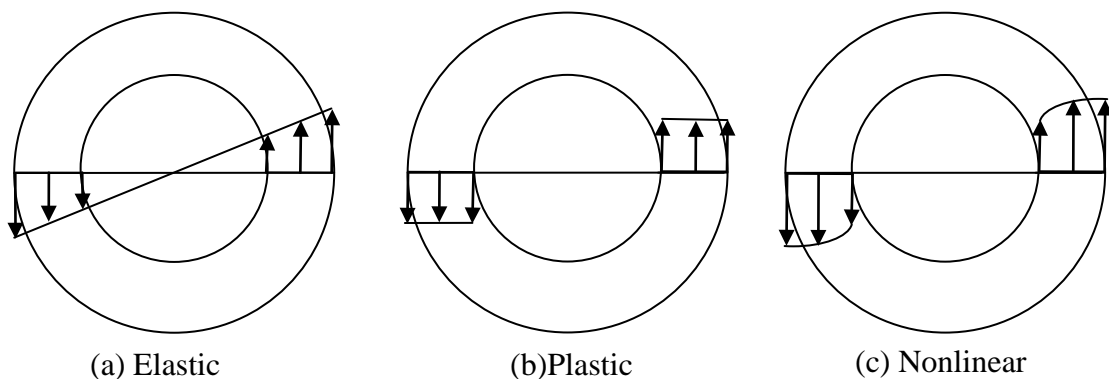


Figure 3-3. Shearing stress along cross-section for (a) Elastic, (b) Plastic, (c) Nonlinear assumptions

Nonlinear shearing stress distribution is bracketed between these two extremes. We can examine how much the nonlinear distribution. Specifically, if we use a Ramberg-Osgood stress-strain model with parameters typical for sands as proposed by Hardin and Drnevich (1972b) the variation with shearing strain for inside and outside radial extremes will look like figure 3-4. The outer radius starts at about 18% difference and the inner radius about 21%. Each drops to about 7-10% difference at higher strain levels.

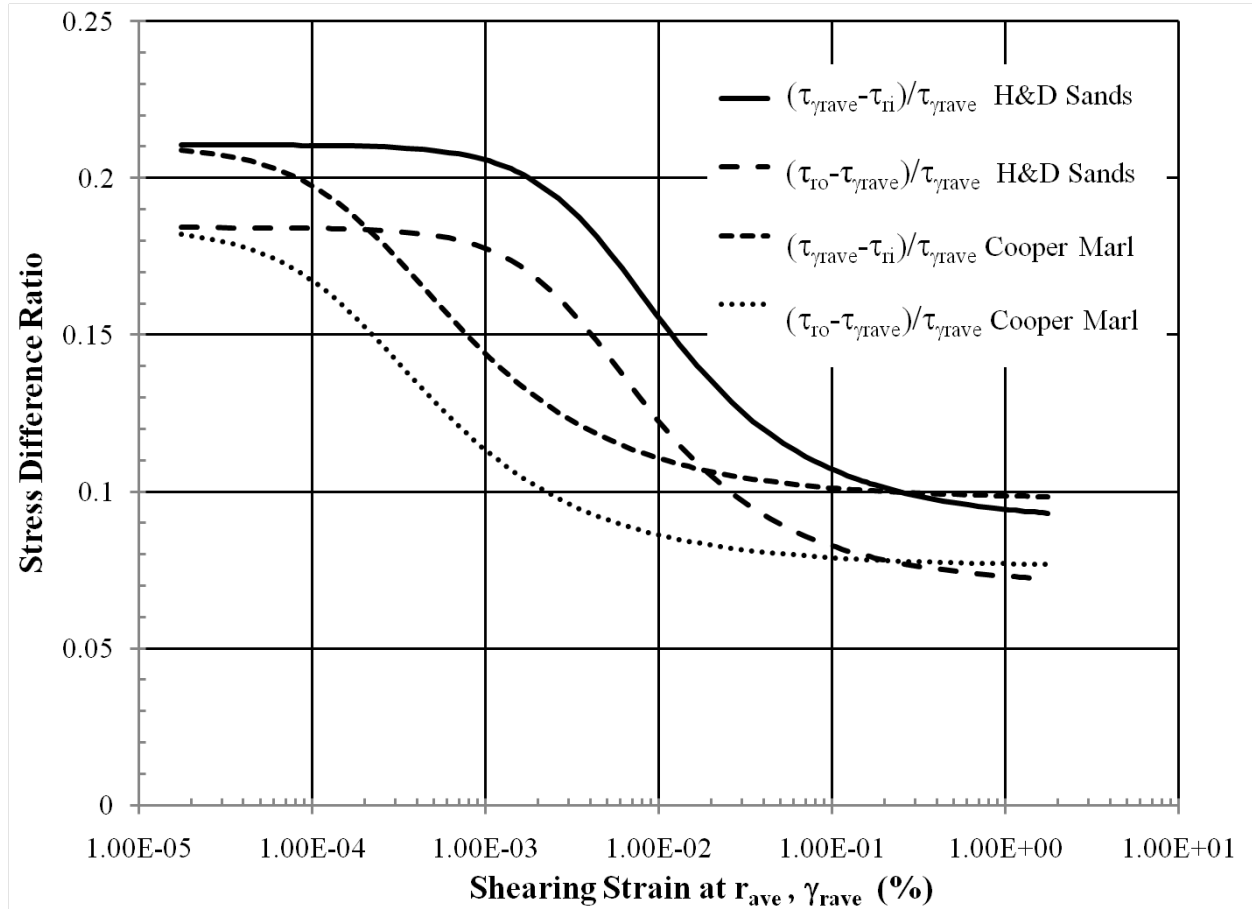


Figure3-4. Plot of shearing stress ratio vs. overall shearing strain for two nonlinear soils

Computing the required torque for such a configuration follows from the above equations in the same manner. One should keep in mind that for torque calculations, given an average shearing stress over the specimen, the elastic distribution is most conservative, ie, the highest stresses have the longest moment arm. For resonant column testing it is difficult to assess the exact power requirements since low-amplitude tests have higher stiffness and less damping. High amplitude tests have lower stiffness but higher damping. Depending on the degree of modulus reduction and damping increase with strain, the device will encounter its maximum limits. What

is also required is some estimate of the low-strain shear modulus G_{max} , of the soils to be tested, as well as some intuition about the degree of modulus degradation one should expect for high amplitude loading. Figure 6 shows estimated torque requirements as well as another estimate of maximum shear modulus, based on an empirical formula by Hardin and Black (1986). Note also the estimated deliverable torque generated at resonance by the present resonant column device.

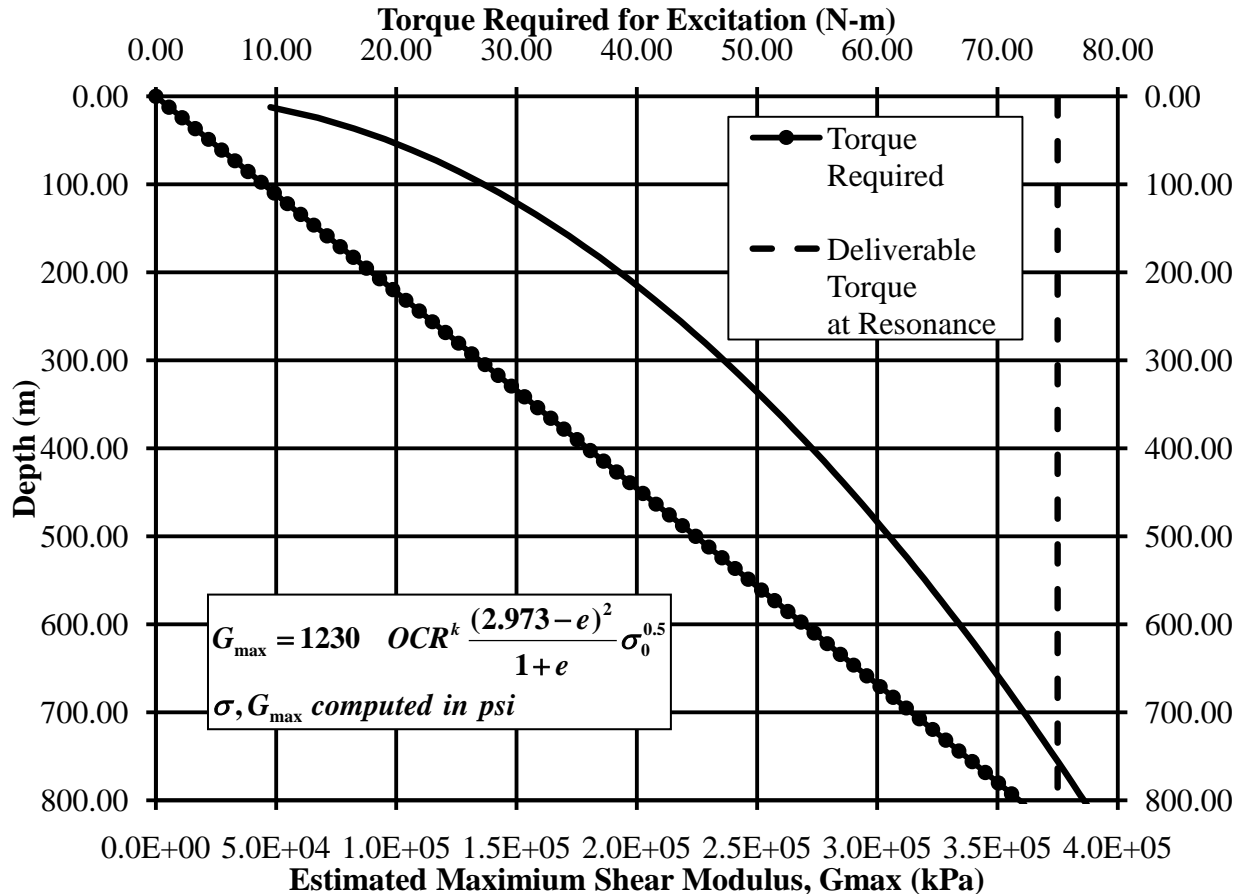


Figure 2. Estimated torque requirements to generate nonlinear behavior

Soils Tested

The testing program started with resonant column tests on glass ballotini, manufactured glass beads used in reflective paints and sand-blasting industries. They are perfectly uniform spheres of silica with polished exteriors and consistent properties. Small diameter (#100 sieve) and large diameter (#40 sieve) ballotini were used. As a second step, 40-60 Ottawa sand was used to further calibrate the machine and gain confidence in the testing technique and data reduction. Finally, samples of Cooper Marl retrieved from field borings were used for testing.

These has a markedly different behavior and it was fortunate that calibration materials were first tested.

Index properties of the soils that were included in the testing program to date are listed below in table 1. Note that the Cooper Marl had a range of index values. Strength values for the three categories were generally similar; however the Cooper marl showed some apparent cohesion in one suite of tests and showed classical cohesionless behavior in another suite. The Cooper Marl 1 set were soils within very close proximity to the soils tested dynamically. They were either specimens in the same sample tube or just above or below the specimens tested. The Cooper Marl 2 data set included a wider distribution of soils including the Cannon Park Core samples that were dynamically tested. This set presented a different set of behaviors than Cooper Marl 1 so the data set was treated as separate. This highlights the important fact that soils in a very small region can exhibit very different behaviors.

Table 1. Index properties of soils used in testing program

Data Set	C_u	% < #200	LL	PI
Ballotini	1.4	0		
40-60 Ottawa	2.5	0		
Cooper Marl	4-6	40-65	20-30	0-5

Table 2. Summary of strength data for soils tested

Data Set	Num Tests	c' (psi)	ϕ' (°)
Ballotini	4	0	29
40-60 Ottawa	4	0	33
Cooper Marl 1	9	7	7.5
Cooper Marl 2	14	0	45.5

Testing Program to Date.

As stated in the introductory remarks, the testing program is not complete, however this is the status of the testing so far. Resonant column tests have been performed on Cooper Marl using the low confining stress system. This is identical to the high confining stress systems

except for the use of a pressure vessel. A more modest confining system was used and confining pressures up to 300 kPa were attained. For most of the testing, confining pressures did not exceed 145 kPa. Table 4 below summarizes the tests

Table 4. Summary of Low Confining Stress Tests

Test	Boring	Sample Depth (m)	Confining Stages (kPa)	Strain Stages (Number)
A	L-1	25.0	103, 124, 145	9, 9, 9
B	L-2	37.2	103, 124, 145	11, 15, 12
C	L-2	21.3	103, 124, 145	12, 13, 13
D	L-2	28	62, 82, 103	6, 6, 7
E	L-2	28.3	103, 124, 145	8, 8, 7
F	W-1	19.8	103, 124, 145	8, 8, 9
G	W-1	42.7	72, 103, 145	7, 10, 7
H	W-2	29.0	82, 103, 145	7, 8, 8
I	W-2	19.8	138, 206, 276	14, 15, 11
CP	CP-1	236.8	103, 206, 309	8, 8, 9

Borings L-1 through L-4 are located around the site where the Arthur Ravenal Bridge was built across the Cooper River in Charleston SC. Borings L-1 and L-2 were located on land, While W-1 and W-2 were located in about 10m water. The location of CP-1 is in Cannon Park, downtown Charleston (Bybell et al, 1998) about 4 km from the other borings.

Chapter 4. Device Construction

The RC-TOSS device uses a coil-magnet drive to load hollow cylindrical soil specimen in torsion. RC-TOSS consists of power supplies, device hardware, measurement transducers, signal conditioners, and a control system (Fig. 3-1) . Each of these component groups is discussed below. More detailed discussion of the instrumentation is in Appendix A.

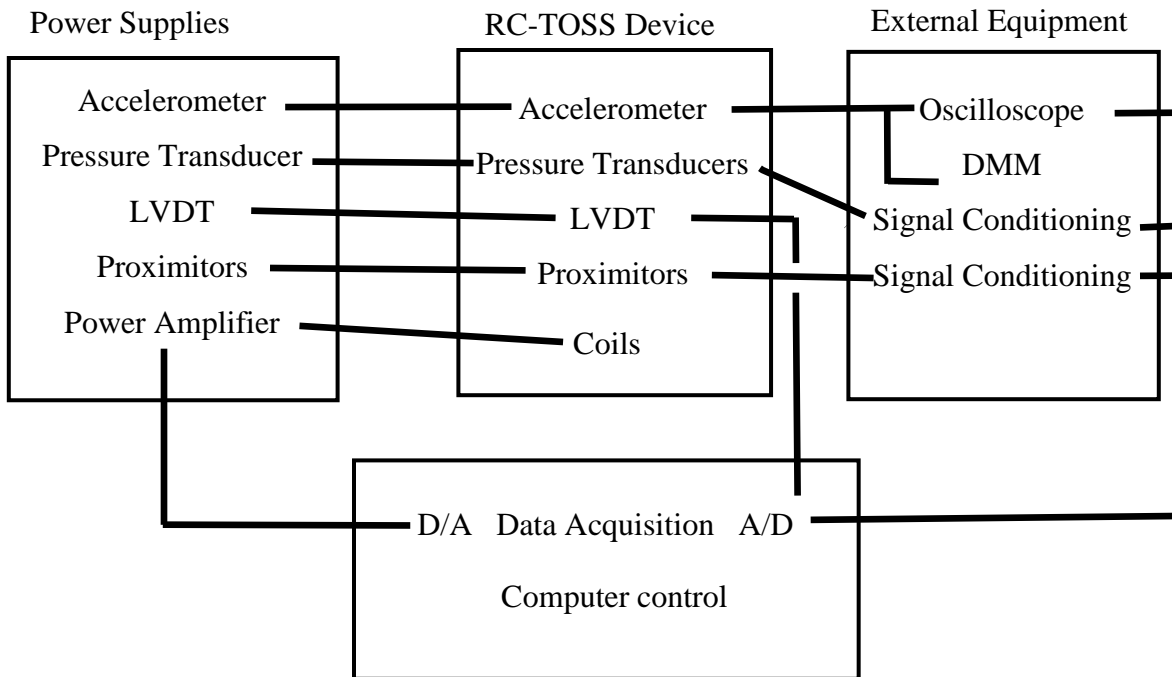


Figure 4-1. Schematic of RC-TOSS testing system

Power supplies provide the necessary source power for instrumentation as well as the drive coils. Each is a separate device; however the accelerometer power source is coupled to its signal conditioning, as are the proximitors and pressure transducers. The power amplifier for the coils is capable of 500 watts of continuous DC power. An oscilloscope is used to watch the resonance output of the accelerometer during RC testing. The DMM can measure RMS amplitude of the accelerometer as well as its frequency. The data acquisition system and computer record transducer outputs during RC test as a logging device, mainly to track any variation in confining pressure or vertical movement during the testing. For TOSS tests they record all the data, make decisions about driving the sample then send drive signals to the power amplifier which drives the coils.

Device hardware holds the sample in place, confines it under pressure, transfers loads to it, and supports the transducers. As shown in figure 3-2, the device rests on a rigid, massive, steel base plate, to which the base assembly is fastened. The plate also anchors the drive coil supports and the measurement post. The base assembly serves as a platform for the test specimen. Inner and outer membranes and split molds fit snugly against the inner and outer diameters of the base assembly. The base assembly is bolted to the base plate to increase fixity at this end of the specimen. A mixture of 8% (wt) epoxy and 10-20 sub-angular sand helps couple the soil and steel and is placed where “porous stone” is indicated in the figure. The mixture is very permeable so pore water movement is not impeded. Steel shear studs help anchor the sand mix and prevent it from sliding along the steel. Appendix A shows the base assembly, and other components in greater detail.

Also note (fig. 4-2) the pore pressure line that travels from the base plate to the base ring and eventually, into the specimen itself. The top assembly connects to the free end of the specimen. Like the base, its inner and outer diameters match those of the specimen. It too, uses a permeable epoxy/sand mixture at the soil/steel interface and has two vents (not shown) for pore water movement. The vents are attached to 1/8” plastic tubing that generates virtually no extra stiffness or damping.

The drive coils mount on their own stands and have an elongated shape. The shape allows for vertical settlement of the specimen during testing. Additionally, the coils’ dimensions provide ample side-to-side space for the magnets. One important aspect of the coil-magnet loading system is the constant nature of the loading force or torque. If the specimen weakens and deforms rapidly, the applied torque will not reduce or relax as proving rings do, rather, the force will remain constant until a strain level is reached (during a strain-controlled test) or device interference occurs. As a result, the stress-strain curve will rarely show strain softening on a single loading curve. The softest condition will plot as a horizontal line.

Proximator targets are made of 4130 Steel and are large enough to allow for some lateral misalignment. The accelerometer (not shown in picture) is mounted directly on the drive head at the front. The LVDT mounts with a spring system that acts as a counter balance to the weight of the drive head and magnets. This helps to maintain isotropic confining stress conditions at low confining pressures.

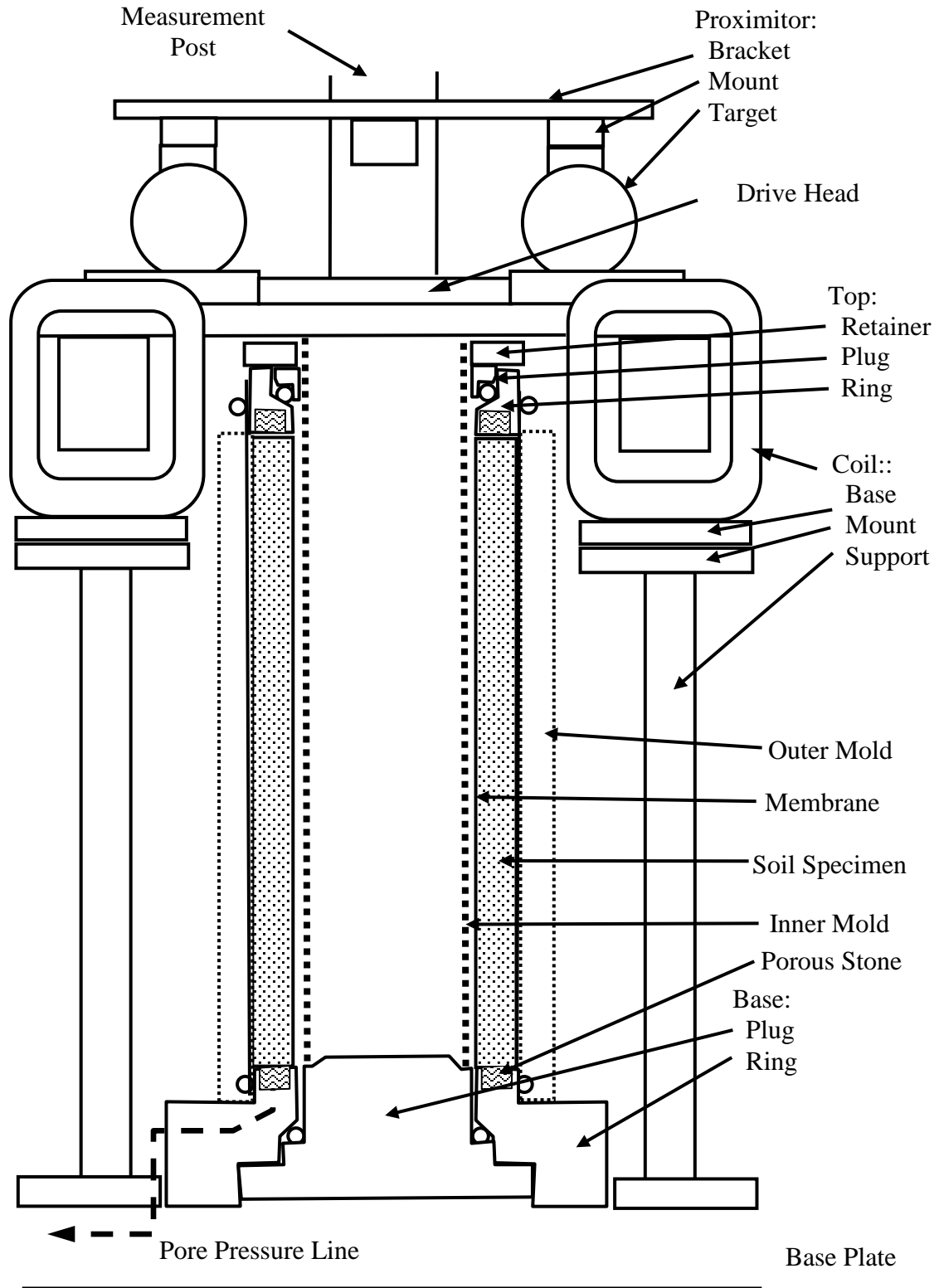


Figure 4-2. RC-TOSS schematic cross section

The inner core of the LVDT is attached and aligned with the centerline of the drive head. A wire and hook system hold the drive head without generating any torque resistance (figure 4-3). The LVDT and spring are held to a rigid measurement post.

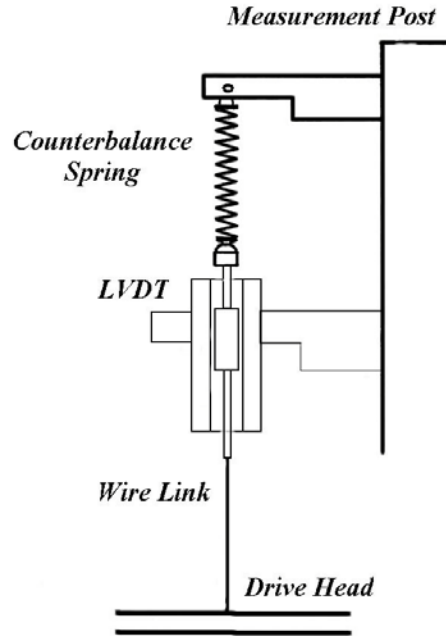


Figure 4-3 Spring counterbalance and LVDT system

The 4-cm inner, 6-cm outer diameter sample has a practical drawback in that no standard membrane sizes fit the molds exactly. One may use 1.4 in. or 1.5 in diameter inner membranes and 2.36 in outer membranes. These work well enough. Butyl O-rings stretch to seal the outer membrane to the device.

Measurement Transducers

The TOSS device can measure rotational displacement and acceleration, longitudinal displacement, torque and pore pressure. These are accomplished by proximity sensors, an accelerometer, an LVDT, by coil current, and a pressure transducer, respectively. Since instrumentation details are discussed in Appendix A. The need for precise measurements placed the heaviest demand on the proximity sensors. For a low-amplitude torsional test, single amplitude strains may range down to 0.002%.

By using an accelerometer, resonant column measurements benefit from the relationship between acceleration and displacement (Appendix A) . This makes measurements at strain amplitudes below 10⁻⁴% routine. DC drift is not a problem since the DMM or oscilloscope reads

only the AC component. With the electronics on hand, the LVDT could measure movements of 0.1 mm.

Signal Conditioning

Signal conditioners alter an input signal to some other form, then pass it on to the next piece of equipment. The alteration may consist of filtering higher frequencies, subtracting or adding signals, amplifying, or offsetting a signal. The circuitry necessary to perform these tasks is part of the respective transducer system. Most of the conditioning allowed for simple gain settings on the acquisition board to maintain a high level of sensitivity and accuracy. Details of the data acquisition system are discussed in Appendix A.

The TOSS system allows for either load or displacement control. The controlling parameter can either be the load generated (and current measured) by the drive coils or the deflection measured by the proximitors. Generally, the displacement controlled tests yield more consistent results. Details of the control program are listed in Appendix D.

Testing Procedure

The testing procedures for the hollow cylinder torsional shear and resonant column test are identical up to application of loads. At that point, the tests diverge with respect to loading frequency and waveform. The computer runs the torsional test while the resonant column test is controlled manually.

Sample preparation

The sample preparation sequence is similar to that described by Ray (1984) with modifications to accommodate the change in equipment. The reader may find it helpful to refer to Fig. 4-2 for terminology.

- 1) Initiate the computer program for the test. The test title, number, soil type, etc. can be entered.
- 2) Place the inner mold onto the base plug and secure it with the mold cap, threaded rod, and nut. Apply talc to the mold so the inner membrane will slide on easier.
- 3) Sprinkle talc inside the inner (4-cm) membrane and slide it down the mold until it overlaps the O-ring on the base plug.

- 4) Apply a thin coating of silicon grease to the beveled surface inside the base ring. Slide the ring down the mold until it mates with the base plug. The O-ring should now be pushing the membrane onto the greased, beveled surface.
- 5) Squeeze the base plug into the base ring further by turning the appropriate screws. To insure even O-ring pressure, tighten screws opposite each other in a star pattern. Each screw should offer equal resistance.
- 6) Attach the base ring to the base plate with the appropriate screws. Again, use the star pattern and even torque to tighten the screws. This attachment must be tight to create good end fixity. The pore pressure line may also be attached at this time.
- 7) Measure the inner diameter and record it on the spreadsheet.
- 8) Grease the polished rim of the base ring and slide the outer membrane onto it. Secure the membrane with an O-ring.
- 9) Fasten the outer mold together with hose clamps and draw a vacuum through it. Fold the membrane over the top of the mold: the vacuum should draw it snugly against the mold. Place an O-ring outside the mold, near the top for later use.
- 10) The soil is ready for placement. Methods of deposition are the same as for any test. Dry pluviation, spooning and tamping, and tremie placement are all possibilities. Pluviation and spooning and tamping produced dense specimens while the tremie technique produced loose ones. When done carefully, all three techniques produced repeatable densities. The soil container should be weighed before and after placement to determine the weight of the specimen
- 10a) Some of the Cooper Marl is cohesive enough to trim with a wire saw. If this is possible, the outer diameter is trimmed then the specimen is placed in a mold with annular end caps.
- 10b).A wood auger is drilled through the centerline of the specimen. A wire garrote is then used to saw out the inside diameter of the specimen.
- 10c) The specimen is then placed onto the base ring and an outer membrane placed on it.
- 11) Grease and place the top ring onto specimen and mold. The top ring must be aligned properly so the magnets and coils fit. Alignment by eye proved sufficient.
- 12) Slip the top plug onto the inner mold and pull the top of the inner membrane outside of it. Work the plug down until it seats within the top ring.

- 13) Slide the top retainer onto the top plug and squeeze the inner o-ring by tightening the appropriate screws. When tightened, the retainer should recess below the highest portions of the top ring.
- 14) Now, draw a vacuum on the sample through the pore pressure lines to create some sample contact. Cut off the vacuum line to the outer mold and fold up the outer membrane to seal against the top ring. Roll up the o-ring from step 9 to secure the membrane. Note: for soils that exhibit a sensitivity to it, the magnitude of the vacuum pressure should not exceed that of the eventual confining pressure.
- 15) Fasten the drive head system onto the top ring. Use the star pattern to tighten the screws.
- 16) Erect the coil supports and position the drive coils to their correct locations, securing them with the adjustment nuts. Check to see if there is sufficient clearance gap around all magnet/coil combinations.
- 17) Remove the inner mold and erect the measurement post. It should align so that the LVDT mount is concentric to the specimen.
- 18) Mount the proximitors and adjust their gaps with the aluminum gage as a start. Carefully slide the proximitors forward or backward to achieve a mid-point output voltage. The connecting cables should be bound to the measurement post with wire to hold them steady.
- 19) Mount and zero the LVDT while hooking up the counterbalance spring.
- 20) Remove the outer mold and measure outer diameters and sample height. Enter them on the data display. Recheck the proximitor and LVDT outputs.
- 21) Compute all the rest of the necessary data and instruct the computer to save the data
- 22a) Low pressure: Assemble the pressure chamber around the sample, being sure to make all the electrical connections. In small steps, increase the confining chamber pressure and reduce the vacuum pressure to maintain a fairly even differential pressure on the sample.
- 22b) High Pressure: Bring the engine lift with the covering pressure vessel carefully over the testing configuration. Before setting it completely down, connect the necessary pore vents and instrument feedthroughs.

23) This is where the resonant column test procedure diverges. From here on the resonant column test is run manually, the torsional shear test continues using the computer.

24) Enter what type of control (stress or strain) then the maximum single amplitude value. Set the data acquisition channel gains to their appropriate scales.

25) With full pressure achieved, instruct the computer to take zero readings for stress and strain.

26) Choose other test parameters as you are prompted.

More details of the computer testing procedure appear in Appendix F. The rest of the test runs automatically and finishes after cycling for the prescribed number of cycles. Collected data appear plotted on the screen and may be saved at any time. The operator may choose to continue the test at another stress or strain level or perform a resonant column test.

Resonant Column

To obtain shear modulus and damping values, the operator replaces the D/A line to the power amplifier with a sine wave generator. Amplitude and frequency are adjusted to obtain first-mode resonance at a particular strain amplitude. The operator then cuts power and records the decaying response on a storage oscilloscope. Methods to compute shear modulus and damping from the data are discussed in Appendix E.

Other Loading Histories

Due to the nature of the control system, one can prescribe almost any sort of loading sequence he wishes: uniform cycles, uniform with offset, varying amplitudes, or totally irregular. Naturally, uniform-cycles mode is the best place to start since the complexity of the problem is reduced. Offsets and irregular loads require minor alterations to the test procedure but hold tremendous potential to study a variety of conditions.

Chapter 5. Test Results

Low Confining Stress RC Results

Results presented here are for low-confining pressure resonant column tests. Torsional shear tests at low confining stress and RC-TOSS tests at high confining pressure will be completed by December 2010. The tests showed markedly different behavior with respect to modulus ratio vs. strain when compared to sands and most silts. Figure 5-1 shows modulus ratio vs shear strain for all 10 specimens tested. Refer to table 3-4 and Appendix B for testing details and more extensive results. Shown with the data are curves from Seed (1982), Vucetic and

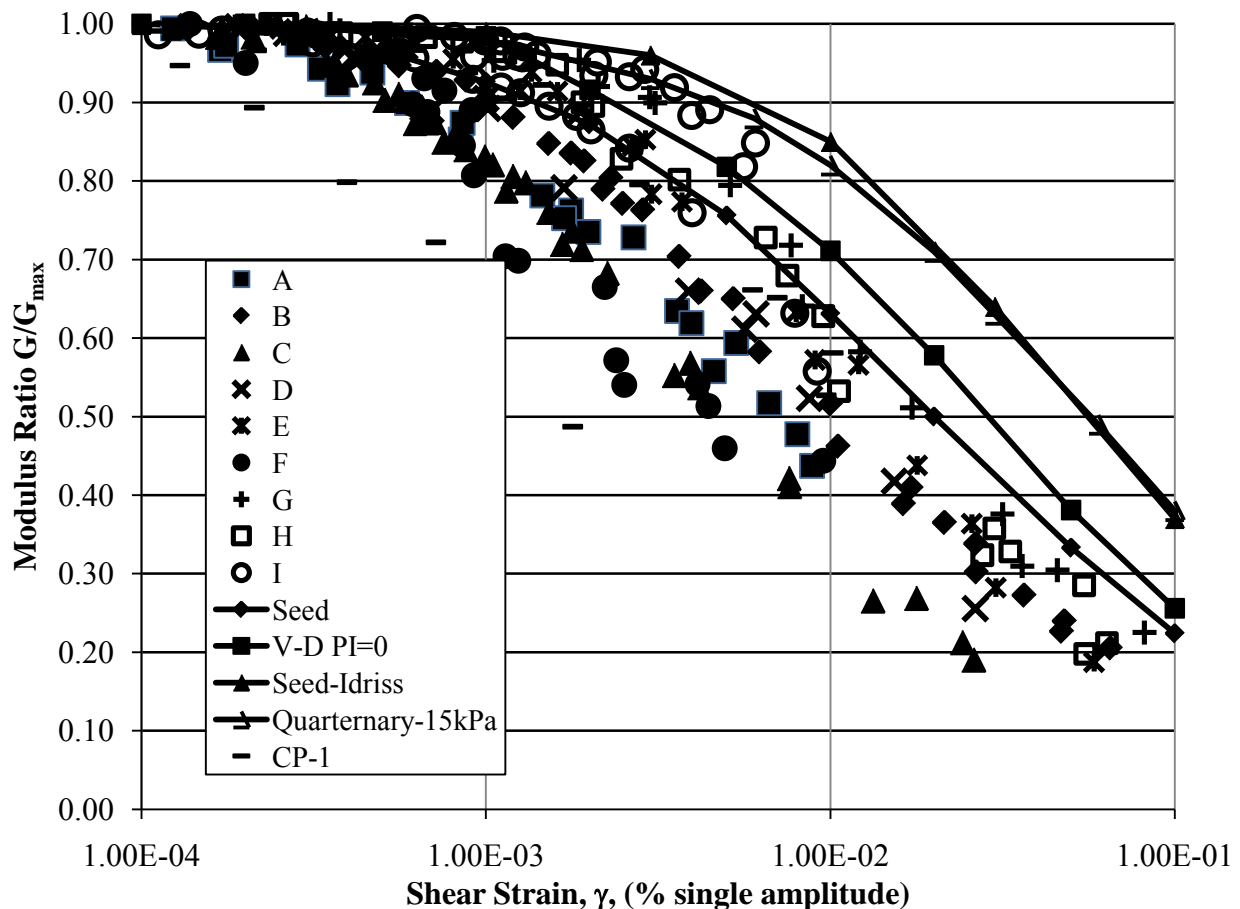


Figure 5-1. Modulus ratio vs shear strain for all test specimens and empirical curves

Dobry (1983), Seed and Idriss (1971) and Andrus (2006). The Andrus curve is for deposits in and around Charleston South Carolina. It is apparent that the Marl loses stiffness at much lower strains than typical sands or non-plastic (PI=0) silts. The impact of this behavior is illustrated in

the next chapter by comparing 1-D earthquake response analyses. When plotted with dimensionless strain, the test data looks better, but the empirical fits are still not encouraging. Most empirical curves do not use dimensionless strain so the comparisons are more difficult. We used a Ramberg-Osgood curve to fit the data in figure 5.2 with better results. The line is plotted without markers. The gray series labeled “Dar-A,B,C” are tests A, B and C plotted using

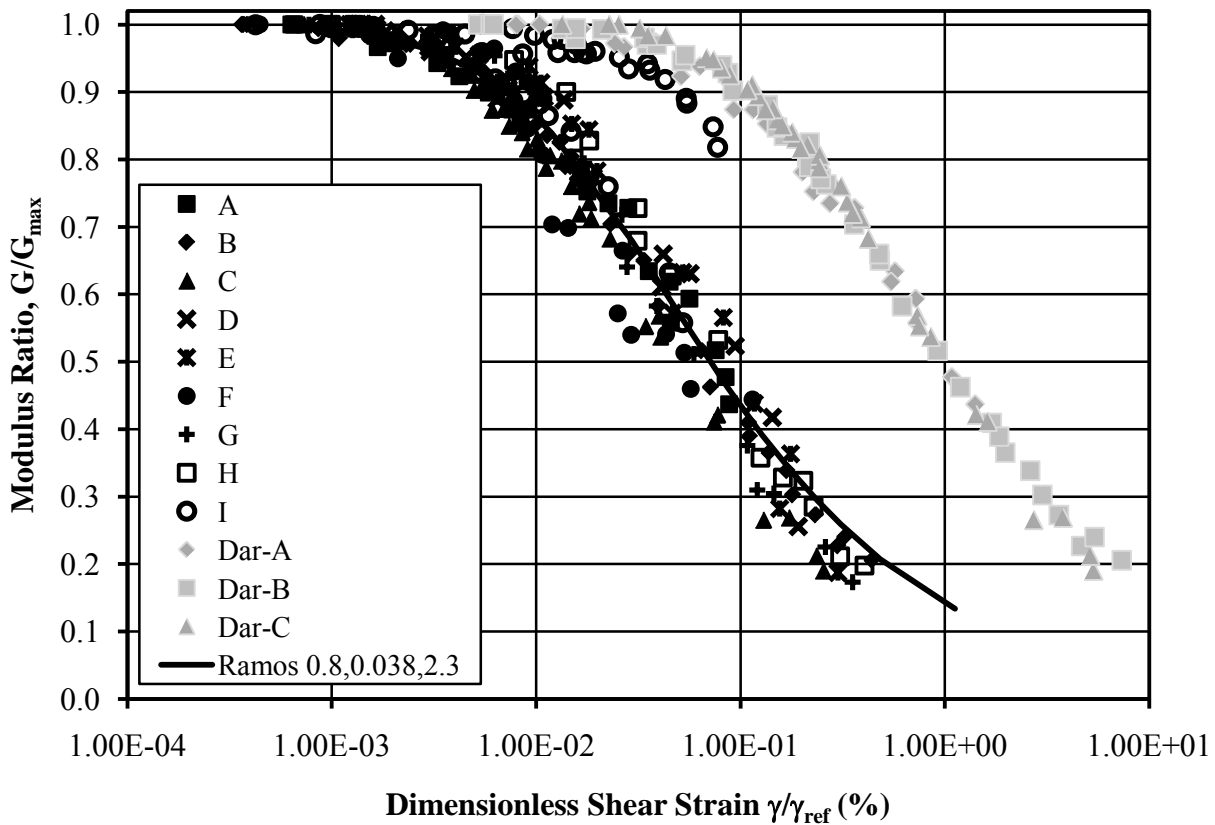


Figure 5-2. Modulus ratio vs. dimensionless shear strain.

Darendeli’s (2006) criteria for reference shear strain. To choose such an approach with this soil would be injudicious. This is because the Darendeli method assumes *a priori* what the reduction curve should look like and never considers the soil strength. This is cause for concern since many researchers accept the Darendeli approach without question. The open circles from test I are results that illustrate the effects of drying in the specimen. This specimen had a small amount of air circulating through the pore spaces for about five days between the first and second confining stages of the test. In that time the soil dried significantly and cemented slightly. The stiffness of the specimen doubled and showed a reduced affinity to weaken at higher strains. Since this was done accidentally and other tests were being conducted, we did not pursue the

phenomenon in our study. Damping behavior of the specimens were more variable and did not present a uniform curve when plotted versus dimensionless strain (figure 5-3) The Ramberg

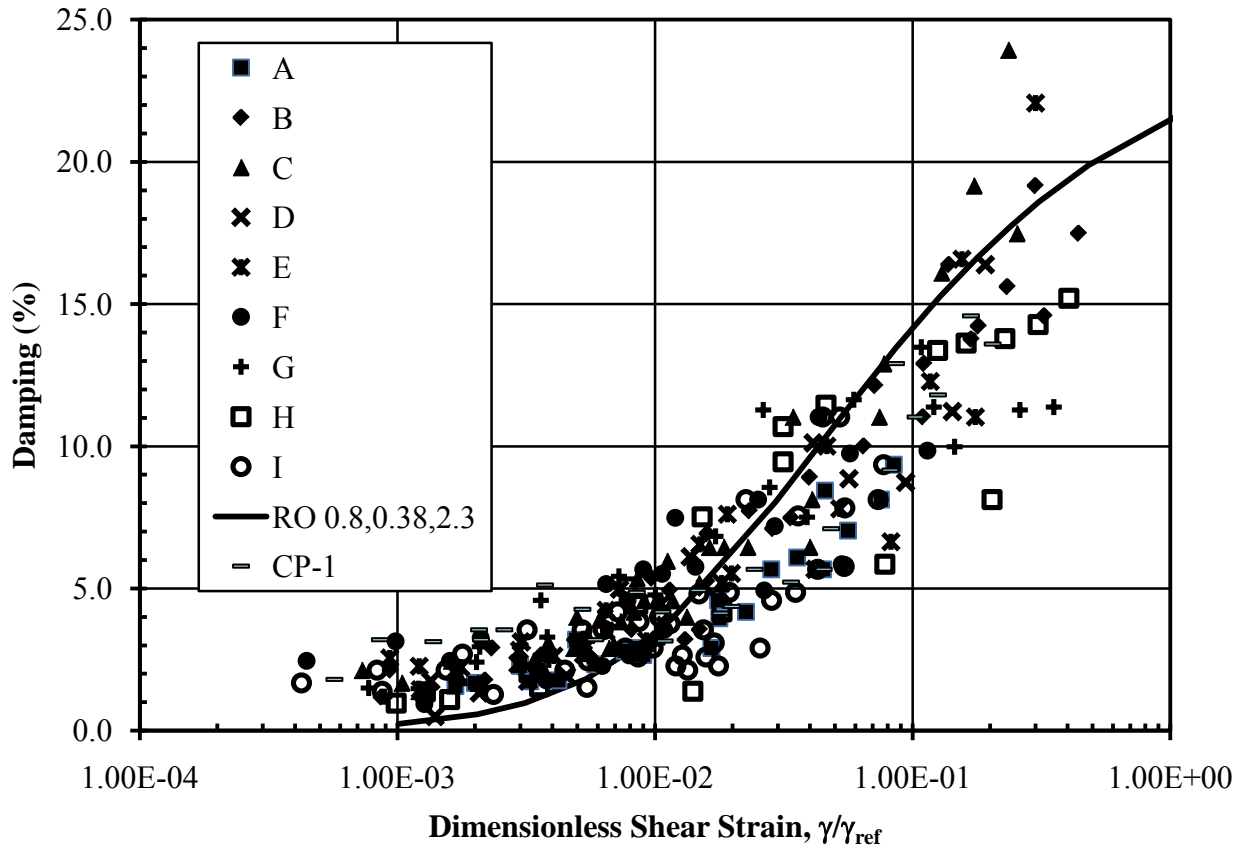


Figure 5-3 Damping vs. dimensionless shear strain-

Osgood curve is shown here as well, assuming a Masing criteria and computing the damping ratio based on the area of the enclosed hysteresis loop. The data is more scattered and the empirical fit does not do as well; however, the dominant feature for the response analysis is stiffness, so the curve is still adequate.

Discussion

The markedly different behavior of Cooper Marl may be due to the high shell content of the soil. Crushed shell particles may have a very different behavior under cyclic loading than granular soils. Some attempts were made to quantify the amount of shell material by using acid digestion methods. While it was obvious that Cooper Marl is composed of a high percentage of calcareous material as shown by the digestion tests, the fabric of the calcareous material and the distribution of particle size and shape is far more difficult. Obviously there is a great deal of room for further research on this soil.

Chapter 6. Application to 1-D Site Response

Introduction

One dimensional seismic response analysis has been a mainstay in earthquake engineering for over 30 years. Most analyses use either a time domain solution (Hashhash and Park, 2001) or a frequency domain solution (Kramer, 1995). While solutions in frequency domain are computationally more convenient, they suffer from inherent inaccuracies. Most of the inaccuracy occurs due to way frequency domain solutions treat non-linear soil behavior. Modulus reductions due to higher strains are applied over the entire duration of the event. This is necessary because there is no sense of time-history in a frequency domain solution. Modulus and damping values are the same throughout the entire event. Given the present state of computational sophistication, this is no longer necessary. Time domain solutions are computationally fast enough to perform the same tasks as their frequency domain cousins, but without the inherent problems associated with equivalent linear approaches.

The method of characteristics is a very efficient method of computing true nonlinear response of soils to earthquake excitation. The problem of a vertically propagating, horizontally polarized shear waves traveling through any number and depth of soil layers is solved in seconds. Numerical damping due to interpolations are reduced to negligible amounts by interpolation in time, as opposed to space, and energy budgets can be tracked and evaluated. Furthermore, stress-strain behavior is evaluated independently from the constitutive model, allowing the operator to verify if the response analysis makes sense.

Method of Characteristics

Most earthquake analysis programs presume a depth of analysis to approximately 100 ft. This assumption is valid for many earthquake-prone areas. However, in and around Charleston, South Carolina, as well as the central U.S. this assumption is incorrect. Soil deposits in these

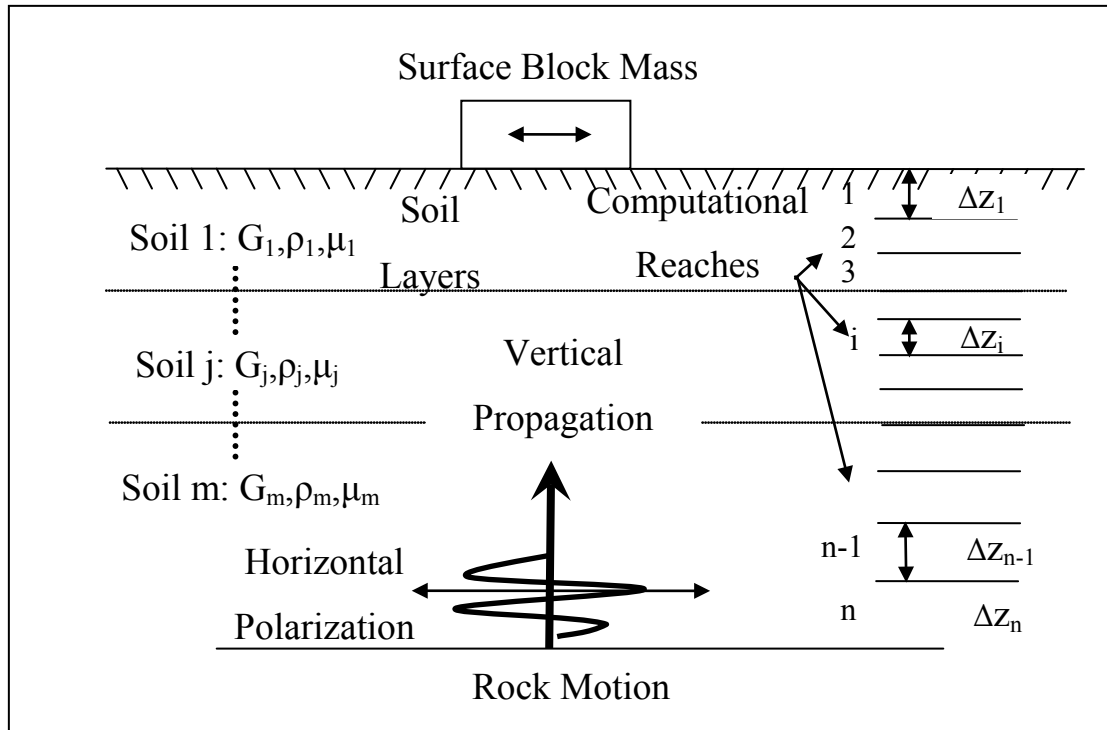


Figure 6-1. Propagating Shear Wave, Soil Layers, Computational Reaches, Surface Mass

areas can be detected to depths over 280 m (Bybell et al. 1998, Hashhash and Park, 2001, Andrus et al, 2006). Such conditions require a robust analysis tool for evaluating earthquake wave propagation to the surface. The method of characteristics has been applied to one-dimensional shear wave propagation through layered soil with non-linear stress-strain properties (Streeter et al. 1974). It has undergone refinements (Wiley and Henke, 1995; Papadakis, 1981) The major advantage of the method is its ability to faithfully model the non-linear, hysteretic, stress-strain behavior of soil when subjected to high levels of acceleration. In the next sections, a brief discussion of governing equations is first presented, followed by methods of numerical interpolation, energy accounting, and finally, application to a deep soil deposit

Governing Equations

An excellent presentation of the derivation of the method has been presented, and often cited, in the literature (Streeter et al. 1974).. A one-dimensional, horizontally-polarized, vertically-propagating shear wave (Fig. 6-2) can be represented by the following equation:

$$\frac{\partial \tau}{\partial z} - \rho \frac{\partial^2 u}{\partial t^2} = \frac{\partial \tau}{\partial z} - \rho \frac{\partial V}{\partial t} = 0 \quad \text{Eq. 6-1}$$

Where ρ = mass density of soil = γ_{wet}/g
 τ = shearing stress
 z = depth
 u = displacement
 V = velocity
 t = time

This is nothing more than the wave equation cast for horizontally polarized, vertically

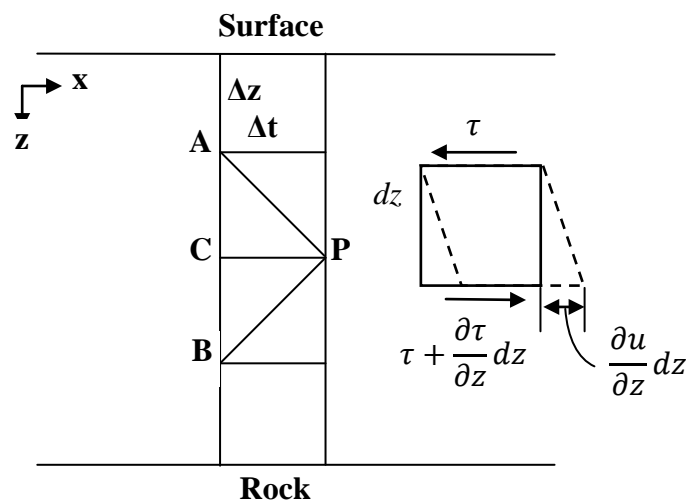


Figure 6-2. Assumptions and configuration for Method of Characteristics (Streeter et al,1974)

propagating shear waves. The dynamic stress-strain relationship for a non-linear viscoelastic material can be expressed by

$$\tau = G(\gamma)\gamma + \mu \frac{\partial \gamma}{\partial t} = G \frac{\partial u}{\partial z} + \mu \frac{\partial^2 u}{\partial z \partial t} \quad \text{Eq. 6-2}$$

where μ = coefficient of viscosity
 $G(\gamma)$ = shear modulus which is a function of strain

If equation 6-2 is differentiated with respect to z , and equation 6-11 is substituted, the equations used by many authors to describe 1-D shear wave propagation is achieved. If Eq. 6-2 is differentiated with respect to t , it can be shown in terms of the particle velocities:

$$\frac{\partial \tau}{\partial t} = G(\gamma) \frac{\partial^2 u}{\partial z \partial t} + \mu \frac{\partial^3 u}{\partial z \partial t^2} = G(\lambda) \frac{\partial V}{\partial z} + \mu \frac{\partial^2 V}{\partial z \partial t} \quad \text{Eq. 6-3}$$

When cast in this formulation, shear modulus is the *tangent* shear modulus because we will be performing an incremental time-stepping analysis.

$$G(\gamma) = \frac{\partial \tau}{\partial \gamma} \quad \text{Eq. 6-4}$$

The second term in equation 3 represents viscous damping. While it is useful when comparing analyses with other software, the hysteresis generated by the stress-strain formulation does an excellent job representing energy dissipation and more-closely models a soil behavior. Nonetheless if the viscous damping term is desired, a good finite difference approximation can be made by

$$\mu \frac{\partial^2 V}{\partial z \partial t} = \mu \left[\frac{\frac{\partial V}{\partial z} - \left(\frac{\partial V}{\partial z} \right)_C}{\Delta t} \right] \quad \text{Eq. 6-5}$$

Where subscript C represents the value determined at point C on the z-t diagram. Equations 6-3 and 6-5 can be combined to give.

$$\frac{\partial \tau}{\partial t} - \left(G(\gamma) + \frac{\mu}{\Delta t} \right) \frac{\partial V}{\partial z} + \frac{\mu}{\Delta t} \left(\frac{\partial V}{\partial z} \right)_C = 0 \quad \text{Eq. 6-6}$$

Equations 6-3 and 6-6 are now transformed into four ordinary differential equations by the method of characteristics. Using the unknown multiplier method, θ is multiplied by equation 6-3 then added to 6-6 to yield

$$\left(\theta \frac{\partial \tau}{\partial z} + \frac{\partial \tau}{\partial t} \right) - \theta \rho \left[\frac{\partial V}{\partial z} \left(G(\gamma) + \frac{\mu}{\Delta t} \right) \frac{1}{\theta \rho} + \frac{\partial V}{\partial t} \right] + \frac{\mu}{\Delta t} \left(\frac{\partial V}{\partial z} \right)_C = 0 \quad \text{Eq. 6-7}$$

The terms in equation 7 have been collected to represent total derivatives, that is

$$\frac{d}{dt} = \frac{dz}{dt} \left(\frac{\partial}{\partial z} \right) + \left(\frac{\partial}{\partial t} \right) \quad \text{Eq. 6-8}$$

if

$$\frac{dz}{dt} = \theta = \frac{1}{\theta \rho} \left(G(\gamma) + \frac{\mu}{\Delta t} \right) \quad \text{Eq. 6-9}$$

Equation 6-9 can be solved for θ to give

$$\theta = \pm \sqrt{\frac{G(\gamma)}{\rho} + \frac{\mu}{\Delta t}} = \pm v_s(\gamma) \quad \text{Eq. 6-10}$$

This is the shear wave velocity of the soil which is dependent on shearing strain (γ). The fact that θ has two real distinct values indicates that equations 3 and 7 are hyperbolic partial differential equations. The equations may be designated C^+ when the plus sign is used and C^- when the minus sign is used. This will yield two sets of (total) differential equations Along the C^+ characteristic

$$(C^+) \quad \frac{d\tau}{dt} - \rho v_s \frac{dV}{dt} + \frac{\mu}{\Delta t} \left(\frac{\partial V}{\partial z} \right)_C = 0 \text{ and } \frac{dz}{dt} = v_s \quad \text{Eq. 6-11}$$

Along the C^- characteristic:

$$(C^-) \quad \frac{d\tau}{dt} + \rho v_s \frac{dV}{dt} + \frac{\mu}{\Delta t} \left(\frac{\partial V}{\partial z} \right)_C = 0 \text{ and } \frac{dz}{dt} = -v_s \quad \text{Eq. 6-12}$$

Equation 6-11 is only valid when the shear wave is travelling downward (positive dz/dt) and equation 6-12 is only valid for upward moving waves. The C^+, C^- lines are interpreted physically as the phase velocity of the shear waves moving up and down the soil column. One may also view them as packets of shear stress/particle velocity information moving at the prescribed velocities. Solutions to these equations can be obtained after they are placed in finite difference form by integration. By choosing an appropriate time step (discussed later) Δt , the finite difference expressions for equations 6-11 and 6-12 become

$$\tau_P - \tau_A - \rho_{AP} v_{AP} (V_P - V_A) + \frac{\mu}{2\Delta z} (V_B - V_A) = 0 \quad \text{Eq. 6-13}$$

$$\tau_P - \tau_B + \rho_{BP} v_{BP} (V_P - V_B) + \frac{\mu}{2\Delta z} (V_B - V_A) = 0 \quad \text{Eq. 6-14}$$

Phase velocities and mass densities may be different for the reach from A to P and B to P, if P happens to reside on a soil layer boundary. If the stress and velocity are known at the previous time step (A, B) then stress and velocity are computed directly at the present time step (P). Additional terms for viscous damping (eg. Park and Hashhash, 2004) are also shown in their finite-difference formulation here.

Boundary Conditions

Earthquake wave input occurs in the form of a velocity vs. time history at the base of the column. Since velocity is prescribed at the base in the form of an earthquake time series, V_P is known and τ_P is determined from the C^+ equation. While no allowance is made for waves travelling back into deeper rock (Joyner and Chen, 1975 Hashash and Park, 2003) further refinements are being added and should become available by December 2010.

At the surface, one may assume a free-stress ($\tau_P = 0$) condition, requiring only the C^- characteristic equation, or more commonly, assume a block of material with weight w , (to represent a building or foundation) at the surface, whereby additional equations of motion are imposed.

$$V_P = \frac{\tau_B}{\rho v} + V_B \quad \text{if } \tau_P = 0 \quad \text{Eq. 6-15a}$$

or with a surface mass,

$$F = \frac{\tau_C + \tau_P}{2} = ma = m \frac{dV}{dt} = m \frac{V_P - V_C}{\Delta t} = \frac{w}{g} \frac{(V_P - V_C)}{\Delta t} \quad \text{Eq. 6-15b}$$

$$V_P = \frac{\tau_B + \tau_C + \frac{2 w V_C}{g \Delta t} + V_B \rho v_B}{\rho v_B + \frac{2 w}{g \Delta t}} \quad \text{Eq. 6-15c}$$

Either way, the surface node requires only the C^- characteristic from the soil below.

Nonlinear Behavior and Interpolations

Nonlinear stress-strain behavior complicates the numerical estimates in that the phase velocities slow down, requiring more time to reach the point of computation (point P). In order to satisfy the requirements for numerical stability, (i.e. the packets of information must arrive on time; the Cauchy criterion) some scheme of interpolation must be invoked. Interpolating in space between the previous points A, B, and C is easily accomplished at the cost of reduced accuracy manifested as “numerical damping”. Values with subscripts R_{space} , S_{space} will replace A and B respectively, in the equations. The precise location of interpolation is not known since one cannot compute reduced phase velocity until stress is known at the destination point. However, a

simple Newton's method can readily solve the problem. Better results are achieved by interpolating in time, rather than space, where R_{time} , S_{time} (figure 6-3) now replace A and B. An average phase velocity can then be computed by the same Newton's method and applied to the equations at point P.

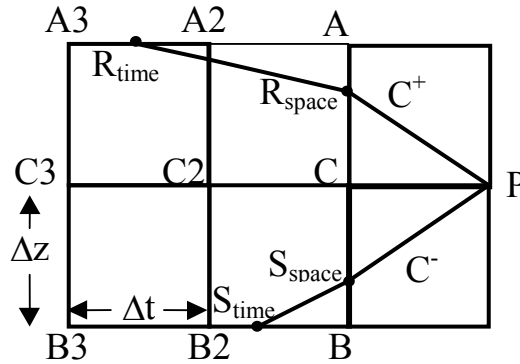


Figure 6-3. Computational Grid

Work-Energy Balance

In order to evaluate the degree of numerical damping that may take place, the computational sequence tracks work input at the base due to the earthquake, and energy stored and dissipated throughout the soil column. Work input is simply calculated as force times displacement at the base of the soil column. In finite difference form; average base stress for a time step times displacement for the same step.

$$dW = \int_t^{t+\Delta t} F \delta dt = \frac{\Delta t}{4} (V_{base\ t+\Delta t} + V_{base\ t}) (\tau_{base\ t+\Delta t} + \tau_{base\ t}) \quad \text{Eq. 6-16}$$

Energy through the column can take the form of stored elastic and dissipated hysteretic energy, and instantaneous kinetic energy. The stored and hysteretic energy is computed by

$$dSH = \int_V \int_{\gamma}^{\gamma+\Delta\gamma} \tau d\gamma d\bar{V} \quad \text{Eq. 6-17}$$

This is simply the area under the stress-strain curve over the volume of soil in question. In terms of computed stress and displacements, as well as discrete reaches, this works out to:

$$SH = \sum_{j=1}^m \frac{\Delta z_j}{4} (\tau_j + \tau_{j+1} + \tau_{j\ old} + \tau_{j+1\ old}) [(\delta_{j+1} - \delta_j) - (\delta_{j+1\ old} - \delta_{j\ old})] \quad \text{Eq. 6-18}$$

For nonlinear behavior, the unloading curve is below its loading counterpart and the hysteretic component is never recovered (but still accounted for). Kinetic energy is computed as the instantaneous value over the soil column at the end of the time step. For a single reach,

$$dKE = \frac{1}{2} \rho \Delta z \left(\frac{V_j + V_{j+1}}{2} \right)^2 \quad \text{Eq. 6-19}$$

Energy and work can be compared as a ratio of stored and kinetic energy divided by work input. An energy/work ratio can be tracked during computation to determine the effect, if any, of numerical damping. An energy ratio value of 1.0 indicates no numerical damping while less than 1.0 indicates some damping has taken place.

Stress Reversals and Forecasting

The numerical method is readily modified to deal with stress reversals using the extended Masing criteria. While the criteria are easily written, the algorithm to apply the criteria is less obvious. One outcome of the algorithm and the use of values from previous time steps is the “loss” of information immediately after the turnaround points (τ_i, γ_i) resulting in stress-strain curves that do not turn around correctly (Fig 2) (Ray, 2002).

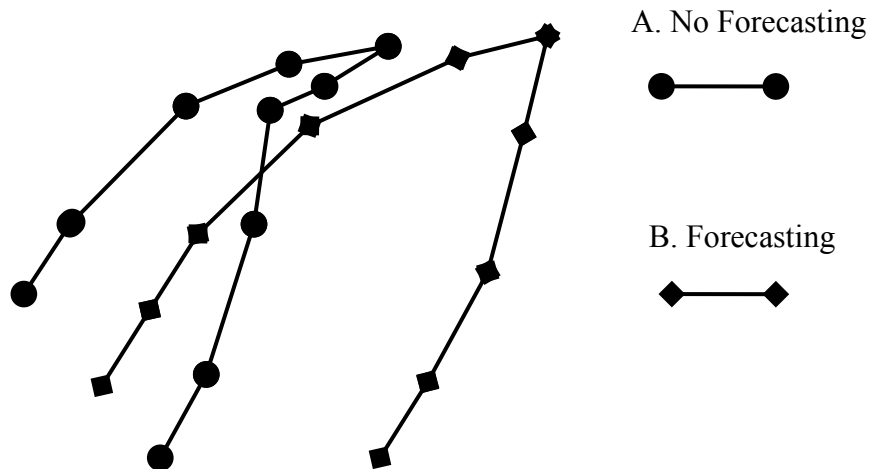


Figure 6-6. Stress-strain loops illustrating turnaround point recovery without (A) and with (B) forecasting

The phase velocity is not properly updated since the existence of a turnaround isn't known until all computations are complete for that time step. The only way to update the analysis properly is to go back in time one step and use the new (anticipated) phase velocity to re-compute values of

velocity (hence displacement and strain) and stress. This procedure works well in the analysis, even without a reversal, since it more accurately represents conditions in the soil over the last time step. Consequently the entire solution algorithm steps forward to estimate the phase velocity, then applies the new phase velocity to the same calculation step again.

Stress-Strain Model

The Ramberg-Osgood model is a convenient numerical representation of shearing stress vs. shearing strain. It is readily made dimensionless and can be scaled to field generated values of shear modulus. The stress strain equation is normally written

$$\gamma = \frac{\tau}{G_o} \left(1 + \alpha \left| \frac{\tau}{C_1 \tau_m} \right|^{R-1} \right) \quad \text{Eq. 6-20}$$

where γ =shearing strain; τ =shearing stress; G_o =maximum (low strain amplitude) shear modulus; α, C_1, R =curve-fitting constants. Stress reversals are computed by the same equation with the substitutions

$$\frac{\gamma - \gamma_i}{2} \text{ and } \frac{\tau - \tau_i}{2} \quad \text{for } \gamma \text{ and } \tau \quad \text{Eq. 6-21}$$

where γ_i, τ_i are values at a reversal point. For computing phase velocity, a value of tangent modulus is required. This is computed by the following equations.

$$v_s = \sqrt{\frac{G_{tan}}{\rho}} \quad G_{tan} = \frac{G_o}{\left(1 + \alpha R \left| \frac{\tau}{C_1 \tau_{max}} \right|^{R-1} \right)} \quad (4a,b) \quad \text{Eq. 6-22}$$

Note that the equations, as cast, render direct calculation of v_s as a function of strain impossible. In order to circumvent this problem, and make the code more generally applicable, a table look-up method is used instead of direct calculation. Prior to running the time sequence, values of γ and G_{tan} are computed for common values of τ/τ_{max} and are stored in an array. In this study, 128 values were computed. During the time sequence, values of strain are known, and G_{tan} is determined by binary search. Each lookup requires 7 comparisons and a final linear interpolation. Such a method can be applied to any soil model with any degree of precision (eg. 256, 512 values). Nonlinear stress-strain models can be represented by any relationship the user wishes (eg. Assimaki et.al., 2000; EPRI, 1993).

Computation of Stress and Strain

Solutions to equations 6-13 and 6-14 lead to values of shearing stress, τ , and particle velocity V , at every reach point. Values for displacement are computed by integration of velocity over time at every reach point. For a specific soil interval between two reach points, shearing strain is computed as the difference in displacements above and below, divided by the interval length. Shearing stress in the interval is computed as the average stress at points above and below. The only computational tie between stress and strain is through calculation of phase velocity (via non-linear models such as Ramberg-Osgood) and its application into equation 6-13 and 6-14. Therefore, if stress strain curves generated from the above calculations along each layer accurately represent nonlinear behavior of the soil, the model is a good one. This is *very different* from applying a stress-strain model to an already-computed stress-time history and observing strain behavior.

Comparison with Equivalent Linear Analysis

In order to show comparison to a familiar profile, WinMoc was used to analyze the profile first given by Schnabel et al (1972) with an acceleration history from the SHAKE (EduPro Civil Systems, 1999) program: Treasure Island, Loma Prieta. The soil models required special handling since the WinMoc program uses a non-dimensional approach to non-linear stress-strain models. However, the parameters chosen matched the Seed and Idriss (1970) sand curves as well as the Sun et al (1988) clay curves. The WinMoc analysis used 50 computational reaches to discretize the profile. The earthquake record was identical to the record used in EduShake. Plots of surface velocity vs. time are shown in figure 6-5. Note that the response is given for the time interval from 10 to 20 seconds in order to increase visibility. The responses are typical for the types of approaches used: the time-stepping approach can carry along high frequencies even at high strains while the equivalent linear approach cannot. The high frequencies can be better imagined when one looks at the impact of turnarounds in the stress-strain behavior during high-amplitude loading. Figure 6-6 shows the stress-strain history for the same profile and event at depths of 40 and 44 m. The stress reversals show a sharp response and stiff behavior which is carried through the rest of the profile. Notice also the Masing behavior (Ray and Woods, 1987) throughout the event. Since these are response stresses and strains, the fidelity of the model is excellent with respect to Masing behavior.

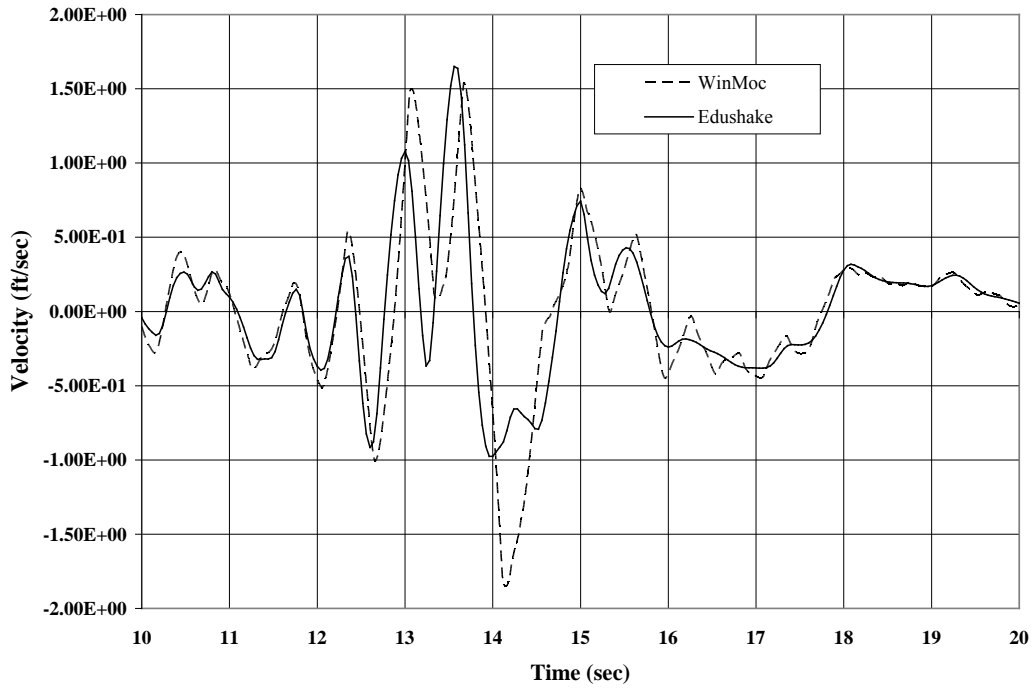


Figure 6-5. Surface Velocity For WinMoc and EduShake

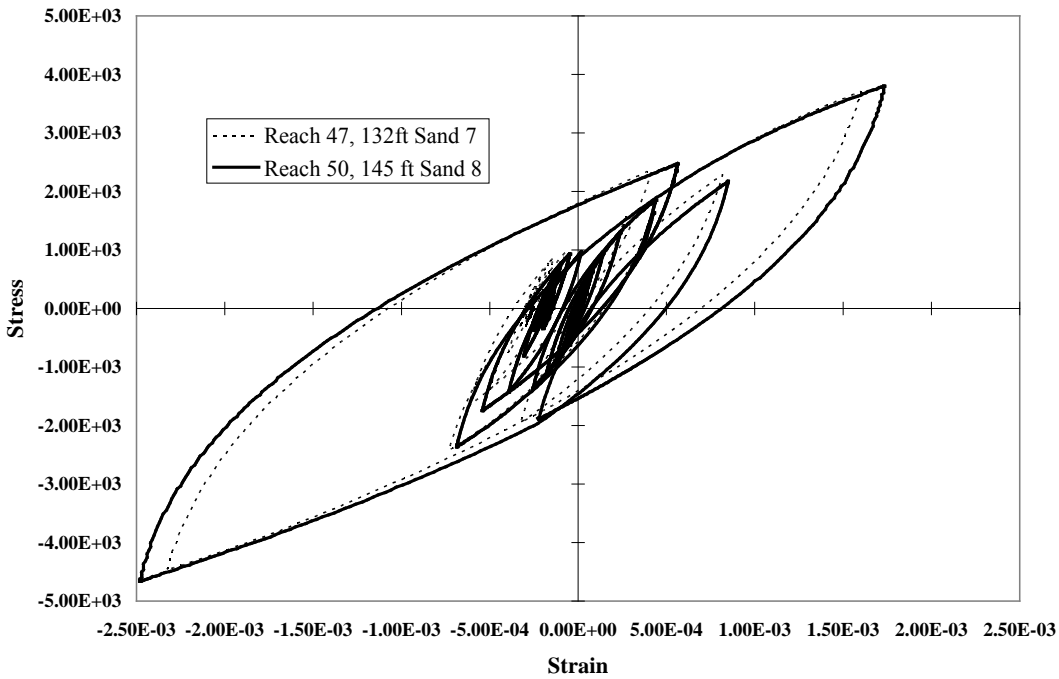


Figure 6-6. Stress-Strain Response in Deep Sands

Energy Results

The ability to track energy is shown in figure 6-7 where work at the base, elastic and hysteretic energy, and kinetic energy are tracked during the entire event. Energy ratio is plotted on the secondary axis and shows a value between 1.00 and 0.992 for the duration of shaking. Virtually no numerical damping is present.

Implications for Liquefaction Evaluation

Since the stress-strain behavior of all individual reaches are tracked for the entire event, approaches to liquefaction evaluation using damage parameters or pore-pressure generation (Bonilla et al, 2005) by exceeding threshold strain levels becomes simply a matter of a subroutine within the analysis. Tracking maximum stresses, maximum strains, number of major cycles of loading are also easily implemented. This program has been used to develop profiles of maximum shear stress, and maximum shear strain in order to compare to liquefaction resistance profiles.

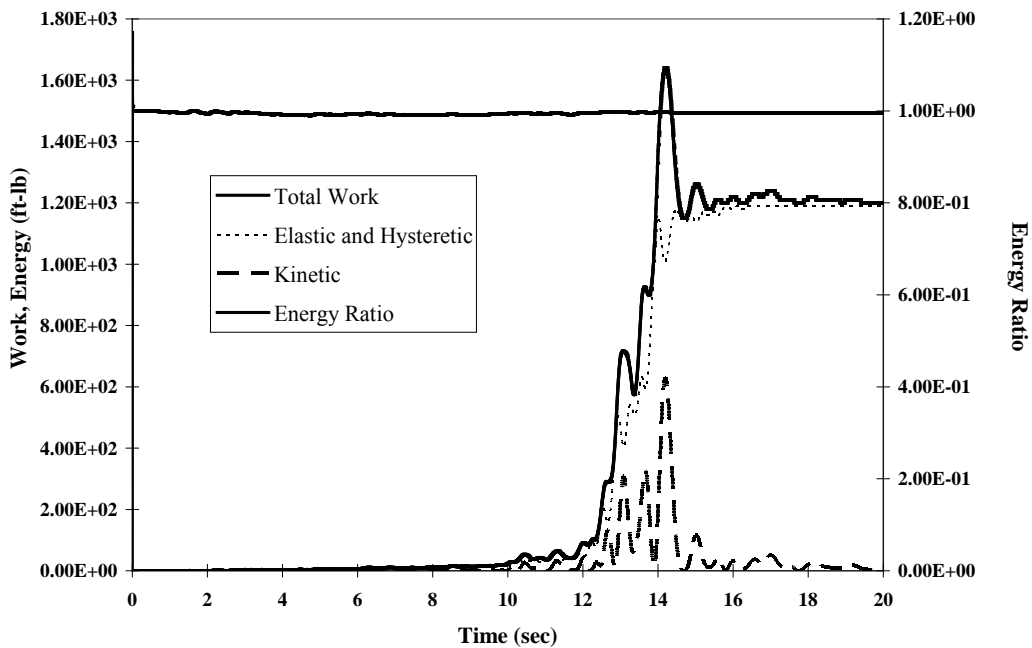


Figure 6-7. Work, Energy, Energy Ratio vs. Time

Effect of Cooper Marl Modulus Reduction

In order to better assess the importance of the difference in behavior noted in Chapter 5. Two computer runs were performed. The first used a profile with sand in the upper 140m while the other used the Cooper Marl curves shown earlier. Results of the analysis are shown below as surface particle velocity vs. time. It is readily apparent that the marl softens faster under high-

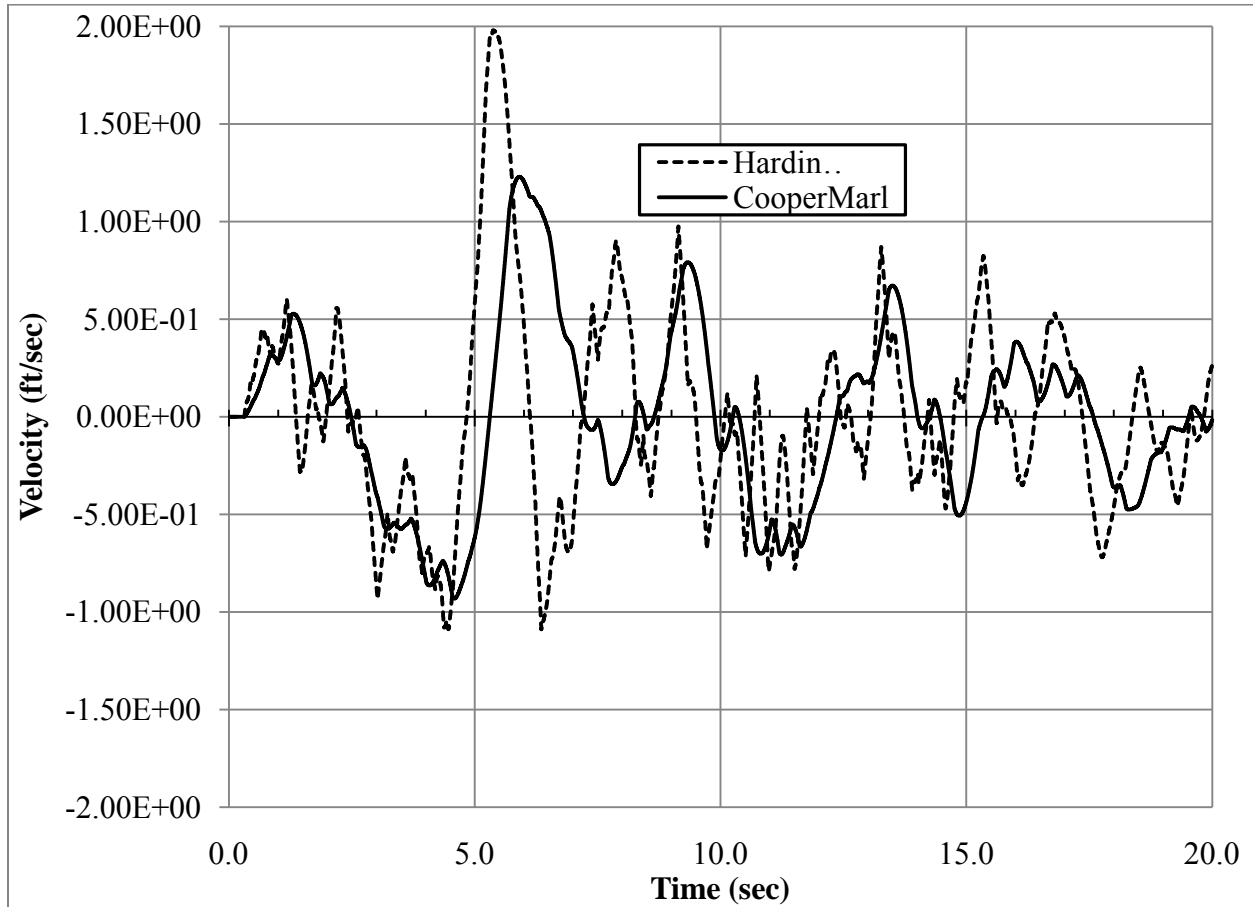


Figure 6-8 Surface velocity vs. time for identical events, H-D sand and Cooper Marl.

amplitude motion. The resulting response shows much lower frequency response. This would also imply reduced acceleration (and inertial forces) and increased lateral drift. As Boore (2006) stated “Soil matters”. Not only does it matter, but the shift in the modulus reduction curve matters as well.

Chapter 7 Analysis of Specimen Behavior in Torsional Shear

Introduction

In order to better comprehend the true behavior of a torsional shear test (and resonant column test), we thought it would be a good idea to model the specimen with a 3D finite element program. We chose the MIDAS GTS finite element program because it was relatively inexpensive and easy to use. It has three dimensional capabilities and can treat nonlinear soil behavior with a variety of models. The finite element model we used is shown below in figure 7-1.. It consists of a hollow cylinder, divided into 16 separate material sections. The top and base sections represent the top and base rings of the device. The other 14 sections are different volumes of the specimen. Each section can have its own soil properties. To simulate a small inclusion or void, the soil properties in a small section are set to be very stiff (like rock) or very soft (like a void). Additional sections can be altered to simulate larger voids or inclusions. The entire model has about 45,000 elements and perhaps 55,000 nodes.

The top of the specimen is loaded with a prescribed rotation. To facilitate this, a beam element (with very stiff modulus and moment of inertia) is attached to the top ring. The center node of the beam, situated on the center line of the specimen, is then applied with a given rotation. The rotation is applied in steps and stresses and deflections for each load step is recorded. The operator can then view the results graphically or numerically in a table. The time for an elastic analysis with ten load steps is about 5 minutes on a new, multi-processor desktop.

Figure 7.2 shows the displacement in the y-direction for the applied torsion. One unfortunate drawback is that cylindrical displacements are not given, they must be computed “by hand” by copying tabular data to a spreadsheet and then performing the calculation. Graphical representation of tangential or radial displacements is not possible. However, solid stresses can be easily displayed and studied. The analysis of the torsional specimen did not move beyond fundamental linear elastic approaches. This is on the “to do” list for continuing this study.

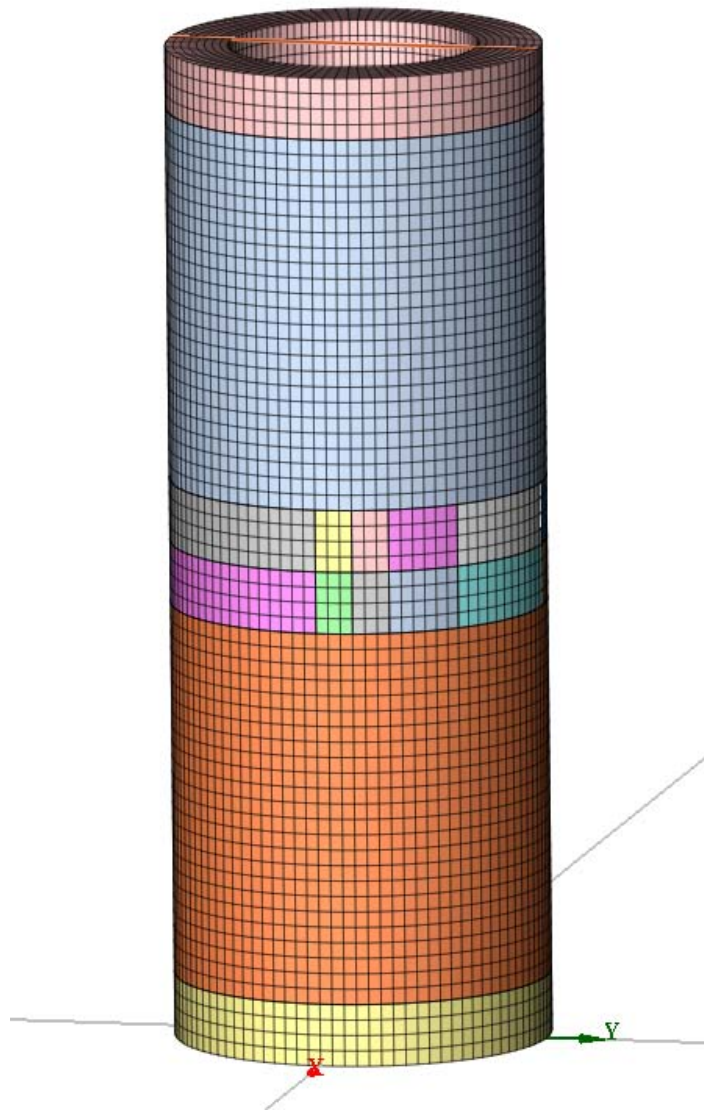


Figure 7.1 Finite element mesh of torsional specimen showing various sections

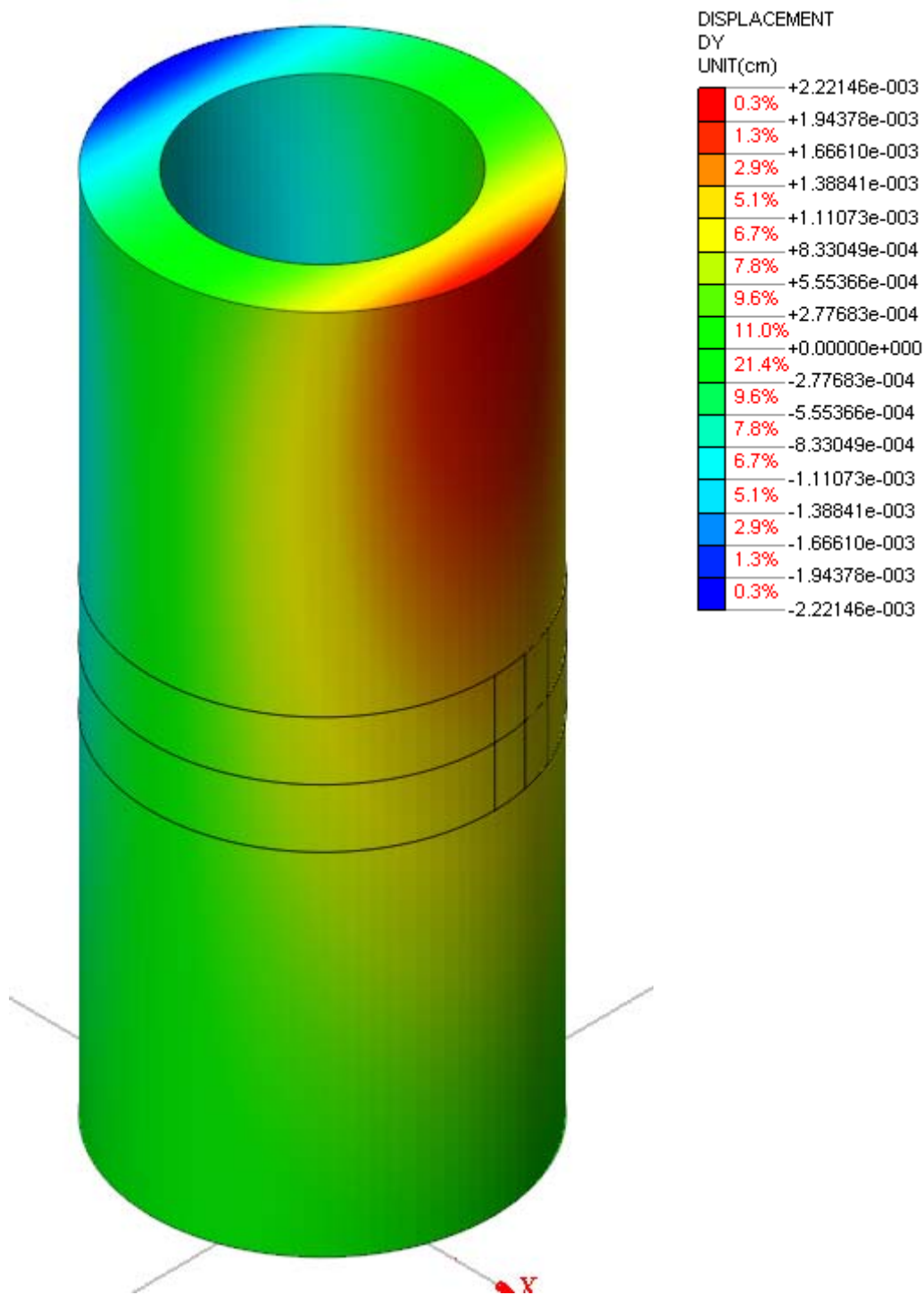


Figure 7-2. Typical displacement output

Chapter 8. Conclusions and Further Study

A resonant column torsional shear device was designed to test soils at high confining stresses. The design was based on known conditions around Charleston South Carolina. The confining vessel has been proven to provide isotropic confinement stresses up to 2600 kPa with the possibility of producing confining stresses to 5500 kPa. This represents sediment depths of over 800 m. Instrumentation has already been shown to work on low-confining stress (100-300 kPa) tests.

Results from low-confining stress tests indicate that Cooper Marl has a markedly different behavior in that it softens at much lower strain levels than typical silts or fine sands. This may be due to the high content of shell fragments present in the marl or other due to other factors yet to be determined.

Using the Ramberg-Osgood model and the Hardin-Drnevich definition for dimensionless strain allowed the data to be accurately represented numerically for use in response analysis programs. Using other dimensionless strain assumptions proved less fruitful.

The method of characteristics faithfully reproduces nonlinear soil response throughout a strong motion event. Stress-strain behavior is easily followed and irregular loading histories present no problems to the calculations. An energy budget method is used to determine the impact of interpolation and numerical damping. For all the cases studied, the impact of numerical damping was negligible.

A three-dimensional finite element model was developed for studying the behavior of a soil specimen when it undergoes testing in the RC-TOSS system. Effects of non-uniform soil properties, hard or soft inclusions, and other imperfections can be studied. Unbalanced rotational inertial, misaligned torque application, and other loading effects can be studied as well.

Areas for Further Study

The immediate area for further study is to perform high-confining stress tests in the device now that is completed. Effects of confining stress and duration of confinement on Cooper Marl will first be examined. Modulus reduction with increasing strain will be quantified over a large range of high confinement. The driving capacity of the device is not known since it has not been reached. Further improvement of the magnet components should triple its torque capacity.

The MOC program is being altered to allow for energy passage to underlying basement structure. Other soil models are being tested so that they may be more easily incorporated into the analysis. The effects of cyclic hardening and softening are also being incorporated. As a future design goal, the use of a pore pressure generation model, based on accumulated strain or dissipated energy will be included.

The three dimensional finite element study will require more analysis and numerical experiments on soil models that are presently the de-facto models in geotechnical software.

References

- Andrus, R.D., Fairbanks, C.D., Zhang, J., Camp, W.M., Casey, T.J., Cleary, T.J., and Wright, W.B., (2006) "Shear-Wave Velocity and Seismic Response of Near-Surface Sediments in Charleston, South Carolina," *Bulletin of the Seismological Society of America*, Vol. 96, No. 5, pp. 1897-1914.
- Assimaki, D., Kausel, E., and Whittle, A (2000) "Model for Dynamic Shear Modulus and Damping for Granular Soils," *Journal of the Geotechnical and Geoenvironmental Division, ASCE*, Vol. 126, No. 10, pp. 859-869.
- Bonilla, L.F., Archuleta, R.J, and Lavalle, D. (2005) "Hysteretic and Dilatant Behavior of Cohesionless Soils and Their Effects on Nonlinear Site Response: Field Data Observations and Modeling", *Bulletin Seismological Society of America*, Vol. 95, No. 6, pp. 2373-2395
- Boore, D.M.(2004) "Can Site Response Be Predicted?" *Journal of Earthquake Engineering*, Vol. 8, Special Issue 1 (2004) 1–41
- Bybell, L.M., Conlon, K.J., Edwards, L.E., Frederiksen, N.O., Gohn, G.S., & Self-Trail, J.M. (1998) Biostratigraphy and physical stratigraphy of the USGS-Cannon Park core (CHN-800), Charleston County, South Carolina. *U.S. Geological Survey Open-file Report 98-246*. Reston, Virginia.
- Chapman, M.C., Martin, J.R., Olgun, C.G. and Beale, J.N. (2006) "Site Response Models of Charleston, South Carolina and Vicinity Developed from Shallow Geotechnical Investigations" *Bull. Seismological. Society of America*, Vol. 96, No. 2, pp. 467-489.
- Chapman, M.C., Talwani, P, and Cannon, R.C. (2003) "Ground motion attenuation in the Atlantic Coastal Plain near Charleston, South Carolina," *Bull. Seismological. Society of America*, Vol. 93, pp. 998-1011.
- Drnevich, V. P., Hardin, B. O. and Shippy D.J. (1978) "Modulus and Damping of Soils by the Resonant Column Method," *Dynamic Geotechnical Testing, ASTM STP 654*, American Society for Testing and Materials, 1978, pp91-125.
- EPRI. Guidelines for determining design basis ground motions. EPRI TR-102293, Palo Alto, CA, 1993.
- EduPro Civil Systems (1999) EduShake Version 1.10, June.
- Finn W.D.L (2000)State-of-the-art of geotechnical earthquake engineering practice," *Soil Dynamics and Earthquake Engineering* 20 pp 1-17
- Hashash, Y.M.A., (2007) DEEPSOIL website, <http://cee-zzvy.cee.uiuc.edu/Website/Deepsoil/>
- Hashash, Y. M. A., and Park, D. (2001). "Non-linear one-dimensional seismic ground motion propagation in the Mississippi embayment." *Engineering Geology*, 62(1-3), 185-206.
- Hashash, Y. M. A., and Park, D. (2002). "Viscous damping formulation and high frequency motion propagation in nonlinear site response analysis." *Soil Dynamics and Earthquake Engineering*, 22(7), pp. 611-624.

- Hardin, B. O. and Drnevich, V. P., (1972a) "Shear Modulus and Damping in Soils: Measurements and Parameter Effects," *ASCE Journal of Soil Mechanics and Foundations Division*, v.98, No. SM 6, June 1972, 603-624.
- Hardin, B. O. and Drnevich, V. P., (1972b) "Shear Modulus and Damping in Soils: Design Equations and Curves," *ASCE Journal of Soil Mechanics and Foundations Division*, v. 98, No. SM 7, July 1972, 667-692
- Idriss, I.M. (1999) "Lecture on Recent Advances in Liquefaction" Geo-Charlotte.
- Jardine, R. J., Potts, D. M., Fourie, A. B. & Burland, J. B. (1986) "Studies of the influence of non-linear stress-strain characteristics in soil-structure interaction" *Geotechnique* 36, No.3, 377-396
- Kramer (1996) *Geotechnical Earthquake Engineering*, Prentice-Hall. ISBN 0-13-374943-6, 653 pp.
- Laird, J.P. and Stokoe, K.H. (1993) "Dynamic properties of remolded and undisturbed soil samples tested at high confining pressure," Geotechnical Engineering Report, GR93-6, Electrical Power Research Institute, Palo Alto CA.
- Martin, J.R. and Clough, G.W. (1990) "Implications from a Geotechnical Investigation of Liquefaction Phenomena Associated with Seismic Events in the Charleston, SC Area" Final report to USGS Research Contract 14-08-001-G-1348, November, 414 pp.
- Mohanan, N., Fairbanks, C.D., Andrus, R.D., Camp, W.M., Cleary, T.J., Casey, T.J., and Wright, W.B.(2006) "Electronic Files of Shear Wave Velocity and Cone Penetration Test Measurements from the Greater Charleston Area, South Carolina," Data Report to USGS, Award 05HQGR0037, 24 pp.
- Park, D. and Hashash, Y.M.A., (2005) "Evaluation of seismic site factors in the Mississippi Embayment. I. Estimation of dynamic properties," *Soil Dynamics and Earthquake Engineering*, No. 25, pp. 133-144.
- Park, D., and Hashash, Y. M. A. (2004). "Soil damping formulation in nonlinear time domain site response analysis." *Journal of Earthquake Engineering*, 8(2), 249-274.
- Pradhan, T.B.S., Tatsuoka, F., and Horii, N.(1988) "Simple Shear Testing of Sand in Torsional Shear Apparatus," *Soils and Foundations*, Vol 28, No. 2 pp 95-112. Japanese Geotechnical Society
- Ramberg, Walter, and Osgood, William R. (1948?) "Description of Stress-Strain Curves by Three Parameters," Technical Note 902 to National Advisory Committee for Aeronautics (now NASA) 28 pp.
- Ray, R.P. (2002) "Modeling Earthquake Response in Deep Soil Deposits," *Numerical Models in Geomechanics* (NUMOG VIII), edited by Pande & Pietruszczak, Swets & Zeitlinger, The Netherlands, pages 667-71, ISBN 90 5809 359X
- Ray, R.P. and Woods R.D., (1987) "Modulus & Damping Due To Uniform and Variable Cyclic Loading," *Journal of the Geotechnical Engineering Division*, ASCE, Vol 114, No, 8, August, pp. 861-876.

- Ray, R.P. (1983). "Changes in Shear Modulus and Damping in Cohesionless Soil due to Repeated Loadings." Ph.D. dissertation, University of Michigan, Ann Arbor, MI., 417 pp.
- Richart, F.E. Jr. (1975) "Some Effects of Dynamic Soil Properties on Soil-Structure Interaction," *Journal of the Geotechnical Engineering Division*, Vol. 101, No. 12, December 1975, pp. 1193-1240
- Saada AS and Townsend FC "State of the Art: Laboratory Strength Testing of Soils," Laboratory Shear Strength of Soil, ASTM STP 740 American Society for Testing and Materials pp 7-77.
- Schnabel, P.B., Lysmer, J., and Seed, H.B. (1972). "SHAKE: A computer program for earthquake response analysis of horizontally layered sites," Report No. EERC 72-12, Earthquake Engineering Research Center, University of California, Berkeley, California
- Seed, H.B. and Idriss, I.M. (1970). "Soil moduli and damping factors for dynamic response analyses," Report No. EERC 70-10, Earthquake Engineering Research Center, University of California, Berkeley.
- Silva, W., Wong, I., Siegel, T. , Gregor, N., Darragh, R. and Lee, R, (2003) "Ground Motion and Liquefaction Simulation of the 1886 Charleston, South Carolina, Earthquake," Bulletin of the Seismological Society of America, Vol. 93, No. 6, pp. 2717-2736, December.
- Stewart, J.P., Kwok, A.O-L., Hashahs, Y.M.A., Matasovic, N., Pyke, R., Wang, Z., and Yang, Z. (2008) "Benchmarking of Nonlinear Geotechnical Ground Response Analysis Procedures," PEER 2008/04, Pacific Earthquake Engineering Research Center, 205 pp.
- Streeter, V.L., Wylie, E.B., & Richart, F.E. 1974 "Soil motion computations by characteristics method". *Journal of the Geotechnical Engineering Division, ASCE* 100,(GT3): 247-263.
- .Sun, J.I., Golesorkhi, R., and Seed, H.B. (1988). "Dynamic moduli and damping ratios for cohesive soils," Report No. EERC-88/15, Earthquake Engineering Research Center, University of California, Berkeley..
- Tatsuoka,F., Iwasaki,T., Tokida,K. and Kon-no,M. (1981), "Cyclic undrained triaxial strength of sampled sand affected by confining pressure", *Soils and Foundations*, Vol.21, No.2, pp.115-120.
- Vucetic, M and Dobry, R (1991)"Effect of Soil Plasticity on Cyclic Response," *Journal of Geotechnical Engineering*, Vol. 117, No. 1, January 1991, pp. 89-107

Appendix A. Device Details

Pressure Vessel Design

The pressure vessel was designed to surround an RC-TOSS testing device and its attached transducers. The size of the vessel is 10-in nominal diameter by 24-in long. The part schedule is shown in figure A1, as produced by the fabricator. It is rated at 800 psi with the lowest temperature rating given to pressure vessels (300° F). Material is steel at the grades given in the drawing. The vessel rests on a pedestal with the lifting lug at the top and the blind flange at the base. The pedestal allows for complete access to the nuts and threaded rod to hold the vessel together. The blind flange has six ¼-20 holes tapped into it to accept a “transfer plate”. The transfer plate has holes drilled and tapped on one side to accept all the RC-TOSS supports as well as six holes for mounting to the blind flange. This will allow for easy modification if necessary since no further drilling of the blind flange is necessary; only modification of the transfer plate.

Pressure Vessel Feedthroughs

One of the most difficult aspects of this project was selecting the proper pressure feedthroughs. Most off-the shelf items were not certified to 800 psi or would not allow the necessary wiring to pass through. The feedthroughs used are shown in figures A2-A5. All were tested to about 800 psi. The most sensitive issues were with the SMA and Microdot feedthroughs. They were necessary for the measurement transducers and could not be altered without compromising the performance of the instruments. Several vendors were contacted and said they could deliver the feed throughs, however only on vendor finally delivered. From the time of initial design the time of delivery was over 9 months of weekly communication with technical and sales people. The feedthroughs and pressure transducers have been tested as an assembled unit in the lab to 400 psi.

Measurement Transducers

The measurement transducers consist of one accelerometer, two proximitors, two pressure transducers and one LVDT. Table A1 lists the instrumentation

Table A1. Instruments used in RC-TOSS device

Device	Make and model	Sensitivity	Manufactured by
Accelerometer	PCB 302-B03	299 mV/g	PCB Piezotronics
Proximitors (2)	KD-2440	~2.75 V/mm	Kaman Aerospace
LVDT	500 DC-EC	0.8 V/mm	Shaevitz Sensors
Differential Pressure	DP-15-58 (800 psi)	33 mV/V FS (10 V DC w/conditioner)	Validyne Engineering

All instruments had repeatable behavior better than 0.1% FS (1 in 1000). The proximitors were nonlinear while all the others had linear outputs. When matched with a good power supply and readouts they achieved these accuracies throughout the testing program. The instruments are shown in figures A-6 through A-9.

The accelerometer is used only for the resonant column test and proximitors are used only for TOSS. Both systems measure tangential movement which is then converted to torsional rotation, then shear strain. Since harmonic acceleration is related to displacement by

$$\delta = \frac{a}{\omega^2} \quad \text{Equation A1}$$

and resonant frequencies during a resonant column test are about $\omega = 300$ rad/sec, the accelerometer is ideally suited for measuring low strain ($< 10^{-4}\%$). Since soil softens as it is strained higher, the accelerometer can measure up to 0.1% easily as well. The major difficulty at this strain level is maintaining a stable resonance as the soil breaks down. Capturing a resonant frequency at very high strains becomes more and more problematical, however, modulus ratio reductions to $G/G_{\max} = 0.2$ are routinely possible. Eventually the specimen will break down or deform excessively so contact is made between magnets and coils.

The proximitors work best for TOSS testing where the loading is too slow for the accelerometer and hysteresis loops of stress and strain are desired. A torque transducer was not used; rather the coil current was calibrated against a steel rod to determine torque, and eventually shear stress. Since the proximitors exhibit nonlinear output with distance, each one had to be

acquired separately, converted then their deflections combined to determine drive head rotation and shear strain.

The LVDT measures vertical movement of the drive head. The iron core of the LVDT is attached via a wire and hook to the drive head. The other end is attached to an adjustable spring which counterbalances the drive head's weight, insuring isotropic stress conditions on the specimen. Vertical movement occurs during the initial cycles of loading in a high amplitude TOSS test. Vertical movement can also be recorded between each frequency stage of the resonant column test.

Data Acquisition

The data acquisition system was a National Instruments NI-PCI-6122 with a 37-pin output connector. The card will convert up to 16 channels (8 channels differential) to 16-bit accuracy. Additional sensitivity is achieved by changing the input range to the level appropriate to the instrumentation used. Accuracy and linearity far exceeded the capability of the instrumentation and the realistic expectations of the soil behavior. Conversion speed for a single channel is 250 kHz. For a TOSS this is more than enough speed to sample four or five channels of data. It also has D/A capability so that the TOSS device can be driven by arbitrary load/deflection histories as well as sinusoidal load or deflection history. The slightly smaller output connection was a cost consideration and had a more robust cable-connector system.

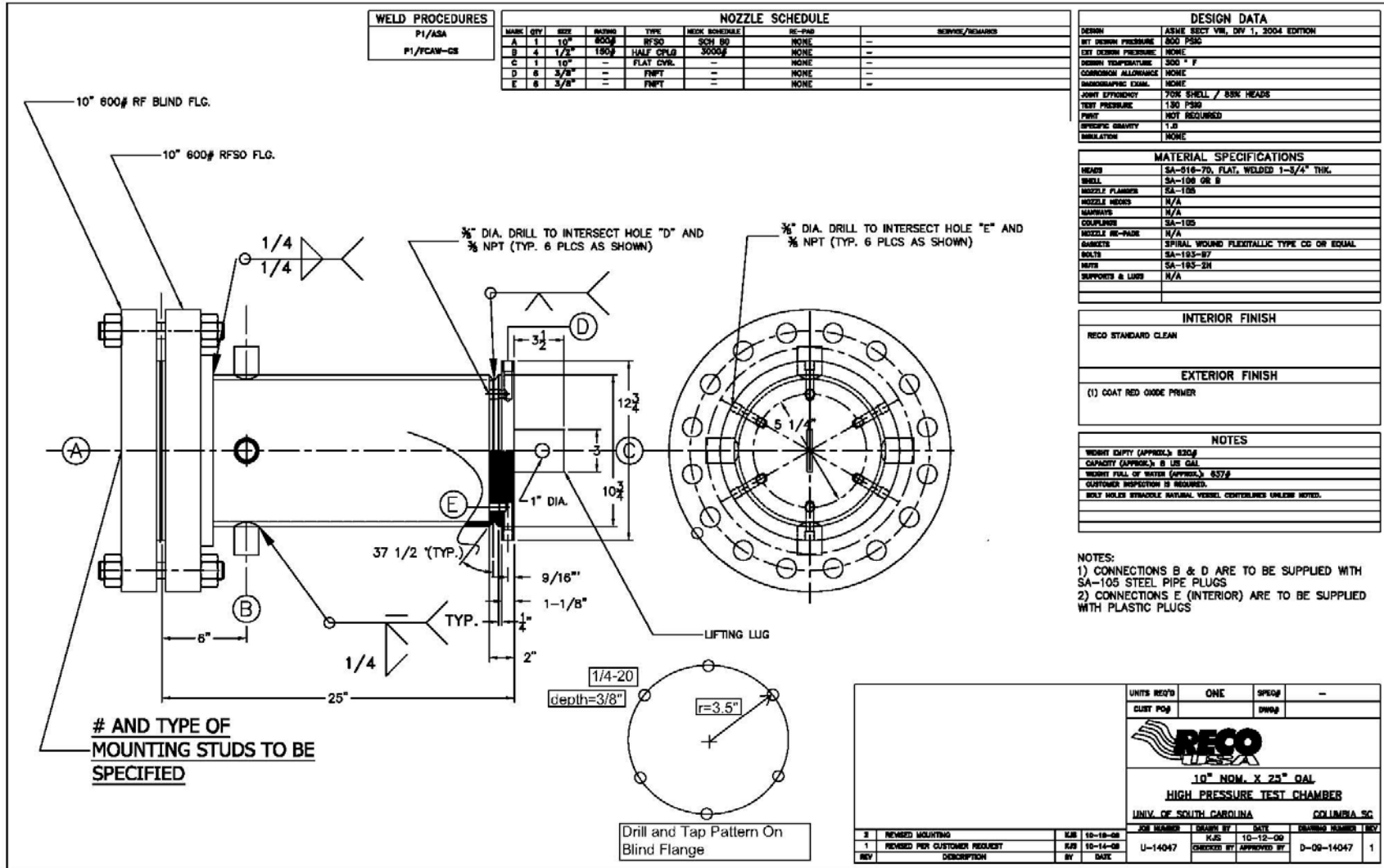


Figure A1. Schematic of pressure vessel, certified to 800 psi (5.5 MPa)

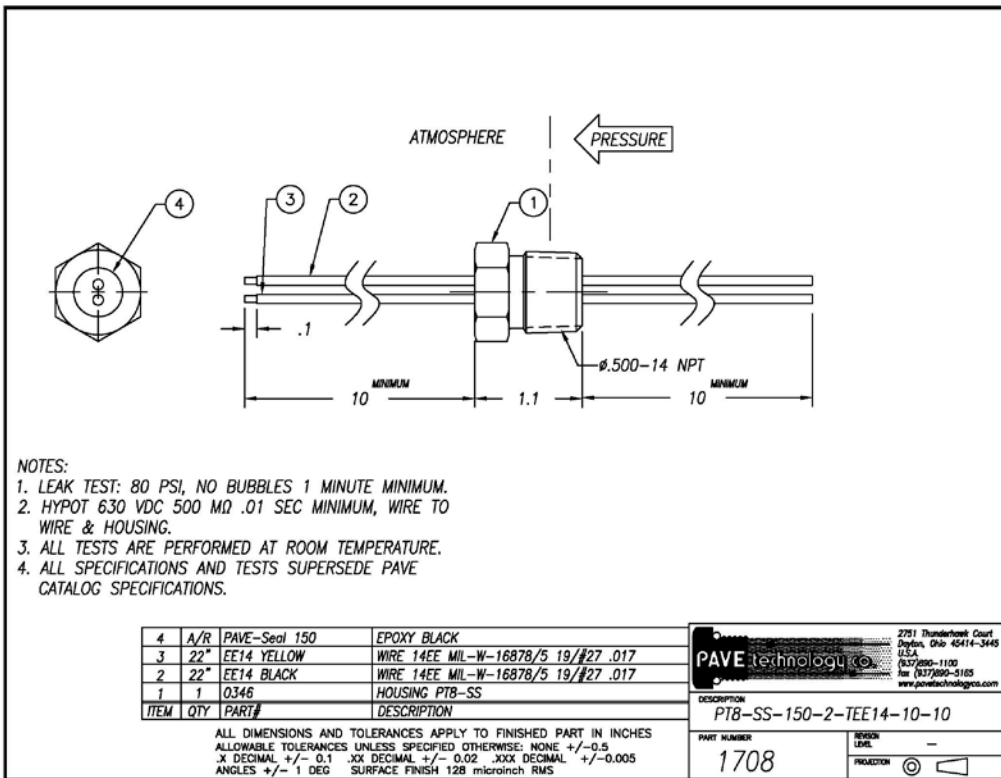


Figure A2. Two-wire power feedthrough for coil power.

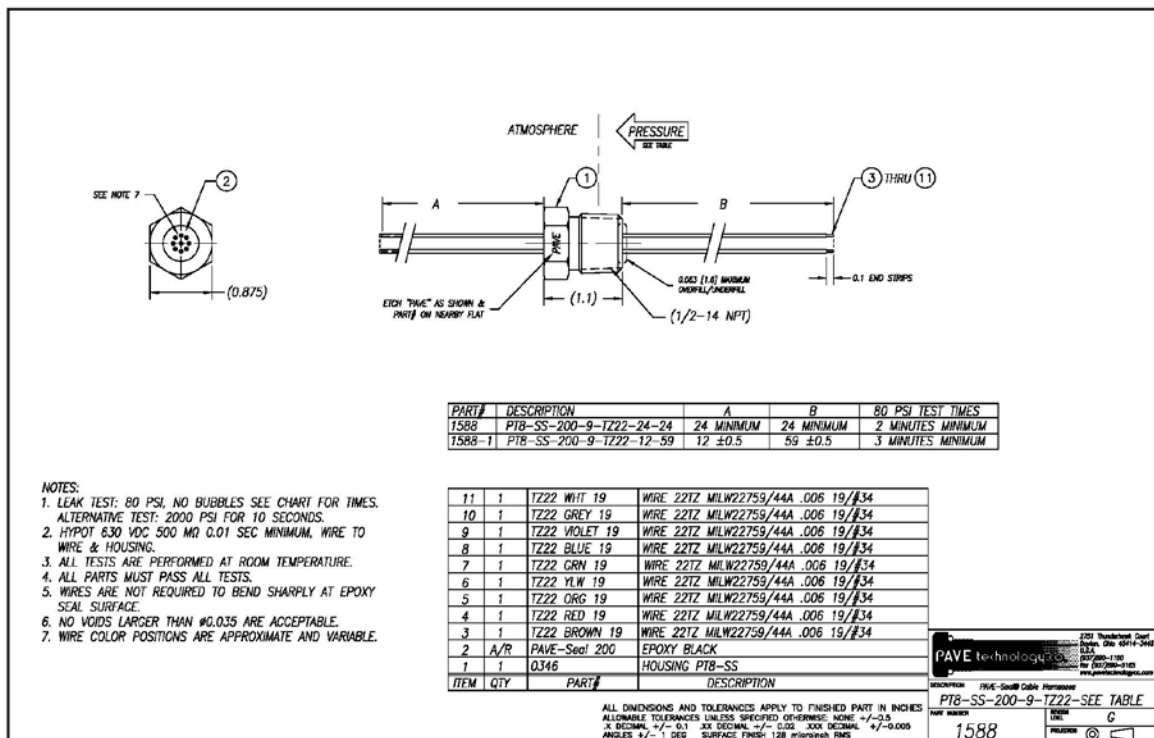


Figure A3. Six-wire feedthrough for LVDT and other instruments

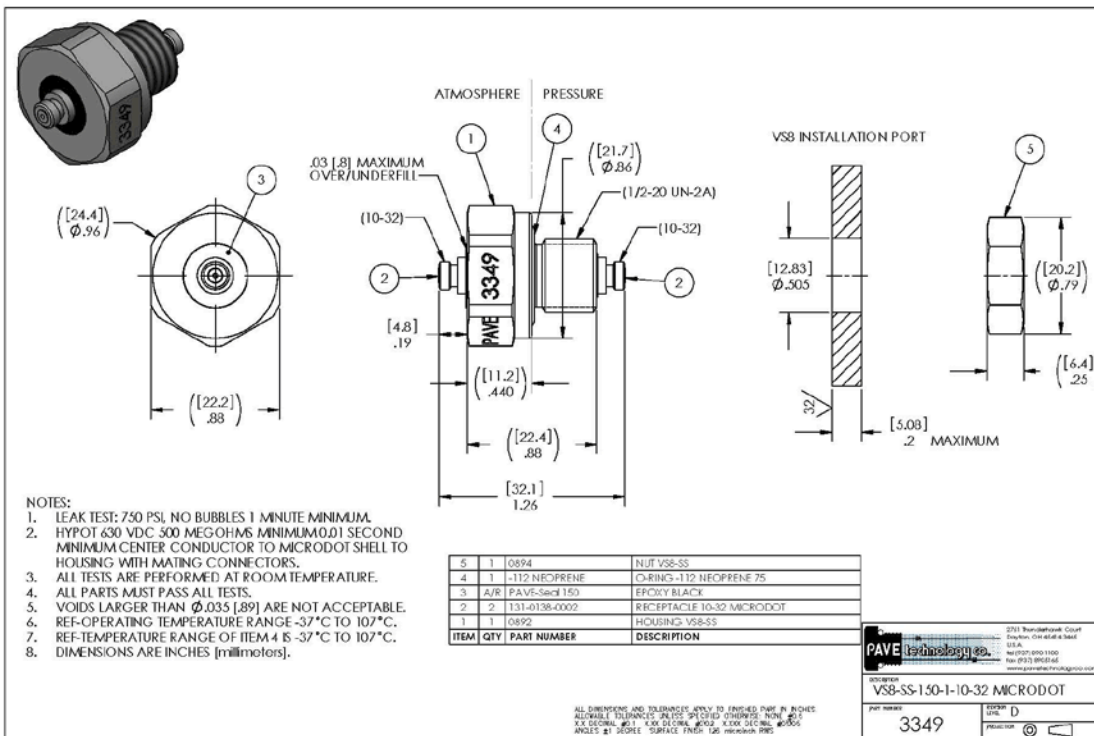


Figure A4. Microdot feedthrough for accelerometer cable.

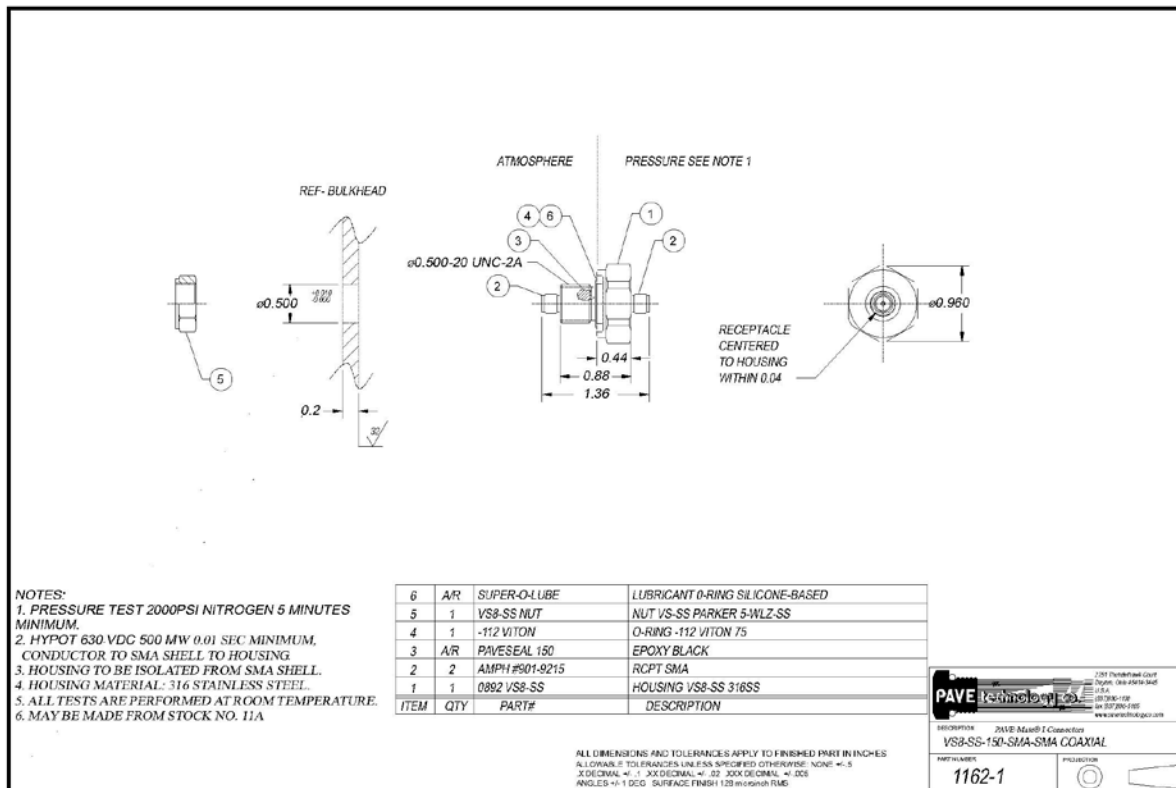
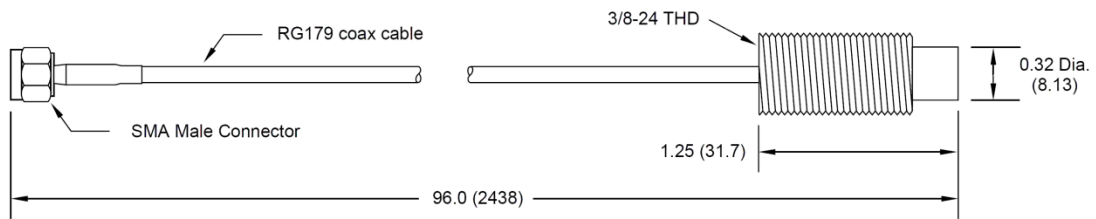


Figure A5. SMA feedthrough for proximator cables (I used two).

KD-2440 SENSORS

9C SENSOR



Dimensions shown are in inches (mm)

ORDERING INFORMATION

9C sensor	P/N 851166-008
Electronics only	P/N 854975-000

Figure A6. Proximitor sensor Kaman KD 2440.

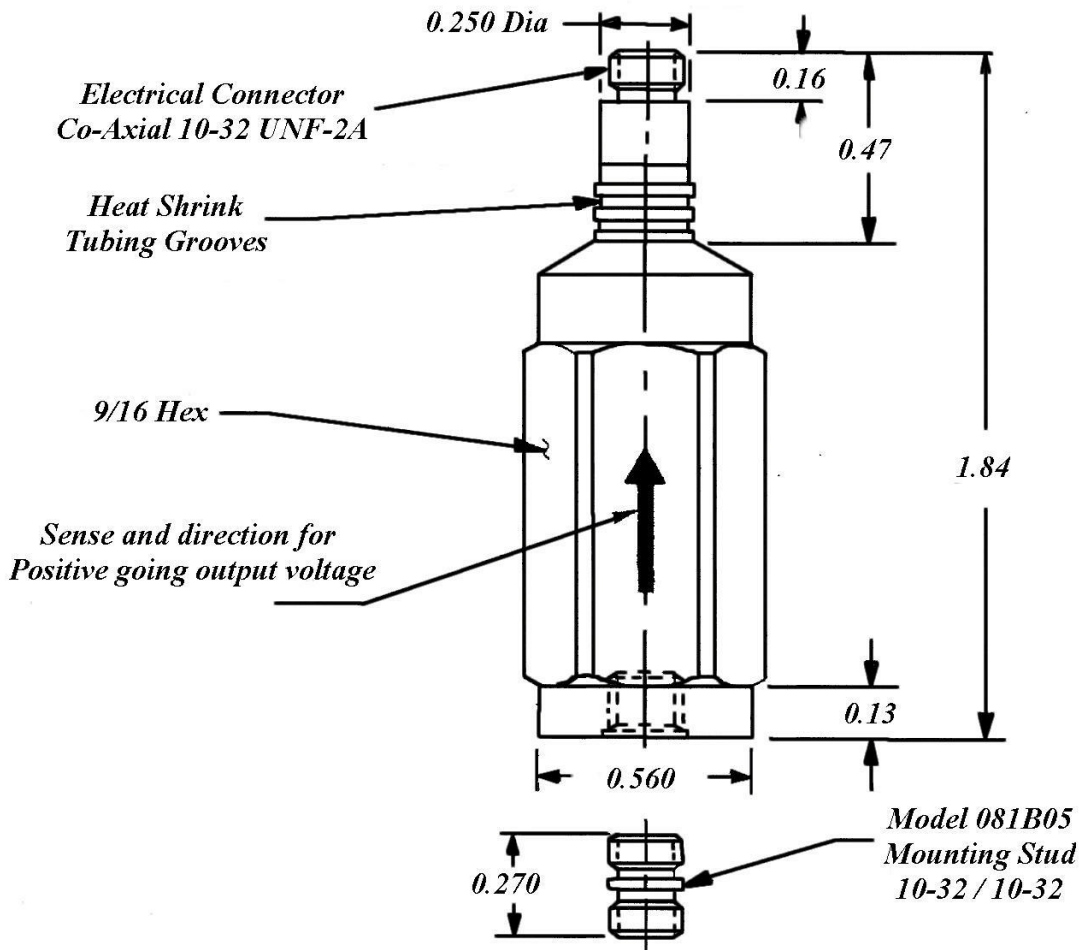


Figure A7. PCB Piezotronics accelerometer 302B03

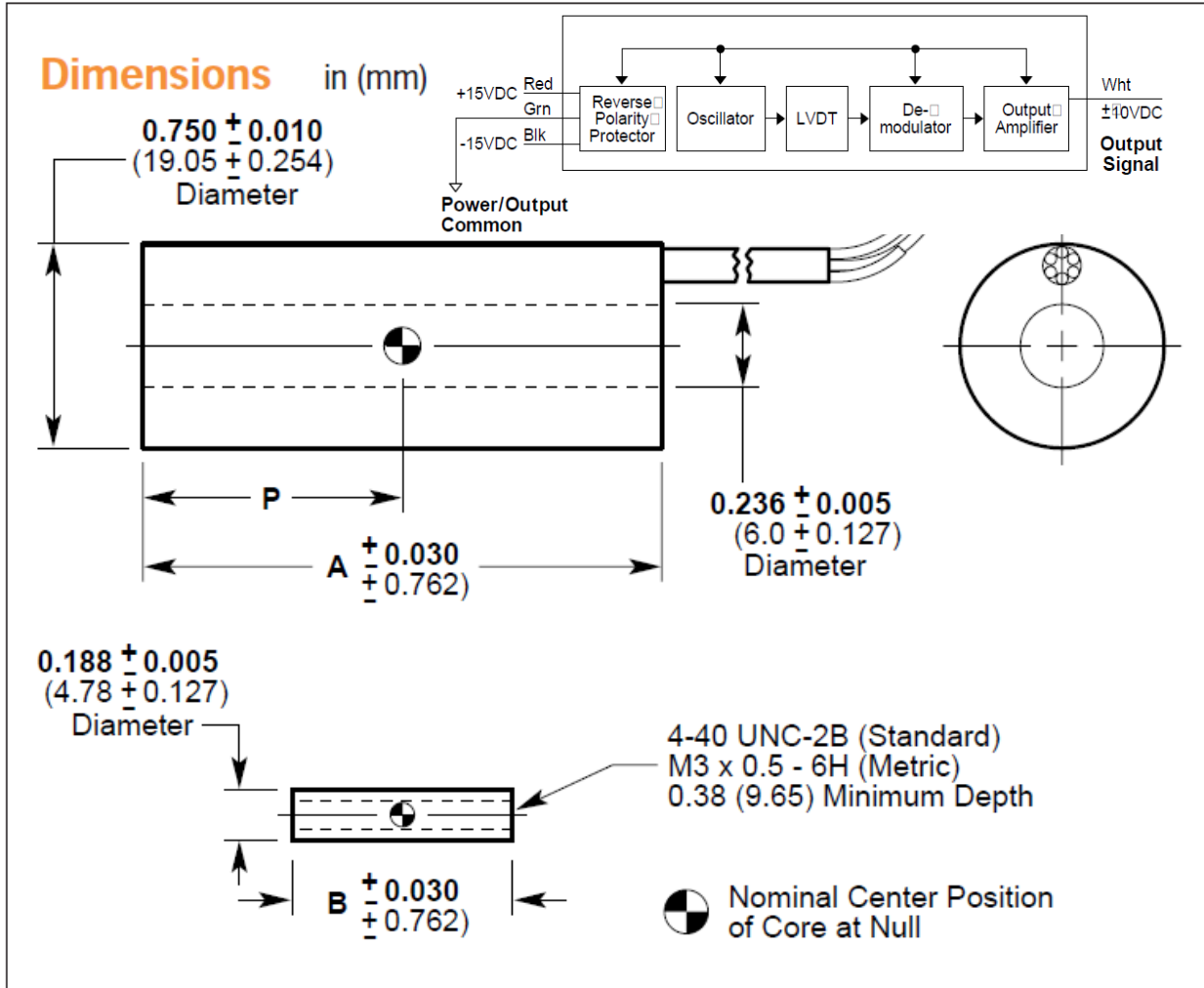


Figure A8. Shaevitz Sensors DC-EC linear variable differential transformer (LVDT)

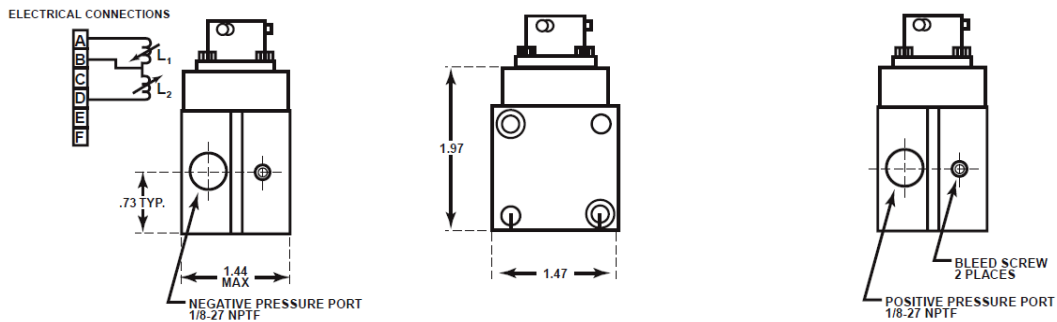


Figure A9. Validyne DP-15-58 differential pressure transducer

Appendix B. Test Analysis/Control Software

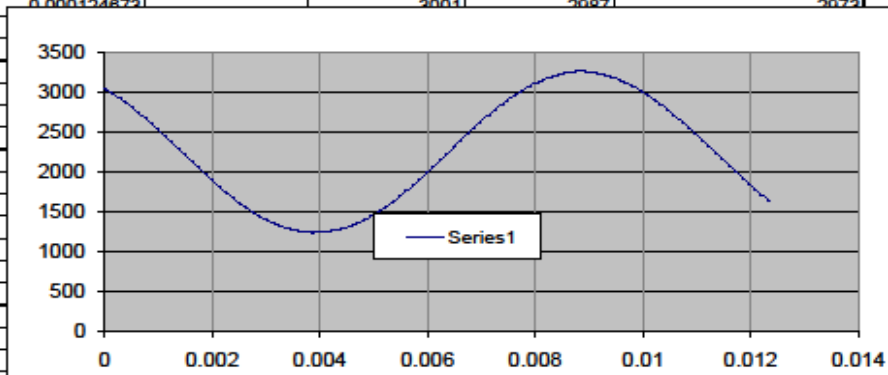
Excel Spreadsheets and Visual Basic

The control program is written in Visual Basic for Applications or VBA. It is similar, but not identical to Microsoft Visual Basic Stand-alone system. The advantage of using VBA is that it resides “behind” Excel and its spreadsheets. The spreadsheets are a very convenient way to enter data and view results. VBA is a very good language to perform simple tasks that are not computationally intense or time critical. This program will perform a torsional shear test at a rate of about 2 cycles per second. I will often deliberately delay the program to avoid any inertial effects of the loading system.

User Interface

The user interface consists of an Excel spreadsheet which is color coded and contains a large amount of load history data or other optional data. A clip of the spreadsheet is shown in figure B-1 where the specimen data and test control parameters are input.

Sample Data		lbs-in	gms-cm	Loading Choices		Legend	
Weight (gms)			400	Stress/Strain	0	0=stress, 1=strain controlled	User Entry Req'd
Height (in)	6.5	16.51		Type	1	0=Sine Cyclic 1=Irregular History	User Entry Complete
Inside Dia (in)	1.42	3.61		Ncycles	2	Maximum =65,000	Computed Value
Outside Dia (in)	2.37	6.02		Ndata Cycles	200	Maximum =200	Constant
				Nirreg hist	1701	Maximum =4000	
RC sample data			Cyclic Settings				
J sample		2462.35	Amplitude	10.00	Maximum Amplitude		
Jo Driver		37467.00	Offset	0.00	Offset value		
B tan B		0.25363				J sample	
Factor		100.00				Jo Driver	
		8000	8021				
Gain		4				B tan B	
Output			Amplitude	G	Strain	Factor	
(min)		(Hz)	(volts rms)	(psi)	(%)		
0		3053	3041	3029	3015	R/C Test Data	
0.000124872		3001	3087	3073	3060		
					304		
					340	Channel Scanning	
					773	Board	1
					703	Low Chan	0
					832	High Chan	0
					580	Num Pts	100
					478	Rate	8000
					898	Gain	4
					819	Output	
					237		
					158		
					079		
					998		
					918		
					844		
					771		
					701		
					834		
					1572		
0.002493405		1618	1601	1588	1572		
0.002618128		1557	1544	1530	1516		



NewTossTest3.0.xlsm


```

    Public RCFactor As Single           'Resonant column calibration factor
    Public RCBtanB As Single            'Resonant factor from BetaTanBeta
    Public RCJo As Single               'Resonant column top cap mass polar
moment of inertia
    Public RCJSample As Single         'Resonant column specimen mass polar
moment of inertia

'*** Data arrays here
'*** Cyclic Stuff
    Public Ncon As Integer
    Public Ncycle As Integer
    Public Ndat As Integer
    Public ControlVec(0 To 201) As Double           'Control vector to drive
cyclic test
    Public Proximator(0 To 200, 1 To 200) As Single 'Proximator reading 200
cycles, 200 data points
    Public PorePress(0 To 200, 1 To 200) As Single 'Pore pressure reading
    Public VertLVDT(0 To 200, 1 To 200) As Single 'Vertical LVDT reading
    Public AmpDrive(0 To 200, 1 To 200) As Single 'Amplifier drive reading
(or writing)

'*** Irregular Stuff
    Public IrregHist(0 To 4000) As Double           'Irregular history drive
vector
    Public IrregProx(0 To 4000) As Single           'Irregular test proximator
reading
    Public IrregDrive(0 To 4000) As Single         'Irregular test driver
value
    Public IrregLVDT(0 To 4000) As Single          'Irregular test LVDT value
    Public IrregPorePress(0 To 4000) As Single     'Irregular test
PorePressure value
'*** Calibration Factors Here
' Public ProxCalFactor As Single                   'Proximator calibration
factor
' Public AmpCalFactor As Single                    'Power amp calibration
factor
    Public PorePresCalFactor As Single             'PorePressure transducer
calibration factor (Volts/(Lb/In^2))
    Public ProxVoltstoInches As Single            'Proximator output to
Specimen Displacement (Volts/In)
    Public AccelVoltstoInSec2 As Single           'Accelerometer output to
Acceleration (Volts/(In/Sec^2))
    Public AmpstoTorque As Single                 'Coil Amps to Torque
(Amps/In-Lb)
    Public CurrDriveVoltstoAmps As Single         'Current Drive
Signal(Volts) (to Amplifier) to Coil Amps (Amps)
    Public TorquetoStress As Single

'Data Acquisition Configuration
    Public taskHandle1 As Long, taskHandle2 As Long
    Public pchnl1 As String, pchnl2 As String, pchnl3 As String, pchnl4 As
String, pchnl5 As String
    Public MinValue1 As Single, MinValue2 As Single, MinValue3 As Single,
MinValue4 As Single, MinValue5 As Single
    Public MaxValue1 As Single, MaxValue2 As Single, MaxValue3 As Single,
MaxValue4 As Single, MaxValue5 As Single
    Public DataGroup(1 To 4) As Double
    Public DAValue As Double

```

```

Public DiffTermConfig As Long
Public SperCh As Long
Public wksIndata As Worksheet, wksInDataAcq As Worksheet
Public taskisrunning As Boolean

Sub CheckStuff()
    Call ReadinputData
    Call PrepAdin
    UserForm1.Show
End
End Sub

Sub runtest()
    Call ReadinputData
    Call PrepAdin

    Select Case NTestType
        Case 0
            Call GenControlVector
            Call Runcyclic
            Call Writecyclic
        Case 1
            Call GenIrregHist
            Call RunIrreg
            Call WriteIrreg
        Case Else
            MsgBox ("bad test type")
    End Select
End Sub

Sub ReadinputData()
    Dim pi As Single
    Dim rout As Single, Rin As Single
    Dim StressElastic As Single, StressPlastic As Single

    Set wksIndata = Worksheets("Sample Data")
    pi = 3.14159
    Weight = wksIndata.Cells(2, 2)
    Length = wksIndata.Cells(3, 2)
    InDia = wksIndata.Cells(4, 2)
    OutDia = wksIndata.Cells(5, 2)
    NStressStrain = wksIndata.Cells(2, 5)
    NTestType = wksIndata.Cells(3, 5)
    NumCyclesMax = wksIndata.Cells(4, 5)
    NumDataMax = wksIndata.Cells(5, 5)
    NumIrregMax = wksIndata.Cells(6, 5)
    InAmp = wksIndata.Cells(8, 5)
    InOffSet = wksIndata.Cells(9, 5)
    rout = OutDia / 2#
    Rin = InDia / 2#
    'Below are average X-sec stress of hollow cylinder assuming elastic and
    plastic conditions

```

```

StressElastic = (4# / 3# * pi) * (rout ^ 3 - Rin ^ 3) / ((rout ^ 2 - Rin ^
2) * (rout ^ 4 - Rin ^ 4))
StressPlastic = (3# / 2# * pi) * (1# / (rout ^ 3 - Rin ^ 3))
'Take the average for our work
TorquetoStress = (StressElastic + StressPlastic) / 2# 'Avg Stress=Torque *
TorquetoStress
AmpstoTorque = 4.1474 'Amps per in-lb
'Drive Voltage -10 to +10 volts for -20 to +20 Amps Current Control

```

```

End Sub
Sub PrepAdin()

```

```

DiffTermConfig = 10106 'Differential Configuration, the supplied constant
doesnt work
Set wksInDataAcq = Worksheets("Data Acquisition")
On Error GoTo ErrorHandler
'DAQmx
' pausetime = 0.005 ' Set duration.
' Create the DAQmx task.
DAQmxErrChk DAQmxCreateTask("", taskHandle1) 'Set up the Analog Input
Task
DAQmxErrChk DAQmxCreateTask("", taskHandle2) 'Set up the Analog Output
Task
taskisrunning = True

' Add an four analog input channels to the task.
' And get one analog output channel to the second task
pchnl1 = wksInDataAcq.Cells(3, 2) 'Amp Drive Read
pchnl2 = wksInDataAcq.Cells(3, 3) 'Proximitior Read
pchnl3 = wksInDataAcq.Cells(3, 4) 'Vertical LVDT Read
pchnl4 = wksInDataAcq.Cells(3, 5) 'Pore Pressusre Read
pchnl5 = wksInDataAcq.Cells(3, 6) 'Amp Drive Write (Should be same as
Amp Drive Read+1)
MinValue1 = wksInDataAcq.Cells(5, 2) 'Max and min ranges for all inputs
MaxValue1 = wksInDataAcq.Cells(7, 2)
MinValue2 = wksInDataAcq.Cells(5, 3)
MaxValue2 = wksInDataAcq.Cells(7, 3)
MinValue3 = wksInDataAcq.Cells(5, 4)
MaxValue3 = wksInDataAcq.Cells(7, 4)
MinValue4 = wksInDataAcq.Cells(5, 5)
MaxValue4 = wksInDataAcq.Cells(7, 5)
MinValue5 = wksInDataAcq.Cells(5, 6)
MaxValue5 = wksInDataAcq.Cells(7, 6)
MsgBox ("up to create channel")
DriveInc = (MaxValue5 - MinValue5) / (2 ^ 16 - 1) 'Make 16-bit drive
increment for D/A
'The first four Creates are identical except for the channel number and
respective
'minimums and maximums
'The last Create is for the analog output

DAQmxErrChk DAQmxCreateAIVoltageChan(taskHandle1, pchnl1, "", _
DiffTermConfig, CStr(MinValue1), CStr(MaxValue1), _
DAQmx_Val_VoltageUnits1_Volts, "")
DAQmxErrChk DAQmxCreateAIVoltageChan(taskHandle1, pchnl2, "", _

```

```

        DiffTermConfig, CStr(MinValue2), CStr(MaxValue2), _
        DAQmx_Val_VoltageUnits1_Volts, "")
DAQmxErrChk DAQmxCreateAIVoltageChan(taskHandle1, pchnl3, "", _
        DiffTermConfig, CStr(MinValue3), CStr(MaxValue3), _
        DAQmx_Val_VoltageUnits1_Volts, "")
DAQmxErrChk DAQmxCreateAIVoltageChan(taskHandle1, pchnl4, "", _
        DiffTermConfig, CStr(MinValue4), CStr(MaxValue4), _
        DAQmx_Val_VoltageUnits1_Volts, "")
DAQmxErrChk DAQmxCreateAOVoltageChan(taskHandle2, pchnl5, "", _
        CStr(MinValue5), CStr(MaxValue5), _
        DAQmx_Val_VoltageUnits1_Volts, "")
Exit Sub
ErrorHandler:
    If taskisrunning = True Then
        DAQmxStopTask taskHandle1
        DAQmxClearTask taskHandle1
        DAQmxStopTask taskHandle2
        DAQmxClearTask taskHandle2
        taskisrunning = False
    End If
    MsgBox "Error:" & Err.Number & " " & Err.Description, , "Error"
End Sub
Sub ReadAllCyclic()
    DAQmxErrChk DAQmxReadAnalogF64(taskHandle1, 1, 10#,
DAQmx_Val_GroupByChannel, DataGroup(1), 4, SperCh, ByVal 0&)
    ' DAQmxErrChk DAQmxWriteAnalogScalarF64(taskHandle2, True, 10#, Outval,
ByVal 0&)
    AmpDrive(Ncycle, Ndat) = DataGroup(1)
    Proximator(Ncycle, Ndat) = DataGroup(2)
    VertLVDT(Ncycle, Ndat) = DataGroup(3)
    PorePress(Ncycle, Ndat) = DataGroup(4)
End Sub
Sub ReadAllIrreg()
    DAQmxErrChk DAQmxReadAnalogF64(taskHandle1, 1, 10#,
DAQmx_Val_GroupByChannel, DataGroup(1), 4, SperCh, ByVal 0&)
    IrregDrive(Ncon) = DataGroup(1)
    IrregProx(Ncon) = DataGroup(2)
    IrregLVDT(Ncon) = DataGroup(3)
    IrregPorePress(Ncon) = DataGroup(4)
End Sub
Function BtanB(i, Io) As Single
    Dim newbeta As Single
    Dim iratio As Single
    Dim oldbeta As Single
    Dim tanbeta As Single

    newbeta = 0.3
    iratio = i / Io
    Do
        oldbeta = newbeta
        tanbeta = Tan(oldbeta)
        newbeta = oldbeta + (iratio - oldbeta * tanbeta) _
            / (oldbeta * (1 / Cos(oldbeta) ^ 2))
    Loop Until (Abs(oldbeta - newbeta) < 0.0001)
    BtanB = newbeta
End Function
Sub GenControlVector()

```

```

'this routine generates the control vector for driving the sample
'it is also used to decide when to take data readings
'This is as stress-controlled test for now
Dim i As Integer

Dim wksControl As Worksheet
Set wksControl = Worksheets("ControlVector")
For i = 1 To NumDataMax
    ControlVec(i) = InOffSet * StresstoVolts + InAmp * StresstoVolts * Cos(2# *
3.14159 * (i - 1) / (1# * NumDataMax))
    wksControl.Cells(i + 2, 1) = i
    wksControl.Cells(i + 2, 2) = ControlVec(i)
Next i
Call PlotControl

End Sub
Sub GenIrregHist()
'this routine generates the Irregular loading history and displays it
Dim i As Integer
Dim wksHist As Worksheet
Set wksHist = Worksheets("Irregular History")
IrregHist(0) = 0
For i = 1 To NumIrregMax
    IrregHist(i) = wksHist.Cells(i + 1, 2) * InAmp * StresstoVolts + InOffSet *
StresstoVolts
Next i
End Sub
Sub Runcyclic()
Dim Mono As Boolean
Dim Ncon As Integer
Dim Ncycles As Integer
    MsgBox ("ready?")
    Mono = True                                'Starts as Monotonic loading (first 0.25
cycle, counted as cycle 0)
    LoadDir = 1                                'Positive loading direction
    Ncon = 3 * NumDataMax / 4                  'Set control counter to 3/4 of cycle
    DriveVal = 0#                              'Set D/A output to 0 volts
    Ncycle = 0                                  '0th cycle is monotonic one
    Do                                          'this test lasts for 200 cycles of loading
        If Mono Then                            'Monotonic portion is a little different
            DriveVal = DriveVal + DriveInc
            If DriveVal > ControlVec(Ncon) Then 'if it is time to read data
                Call ReadAllCyclic              'then go read it
                Ncon = Ncon + 1                 'increment the control vector
            End If 'DriveVal > ControlVec(Ncon)
        Else 'Mono not true, cyclic
            LoadDir = -1                        'start of cyclic is negative dir
            DriveInc = -Abs(DriveInc)
            If ControlVec(Ncon + 1) > ControlVec(Ncon) Then 'if positive going
                LoadDir = 1
                DriveInc = Abs(DriveInc)
            Else
                LoadDir = -1
                DriveInc = -Abs(DriveInc)
            End If 'positive going
            DriveVal = DriveVal + DriveInc

```

```

    If LoadDir > 0 And DriveVal >= ControlVec(Ncon) Then 'Positive going
load, hit control pt
    Call ReadAllCyclic          'Read the ad channels
    Ncon = Ncon + 1            'Bump the contorl pointer
    ElseIf LoadDir < 0 And DriveVal <= ControlVec(Ncon) Then 'Negative
going load
    Call ReadAllCyclic
    Ncon = Ncon + 1
    End If 'Check on readings
End If 'Mono or cyclic
WriteDA (DriveVal) 'push the device
If Ncon > NumDataMax Then      'finished with the cycle of data pts
Ncycle = Ncycle + 1          'on to next cycle
wksIndata.Cells(7, 4) = Ncycle 'report on the cycle
Ncon = 1                      'reset control value
Mono = False                  'set flag
End If
Loop Until Ncycle > NumCyclesMax
Call Unload
End Sub
Sub Unload()
    Dim i As Integer

    While Abs(DriveVal) > 0.01
        DriveVal = DriveVal - DriveInc
        WriteDA (DriveVal)
    Wend
    DriveVal = 0#
End Sub
Sub RunIrreg()

Dim Ncon As Integer
MsgBox ("ready?")
Ncon = 0
DriveVal = 0#
ReadAllIrreg

Do                                'this test lasts for 200 cycles of loading
If IrregHist(Ncon + 1) > IrregHist(Ncon) Then 'if positive going
    LoadDir = 1
    DriveInc = Abs(DriveInc)
Else
    LoadDir = -1
    DriveInc = -Abs(DriveInc)
End If 'positive going
DriveVal = DriveVal + DriveInc
If LoadDir > 0 And DriveVal >= IrregHist(Ncon) Then 'Positive going
load, hit control pt
    ReadAllIrreg                'Read the ad channels
    Ncon = Ncon + 1            'Bump the contorl pointer
ElseIf LoadDir < 0 And DriveVal <= IrregHist(Ncon) Then 'Negative going
load
    ReadAll
    Ncon = Ncon + 1
    End If 'Check on readings
    WriteDA (DriveVal) 'push the device
Loop Until Ncon > NumIrregMax

```

```

End Sub
Sub WriteDA(Volts)
    DAQmxErrChk DAQmxWriteAnalogScalarF64(taskHandle2, True, 10#, Volts, ByVal
0&)
End Sub

Sub Writecyclic()
Dim wksOutdata As Worksheet
Dim NewSheetName As String
Dim ColumnLoop As Integer
Dim Nrow As Integer, Ncol As Integer, Nsec As Integer, NRowSec As Integer
Dim Ncycle As Integer, NCyclesLeft As Integer, j As Integer, k As Integer

NewSheetName = "CyTest " + CStr(Sheets.Count + 1)
Sheets.Add.Name = NewSheetName 'make a new sheet
Application.CutCopyMode = False 'turn off cut-copy mode just in case
Set wksOutdata = Worksheets(NewSheetName)
'loop for all cycles of data, divide into groups of 10
'then enter in the three sets of data for each cycle,
'number of rows is number of data per cycle
NRowSec = NumDataMax + 4 'number of rows in a section is 4+datas
NCyclesLeft = NumCyclesMax + 1
Ncycle = 0
Nsec = 0
Nrow = 1

Do
    Nrow = Nsec * NRowSec
    If NCyclesLeft < 20 Then
        ColumnLoop = NCyclesLeft
    Else
        ColumnLoop = 20
    End If
    For j = 1 To ColumnLoop
        Ncol = 1 + 4 * (j - 1)
        wksOutdata.Cells(Nrow + 2, Ncol + 1) = "Cycle"
        wksOutdata.Cells(Nrow + 2, Ncol + 2) = Ncycle
        wksOutdata.Cells(Nrow + 3, Ncol) = "AmpDrive"
        wksOutdata.Cells(Nrow + 3, Ncol + 1) = "Proximator"
        wksOutdata.Cells(Nrow + 3, Ncol + 2) = "PorePres"
        wksOutdata.Cells(Nrow + 3, Ncol + 3) = "VertLVDT"
        For k = 1 To NumDataMax
            wksOutdata.Cells(Nrow + 3 + k, Ncol) = AmpDrive(Ncycle, k)
            wksOutdata.Cells(Nrow + 3 + k, Ncol + 1) = Proximator(Ncycle, k)
            wksOutdata.Cells(Nrow + 3 + k, Ncol + 2) = PorePress(Ncycle, k)
            wksOutdata.Cells(Nrow + 3 + k, Ncol + 3) = VertLVDT(Ncycle, k)
        Next k
        NCyclesLeft = NCyclesLeft - 1
        Ncycle = Ncycle + 1
    Next j
    Nsec = Nsec + 1 'add another section down the page
Loop Until NCyclesLeft = 0
End Sub

Sub WriteIrreg()
Dim wksOutdata As Worksheet
Dim i As Integer

```

```

Dim NewSheetName As String

NewSheetName = "IrregTest" + CStr(Sheets.Count + 1)
Sheets.Add.Name = NewSheetName 'make a new sheet
Application.CutCopyMode = False 'turn off cut-copy mode just in case
Set wksOutdata = Worksheets(NewSheetName)
wksOutdata.Cells(1, 1) = "AmpDrive"
wksOutdata.Cells(1, 2) = "Proximator"
wksOutdata.Cells(1, 3) = "PorePres"
wksOutdata.Cells(1, 4) = "VertLVDT"
For i = 0 To NumIrregMax
    wksOutdata.Cells(i + 2, 1) = IrregDrive(i)
    wksOutdata.Cells(i + 2, 2) = IrregProx(i)
    wksOutdata.Cells(i + 2, 3) = IrregPorePress(i)
    wksOutdata.Cells(i + 2, 4) = IrregLVDT(i)
Next i
End Sub

Public Sub DAQmxErrChk(errorCode As Long)
'
' Utility function to handle errors by recording the DAQmx error code
' and message.
'
Dim errorString As String
Dim bufferSize As Long
Dim status As Long
If (errorCode < 0) Then
    ' Find out the error message length.
    bufferSize = DAQmxGetErrorString(errorCode, 0, 0)
    ' Allocate enough space in the string.
    errorString = String$(bufferSize, 0)
    ' Get the actual error message.
    status = DAQmxGetErrorString(errorCode, errorString, bufferSize)
    ' Trim it to the actual length, and display the message
    errorString = Left(errorString, InStr(errorString, Chr$(0)))
    Err.Raise errorCode, , errorString
End If

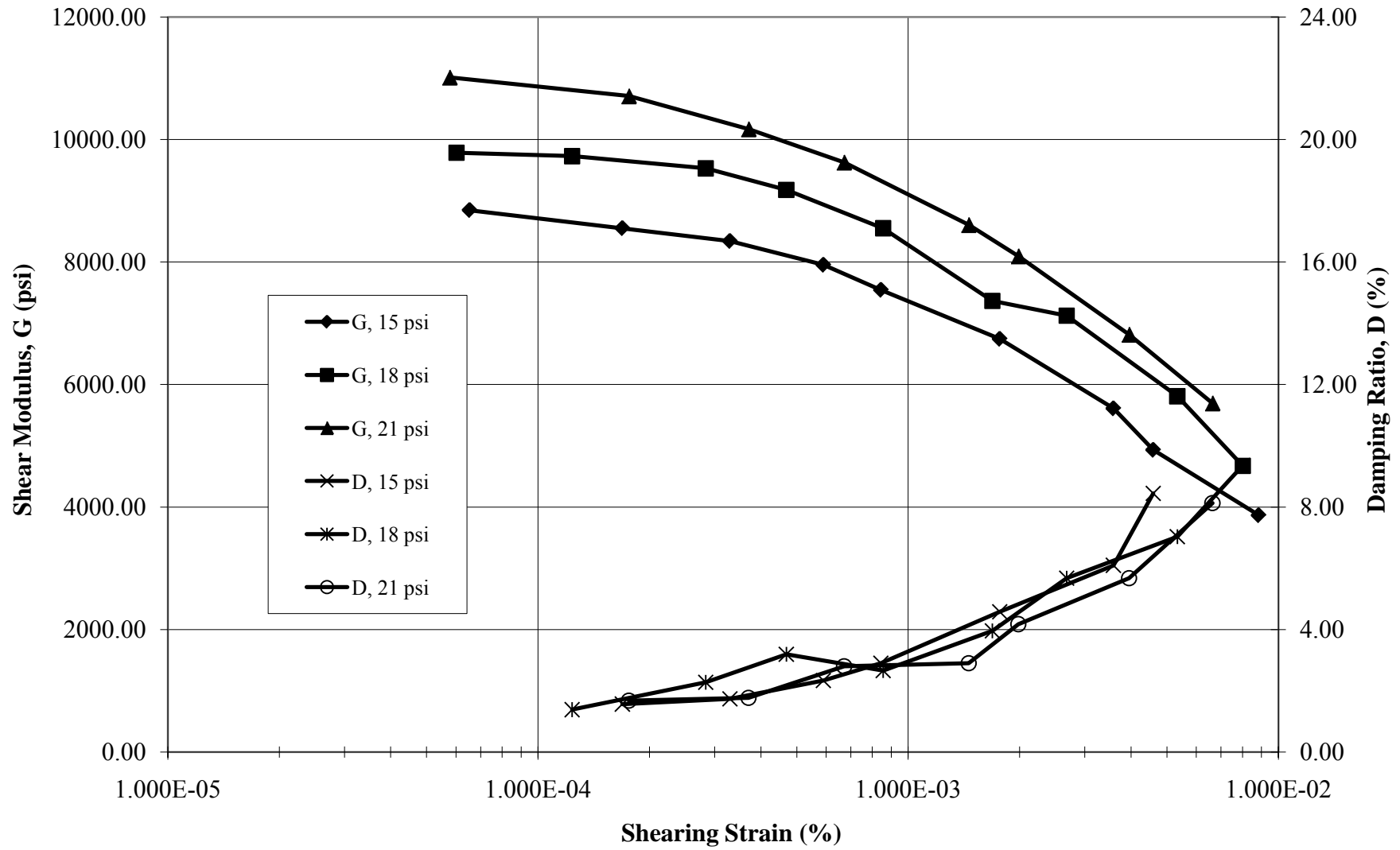
End Sub

```

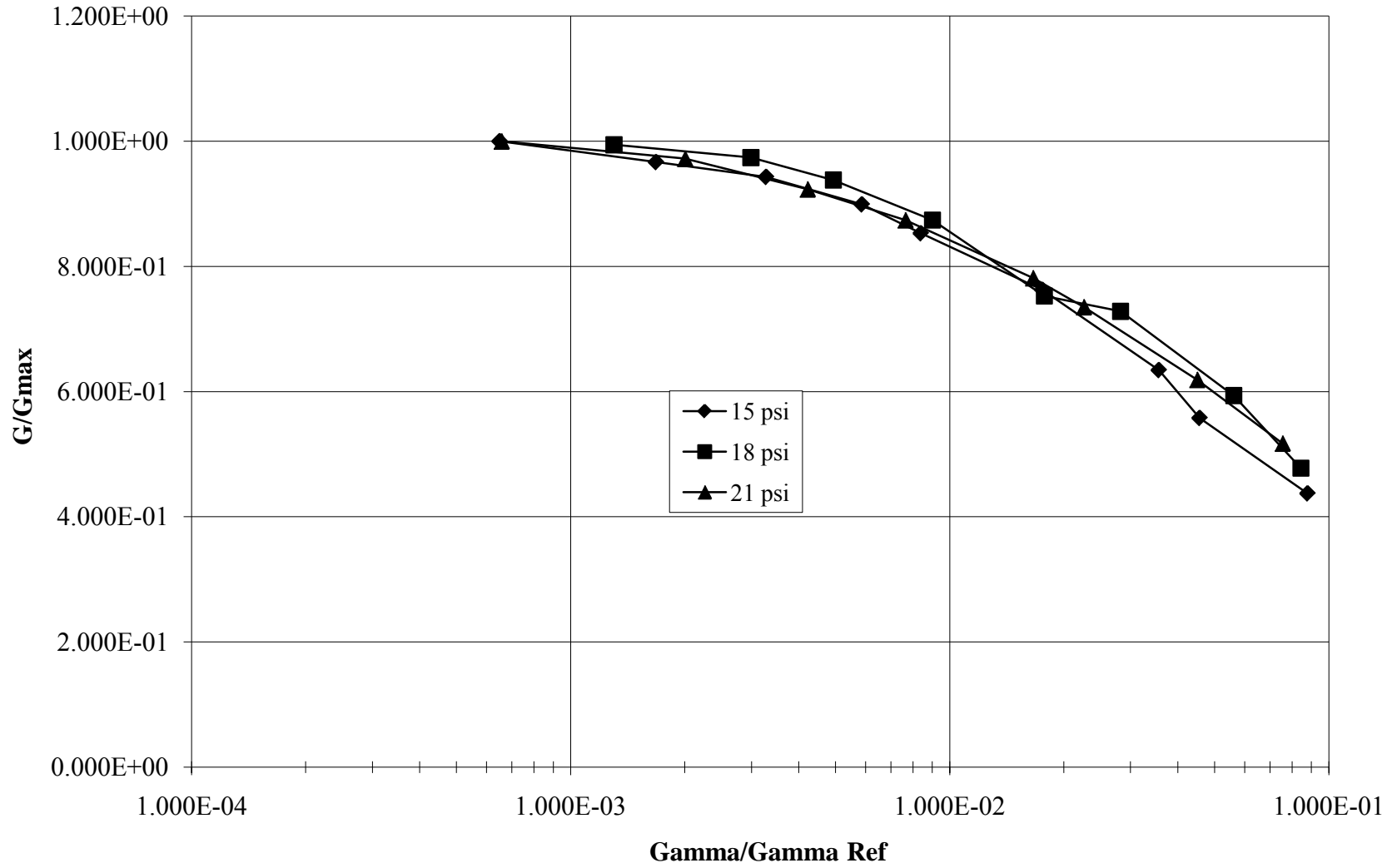
Appendix C Detailed Test Data

Sample				Conf. Press	Date	Time	Elapsed Time	Period	Freq	Shear Wave	G	Accel Volts	Accel Disp	Strain	G/Gmax	Gam/Gam Ref	Z	Z+1	Damping	
Test A	Inside Dia	Outside Dia	Length	(psi)		(clock)	(min)	(msec)	(rad/sec)	(ft/sec)	(psi)	(volts rms)	(cm p-p)	(% s-a)					(%)	
	(cm)	(cm)	(cm)	3.872983346	15	6/17/2008	19:18	1	20.82	301.79	565.57	6692.80	0.0041	3.7E-05	7.080E-05					
	3.937	6.0452	14.25	Meas 1	Taumax	6/17/2008	19:45	28	18.69	336.18	630.02	8305.21	0.0049	3.6E-05	6.819E-05					
				Meas 2	8.8980054	6/17/2008	20:05	48	18.11	346.95	650.20	8845.70	0.005	3.4E-05	6.533E-05	1.000E+00	6.494E-04			
				Meas 3	Gmax	6/17/2008	20:06	49	18.42	341.11	639.26	8550.47	0.0125	8.9E-05	1.690E-04	9.667E-01	1.680E-03	16	14.5	1.57
	3.937	6.0452	14.25	Average	8845	6/17/2008	20:07	50	18.65	336.90	631.38	8340.87	0.0238	0.00017	3.298E-04	9.430E-01	3.278E-03	14.5	13	1.74
			C est (psi)	Phi est (deg)	Gam Ref	6/17/2008	20:08	51	19.10	328.96	616.50	7952.48	0.0406	0.00031	5.901E-04	8.991E-01	5.866E-03	11	9.5	2.33
	Sample X-sec	Sample Volume	7	7.5	0.001006	6/17/2008	20:09	52	19.61	320.41	600.47	7544.21	0.0551	0.00045	8.441E-04	8.529E-01	8.391E-03	6	5	2.90
	(mm^2)	(mm^3)	Ko est			6/17/2008	20:10	53	20.74	302.95	567.75	6744.53	0.1031	0.00093	1.767E-03	7.625E-01	1.756E-02	12	9	4.58
	16.528	235.528	1			6/17/2008	20:11	54	22.74	276.31	517.82	5610.33	0.174	0.00189	3.585E-03	6.343E-01	3.563E-02	11	7.5	6.10
	Sample Wet Wt	Sample Dry Wt	Water Content	Wet Unit wt		6/17/2008	20:12	55	24.25	259.10	485.57	4933.39	0.196	0.00242	4.592E-03	5.578E-01	4.565E-02	8.5	5	8.45
	(gms)	(gms)	(%)	(gm/cm^3)		6/17/2008	20:13	56	27.39	229.40	429.91	3867.10	0.296	0.00466	8.847E-03	4.372E-01	8.794E-02			
	365.9	273	34.03	1.554	18	6/17/2008	20:18	1	18.27	343.91	644.51	8691.45	0.0047	3.3E-05	6.250E-05					
	Mass Polar Moment of Inertia, J			4.242640687	Taumax	6/17/2008	21:00	43	17.22	364.88	683.81	9783.69	0.0051	3.2E-05	6.025E-05	1.000E+00	6.345E-04			
	(gm-cm^2)			9.2895836	6/17/2008	21:01	44	17.27	363.82	681.83	9727.12	0.0104	6.5E-05	1.236E-04	9.943E-01	1.301E-03	12	11	1.38	
	2380.38			Gmax	6/17/2008	21:02	45	17.45	360.07	674.79	9527.48	0.0234	0.00015	2.839E-04	9.739E-01	2.989E-03	15	13	2.28	
	Drive Head Mass Polar Moment of Intertia, Jo			9783	6/17/2008	21:03	46	17.78	353.39	662.27	9177.10	0.0372	0.00025	4.685E-04	9.381E-01	4.934E-03	11	9	3.19	
	(gm-cm^2)			Gam Ref	6/17/2008	21:04	47	18.42	341.11	639.26	8550.47	0.0633	0.00045	8.556E-04	8.740E-01	9.011E-03	6.5	5.5	2.66	
	37467.00			0.0009496	6/17/2008	21:05	48	19.85	316.53	593.21	7362.89	0.1075	0.00089	1.687E-03	7.526E-01	1.777E-02	10	7.8	3.95	
	Beta				6/17/2008	21:06	49	20.18	311.36	583.51	7124.05	0.1652	0.00141	2.680E-03	7.282E-01	2.823E-02	10	7	5.68	
	0.24947				6/17/2008	21:07	50	22.35	281.13	526.85	5807.83	0.268	0.00281	5.333E-03	5.937E-01	5.617E-02	14	9	7.03	
					6/17/2008	21:08	51	24.92	252.13	472.52	4671.68	0.324	0.00423	8.016E-03	4.775E-01	8.442E-02	9	5	9.35	
	Sigma	Sqrt Sigma	Gmax	4.582575695	21	6/17/2008	21:15	1	16.97	370.25	693.88	10074.08	0.0052	3.1E-05	5.966E-05					
				Taumax	6/17/2008	21:32	18	16.44	382.19	716.25	10734.10	0.0055	3.1E-05	5.922E-05						
				9.6811619	6/17/2008	21:37	23	16.23	387.13	725.52	11013.67	0.0055	3E-05	5.772E-05	1.000E+00	6.566E-04				
				Gmax	6/17/2008	21:38	24	16.46	381.72	715.38	10708.03	0.0163	9.3E-05	1.759E-04	9.723E-01	2.001E-03	10	9	1.68	
				11013	6/17/2008	21:39	25	16.89	372.01	697.17	10169.74	0.0326	0.0002	3.705E-04	9.234E-01	4.215E-03	9.5	8.5	1.77	
				Gam Ref	6/17/2008	21:40	26	17.36	361.93	678.29	9626.53	0.0559	0.00035	6.712E-04	8.741E-01	7.635E-03	15.5	13	2.80	
				0.0008791	6/17/2008	21:41	27	18.36	342.22	641.35	8606.44	0.1085	0.00077	1.457E-03	7.815E-01	1.658E-02	6	5	2.90	
					6/17/2008	21:42	28	18.93	331.92	622.04	8095.95	0.139	0.00105	1.984E-03	7.351E-01	2.257E-02	6.5	5	4.18	
					6/17/2008	21:43	29	20.63	304.57	570.78	6816.64	0.233	0.00208	3.951E-03	6.190E-01	4.494E-02	5	3.5	5.68	
					6/17/2008	21:44	30	22.57	278.39	521.72	5695.16	0.327	0.0035	6.636E-03	5.171E-01	7.549E-02	5	3	8.13	

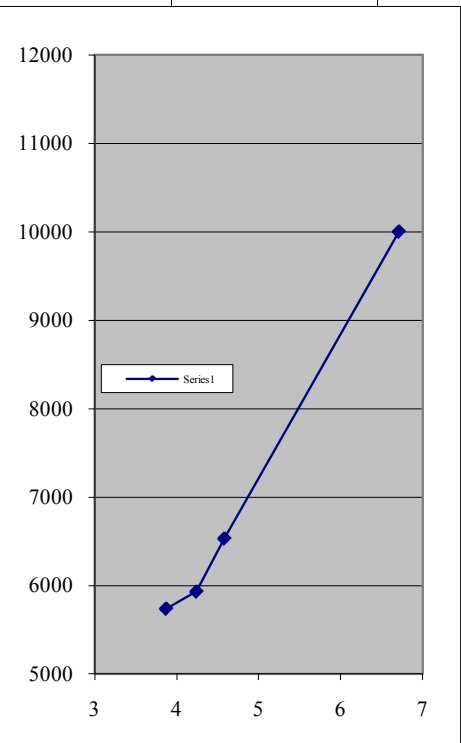
Test A G and D vs. Shearing Strain



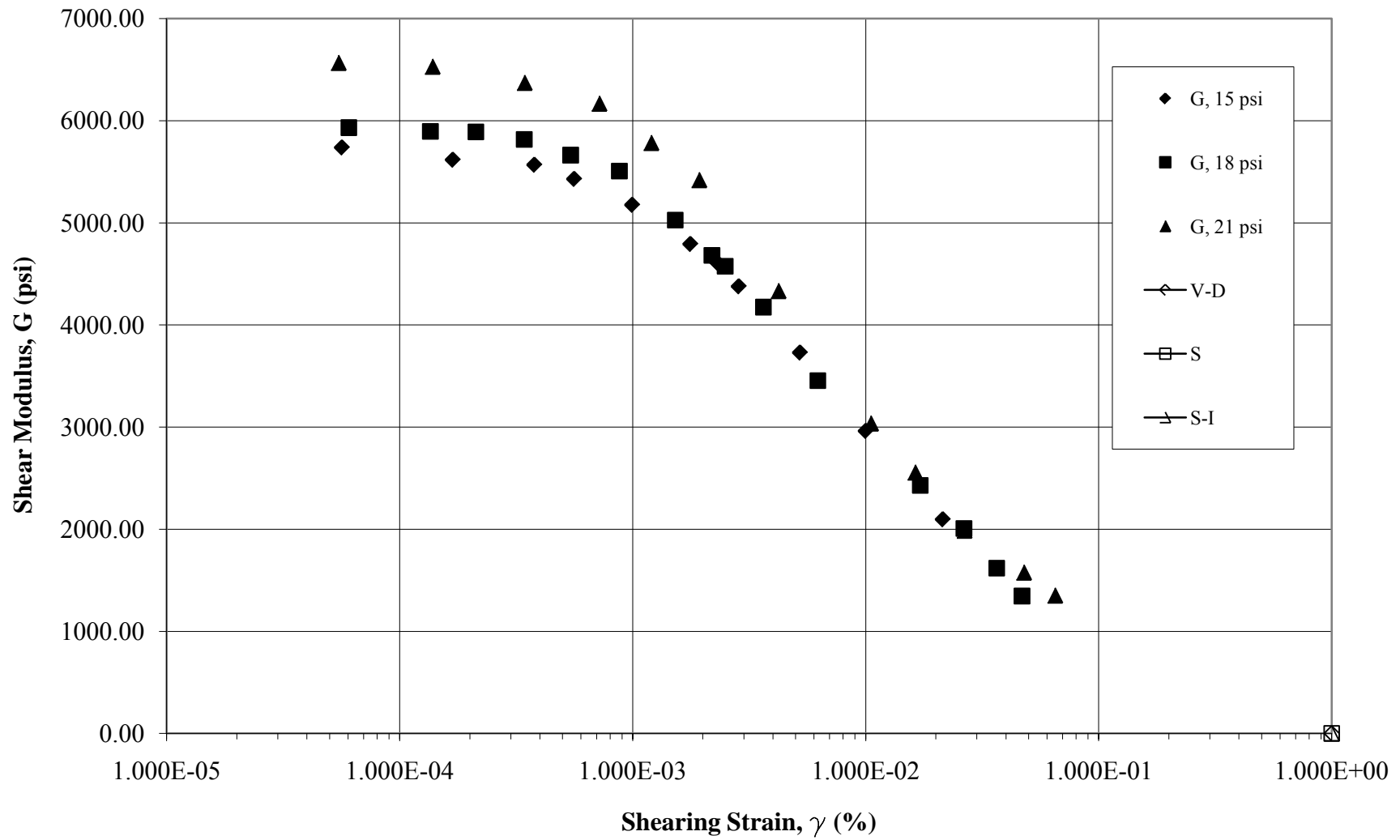
Test A
G/Gmax vs. Gamma/Gamma Ref



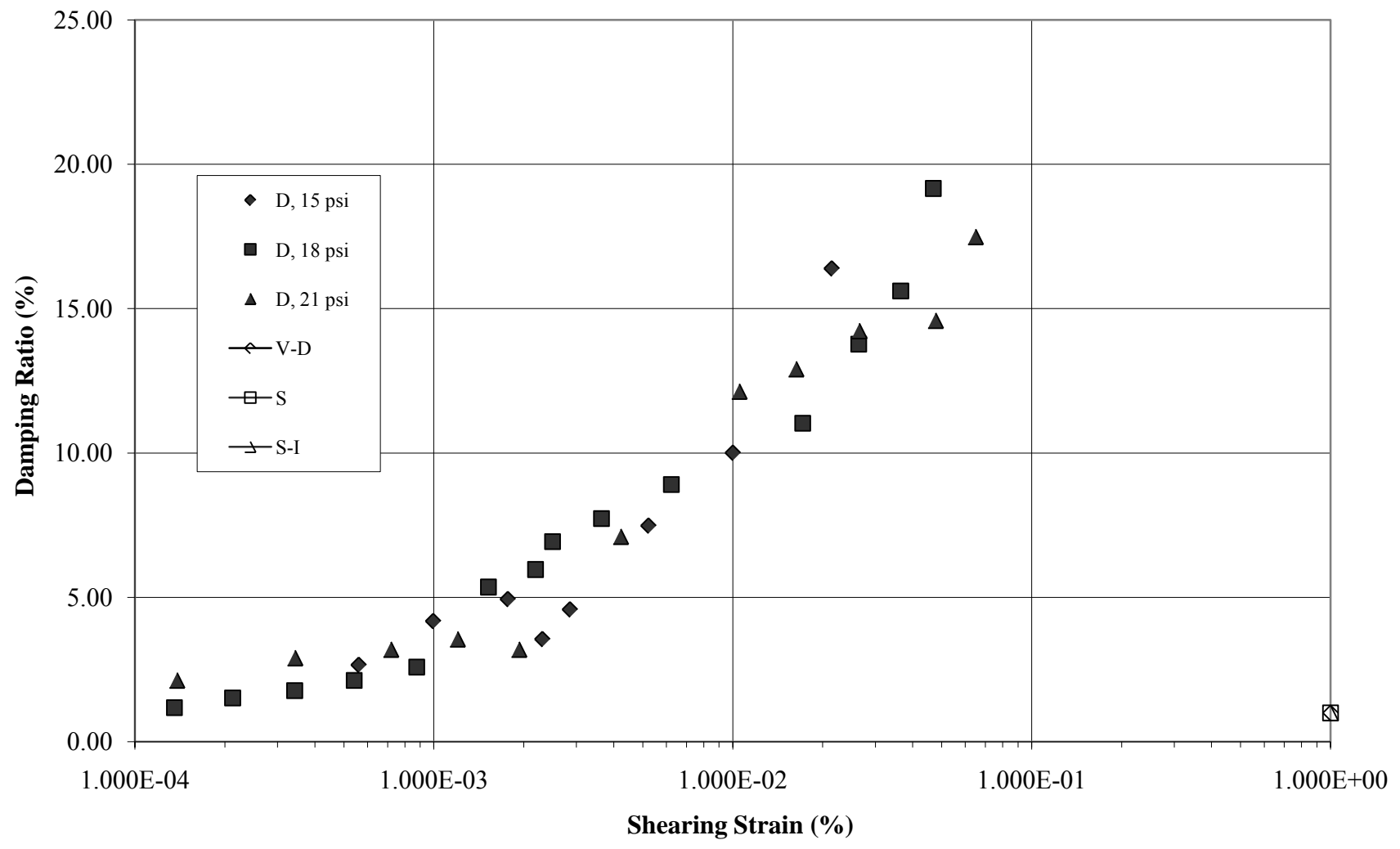
Sample	Test B	Inside Dia	Outside Dia	Length	Conf. Pres	Date	Time	Elapsed Tim	Period	Freq	Shear Wave	G	Accel Volts	Accel Displ	Strain	G/Gmax	Gam/Gam Ref	Z	Z+1	Damping
(cm)	(cm)	(cm)	(psi)		(clock)	(min)	(msec)	(rad/sec)	(ft/sec)	(psi)	(volts rms)	(cm p-p)	(% s-a)							(%)
		3.937	6.0452	14.25	3.8729833	15	6/24/2008	13:30	1	24.19	259.74	471.53	4964.97	0.0023	2.8E-05	5.362E-05	8.653E-01	3.458E-04		
					Meas 1	Taumax	6/24/2008	13:50	21	22.97	273.54	496.58	5506.38	0.0027	3E-05	5.675E-05		3.660E-04		
					Meas 2	8.898005	6/24/2008	14:50	81	22.73	276.43	501.82	5623.28	0.0029	3.1E-05	5.969E-05		3.849E-04		
					Meas 3	Gmax	6/24/2008	15:00	91	22.50	279.25	506.95	5738.83	0.0028	3E-05	5.647E-05	1.000E+00	3.642E-04		
		3.937	6.0452	14.25	Average	5738	6/24/2008	15:01	92	22.74	276.31	501.60	5618.33	0.0082	8.9E-05	1.689E-04	9.791E-01	1.089E-03		
				C est (psi)	Phi est (deg)	Gam Ref	6/24/2008	15:02	93	22.84	275.10	499.40	5569.24	0.0182	0.0002	3.782E-04	9.706E-01	2.439E-03		
Sample X-sec	Sample Volume	7	7.5	0.001551		6/24/2008	15:03	94	23.13	271.65	493.14	5430.46	0.0263	0.0003	5.606E-04	9.464E-01	3.615E-03	13	11	2.66
(mm^2)	(mm^3)	Ko est				6/24/2008	15:04	95	23.69	265.23	481.48	5176.76	0.0445	0.00052	9.949E-04	9.022E-01	6.416E-03	13	10	4.18
16.528	235.528	1				6/24/2008	15:05	96	24.62	255.21	463.30	4793.05	0.0732	0.00093	1.768E-03	8.353E-01	1.140E-02	7.5	5.5	4.94
Sample Wet Wt	Sample Dry Wt	Water Content	Wet Unit wt			6/24/2008	15:06	97	25.10	250.33	454.44	4611.48	0.0919	0.00122	2.307E-03	8.037E-01	1.487E-02	6.5	5.2	3.55
(gms)	(gms)	(%)	(gm/cm^3)			6/24/2008	15:07	98	25.76	243.91	442.79	4378.21	0.1079	0.0015	2.852E-03	7.630E-01	1.839E-02	10	7.5	4.58
390.5	273	43.04	1.658			6/24/2008	15:08	99	27.91	225.12	408.68	3729.65	0.1683	0.00275	5.223E-03	6.500E-01	3.368E-02	8	5	7.48
Mass Polar Moment of Inertia, J						6/24/2008	15:09	100	31.32	200.61	364.19	2961.72	0.256	0.00527	1.000E-02	5.162E-01	6.452E-02	7.5	4	10.00
(gm-cm^2)						6/24/2008	15:10	101	37.23	168.77	306.38	2096.05	0.388	0.0113	2.143E-02	3.653E-01	1.382E-01	7	2.5	16.39
2540.42			4.2426407	18		6/24/2008	15:25	1	23.93	262.57	476.65	5073.44	0.0024	2.9E-05	5.475E-05					
Drive Head Mass Polar Moment of Intertia, Jo					Taumax	6/24/2008	15:37	13	22.94	273.90	497.23	5520.79	0.0028	3.1E-05	5.870E-05					
(gm-cm^2)					9.289584	6/24/2008	16:13	49	22.13	283.92	515.42	5932.33	0.0031	3.2E-05	6.048E-05	1.000E+00	3.862E-04			
37467.00	Confining	sqrt Conf	G	Gmax	6/24/2008	16:14	50	22.20	283.03	513.80	5894.98	0.0069	7.1E-05	1.355E-04	9.938E-01	8.651E-04	7	6.5	1.18	
Beta	15	3.87298335	5738.83	5932	6/24/2008	16:15	51	22.21	282.90	513.57	5889.67	0.0108	0.00011	2.122E-04	9.929E-01	1.355E-03	11	10	1.52	
0.25753	18	4.24264069	5932.3309	Gam Ref	6/24/2008	16:16	52	22.35	281.13	510.35	5816.12	0.0172	0.00018	3.423E-04	9.805E-01	2.186E-03	9.5	8.5	1.77	
	21	4.58257569	6531.8325	0.001566	6/24/2008	16:17	53	22.65	277.40	503.59	5663.07	0.0265	0.00029	5.416E-04	9.547E-01	3.459E-03	8	7	2.13	
	45	6.70820393	10000		6/24/2008	16:18	54	22.97	273.54	496.58	5506.38	0.0417	0.00046	8.765E-04	9.283E-01	5.597E-03	10	8.5	2.59	
					6/24/2008	16:19	55	24.04	261.36	474.47	5027.12	0.0661	0.0008	1.522E-03	8.475E-01	9.718E-03	7	5	5.36	
					6/24/2008	16:20	56	24.91	252.24	457.90	4682.10	0.0885	0.00115	2.188E-03	7.893E-01	1.397E-02	8	5.5	5.96	
					6/24/2008	16:21	57	25.20	249.33	452.63	4574.96	0.0986	0.00132	2.495E-03	7.712E-01	1.593E-02	8.5	5.5	6.93	
					6/24/2008	16:22	58	26.38	238.18	432.39	4174.83	0.1312	0.00192	3.637E-03	7.038E-01	2.323E-02	6.5	4	7.73	
					6/24/2008	16:23	59	29.00	216.66	393.32	3454.56	0.186	0.00329	6.232E-03	5.824E-01	3.979E-02	7	4	8.91	
					6/24/2008	16:24	60	34.58	181.70	329.85	2429.62	0.36	0.00904	1.715E-02	4.096E-01	1.095E-01	5	2.5	11.03	
					6/24/2008	16:25	61	38.04	165.17	299.85	2007.74	0.458	0.01392	2.640E-02	3.385E-01	1.686E-01	9.5	4	13.77	
					6/24/2008	16:26	62	42.37	148.29	269.21	1618.35	0.51	0.01923	3.648E-02	2.728E-01	2.329E-01	4	1.5	15.61	
					6/24/2008	16:27	63	46.46	135.24	245.51	1345.95	0.545	0.02471	4.687E-02	2.269E-01	2.993E-01	4	1.2	19.16	
					4.5825757	21	6/24/2008	16:32	1	23.18	271.06	492.08	5407.06	0.0026	2.9E-05	5.566E-05				
					Taumax	6/24/2008	16:50	19	22.06	284.82	517.06	5970.04	0.003	3.1E-05	5.816E-05					
					9.681162	6/24/2008	17:15	44	21.50	292.24	530.53	6285.09	0.0031	3E-05	5.709E-05					
					Gmax	6/24/2008	18:00	89	21.03	298.77	542.38	6569.16	0.0031	2.9E-05	5.462E-05	1.000E+00	3.706E-04			
					6569	6/24/2008	18:01	90	21.09	297.92	540.84	6531.83	0.0078	7.3E-05	1.382E-04	9.943E-01	9.378E-04	8	7	2.13
					Gam Ref	6/24/2008	18:02	91	21.35	294.29	534.25	6373.71	0.0189	0.00018	3.432E-04	9.703E-01	2.329E-03	9	7.5	2.90
					0.001474	6/24/2008	18:03	92	21.70	289.55	525.64	6169.77	0.0383	0.00038	7.185E-04	9.392E-01	4.875E-03	11	9	3.19
						6/24/2008	18:04	93	22.41	280.37	508.98	5785.01	0.06	0.00063	1.200E-03	8.807E-01	8.145E-03	7.5	6	3.55
						6/24/2008	18:05	94	23.15	271.41	492.71	5421.08	0.0903	0.00102	1.928E-03	8.253E-01	1.308E-02	5.5	4.5	3.19
						6/24/2008	18:06	95	25.89	242.69	440.57	4334.35	0.158	0.00222	4.219E-03	6.598E-01	2.863E-02	7.5	4.8	7.10
						6/24/2008	18:07	96	30.93	203.14	368.78	3036.89	0.276	0.00555	1.052E-02	4.623E-01	7.138E-02	7.5	3.5	12.13
						6/24/2008	18:08	97	33.71	186.39	338.37	2556.65	0.36	0.00859	1.630E-02	3.892E-01	1.106E-01	9	4	12.91
						6/24/2008	18:09	98	38.24	164.31	298.28	1986.79	0.455	0.01398	2.651E-02	3.024E-01	1.799E-01	11	4.5	14.23
						6/24/2008	18:10	99	42.93	146.36	265.70	1576.40	0.65	0.02516	4.772E-02	2.400E-01	3.238E-01	5	2	14.58
						6/24/2008	18:11	100	46.37	135.50	245.99	1351.18	0.758	0.03424	6.493E-02	2.057E-01	4.406E-01	6	2	17.48



Test B G and D vs. Shearing Strain

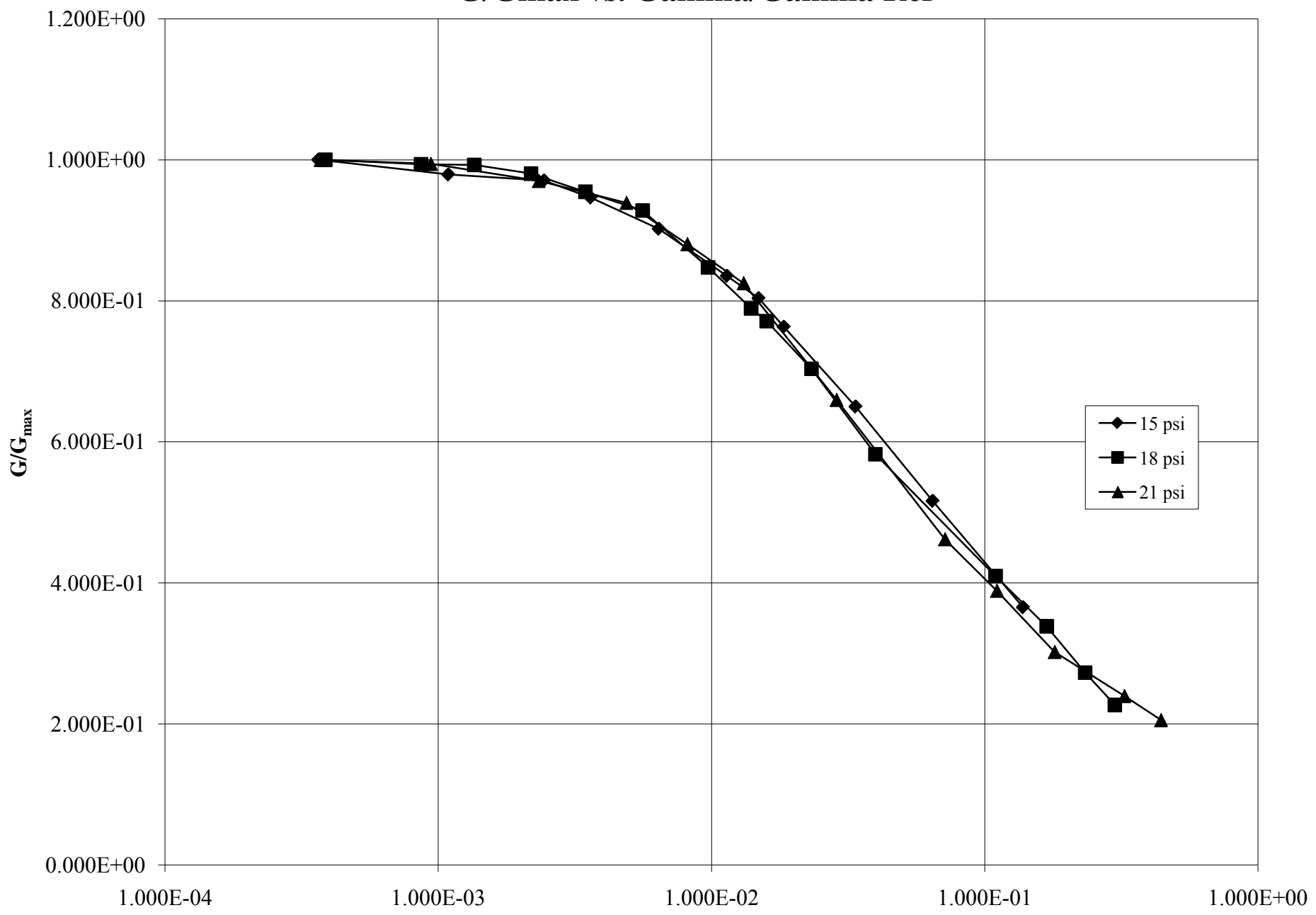


Test B D vs. Shearing Strain



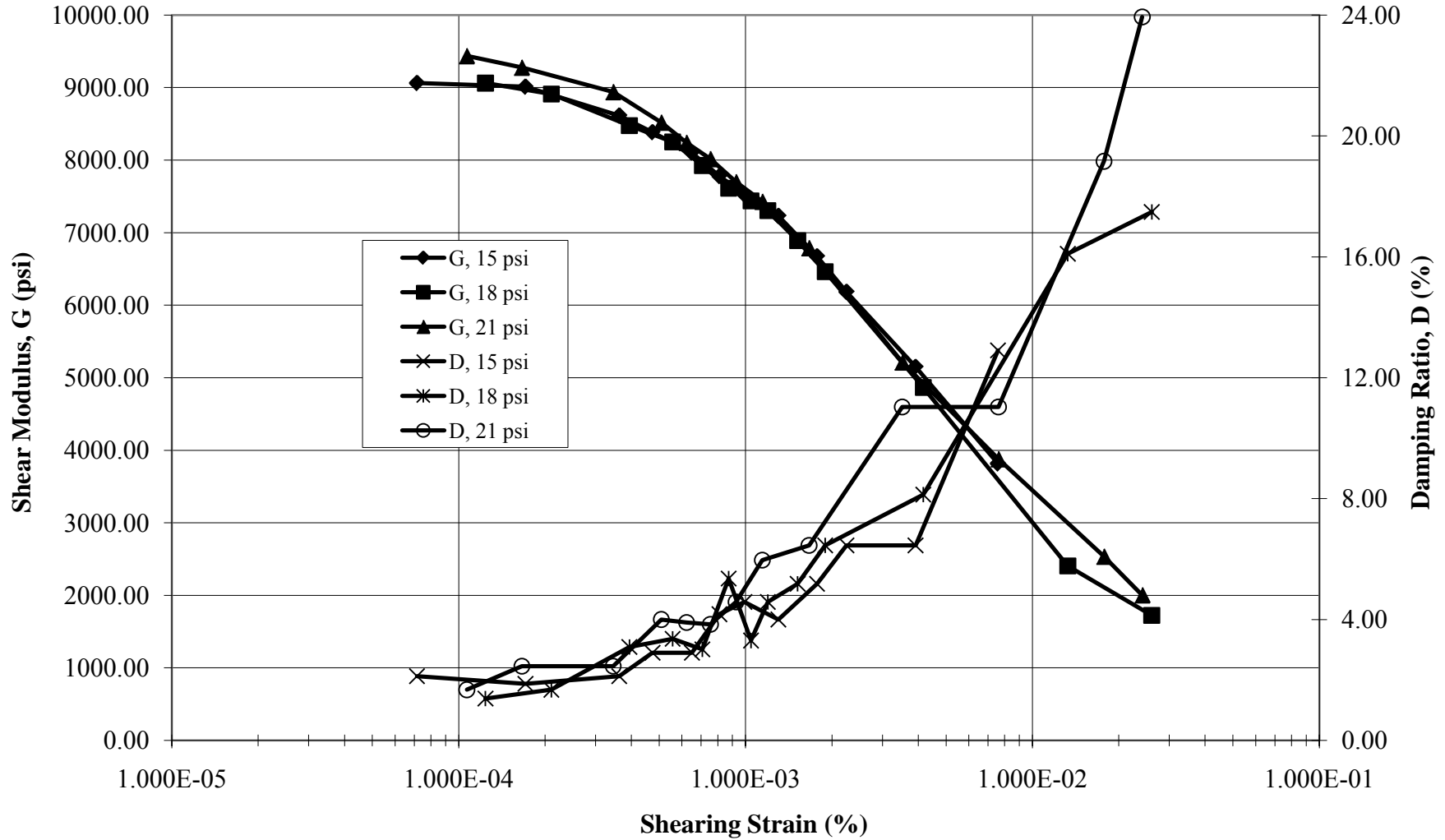
Test B

G/G_{max} vs. Gamma/Gamma Ref

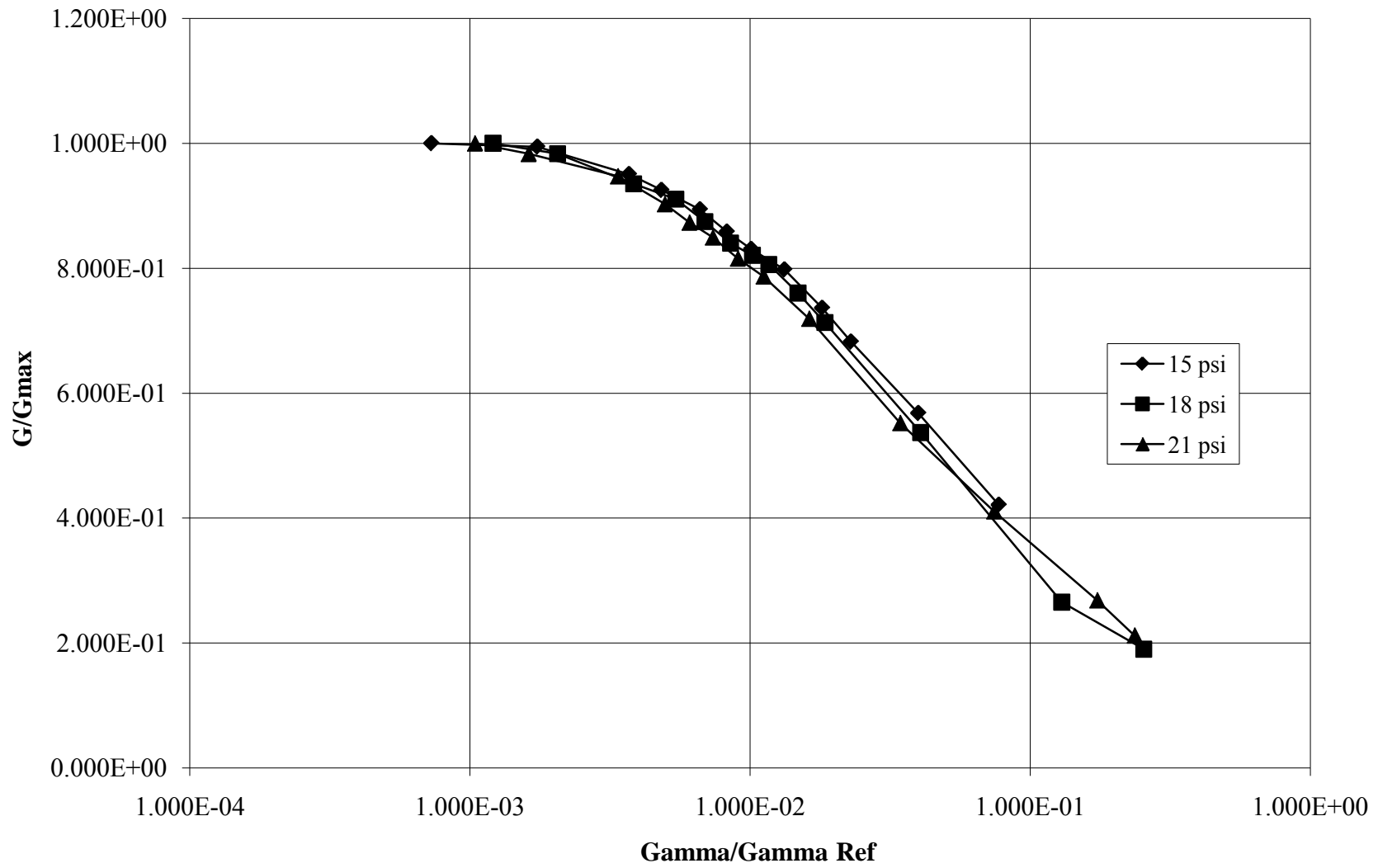


Sample	Test C	Inside Dia	Outside Dia	Length	Conf. Pres	Date	Time	Elapsed Time	Period	Freq	Shear Wave	G	Accel Volts	Accel Disp	Strain	G/Gmax	Gam/Gam Ref	Z	Z+1	Damping
(cm)	(cm)	(cm)	(psi)	(clock)	(min)	(msec)	(rad/sec)	(ft/sec)	(psi)	(volts rms)	(cm p-p)	(% s-a)								(%)
			3.8729833	15	6/22/2008	14:08	1	37.21	168.86	303.63	2099.23	0.0095	0.0002763	5.240E-04						
3.937	6.0452	14.25	Meas 1	Taumax	6/22/2008	16:26	139	21.36	294.16	528.93	6370.54	0.0046	4.408E-05	8.361E-05						
			Meas 2	8.898005	6/23/2008	10:28	1221	17.91	350.82	630.82	9061.24	0.0056	3.773E-05	7.156E-05	1.000E+00	7.287E-04	4	3.5	2.13	
			Meas 3	Gmax	6/23/2008	10:29	1222	17.96	349.84	629.06	9010.86	0.0133	9.011E-05	1.709E-04	9.945E-01	1.740E-03	9	8	1.87	
3.937	6.0452	14.25	Average	9061	6/23/2008	10:30	1223	18.37	342.04	615.02	8613.12	0.027	0.0001914	3.630E-04	9.506E-01	3.696E-03	8	7	2.13	
		C est (psi)	Phi est (deg)	Gam Ref	6/23/2008	10:31	1224	18.62	337.44	606.77	8383.39	0.0343	0.0002498	4.738E-04	9.252E-01	4.824E-03	9	7.5	2.90	
Sample X-sec	Sample Volume	7	7.5	0.000982	6/23/2008	10:32	1225	18.94	331.74	596.52	8102.50	0.0455	0.0003428	6.503E-04	8.942E-01	6.622E-03	12	10	2.90	
(mm^2)	(mm^3)	Ko est			6/23/2008	10:33	1226	19.33	325.05	584.48	7778.85	0.0545	0.0004277	8.113E-04	8.585E-01	8.261E-03	6.5	5	4.18	
16.528	235.528	1			6/23/2008	10:34	1227	19.65	319.75	574.96	7527.55	0.0644	0.0005223	9.907E-04	8.308E-01	1.009E-02	8	6	4.58	
Sample Wet Wt	Sample Dry Wt	Water Content	Wet Unit wt		6/23/2008	10:35	1228	20.05	313.38	563.49	7230.20	0.0813	0.0006865	1.302E-03	7.979E-01	1.326E-02	9	7	4.00	
(gms)	(gms)	(%)	(gm/cm^3)		6/23/2008	10:36	1229	20.87	301.06	541.35	6673.20	0.1023	0.0009359	1.775E-03	7.365E-01	1.808E-02	9	6.5	5.18	
398.2	273	45.86	1.691		6/23/2008	10:37	1230	21.68	289.81	521.13	6183.87	0.1201	0.0011857	2.249E-03	6.825E-01	2.290E-02	9	6	6.45	
Mass Polar Moment of Inertia, J					6/23/2008	10:38	1231	23.76	264.44	475.51	5148.56	0.174	0.0020633	3.913E-03	5.682E-01	3.985E-02	6	4	6.45	
(gm-cm^2)					6/23/2008	10:56	1249	27.59	227.73	409.50	3818.35	0.25	0.0039973	7.581E-03	4.214E-01	7.720E-02	4.5	2	12.91	
2590.51			4.2426407	18	6/23/2008	11:30	1	17.91	350.82	630.82	9061.24	0.0097	6.536E-05	1.240E-04	1.000E+00	1.209E-03	6	5.5	1.38	
Drive Head Mass Polar Moment of Intertia, Jo				Taumax	6/23/2008	11:32	3	18.06	347.91	625.58	8911.35	0.0162	0.000111	2.105E-04	9.835E-01	2.053E-03	10	9	1.68	
(gm-cm^2)				9.289584	6/23/2008	11:34	5	18.52	339.26	610.04	8474.16	0.0288	0.0002075	3.935E-04	9.352E-01	3.839E-03	8.5	7	3.09	
37467.00				Gmax	6/23/2008	11:36	7	18.77	334.75	601.92	8249.93	0.0397	0.0002938	5.572E-04	9.105E-01	5.435E-03	10.5	8.5	3.36	
Beta				9061	6/23/2008	11:38	9	19.15	328.10	589.97	7925.77	0.0484	0.0003728	7.071E-04	8.747E-01	6.897E-03	14.5	12	3.01	
0.26000				Gam Ref	6/23/2008	11:40	11	19.54	321.56	578.20	7612.54	0.0574	0.0004603	8.731E-04	8.401E-01	8.516E-03	7	5	5.36	
				0.001025	6/23/2008	11:42	13	19.77	317.81	571.47	7436.45	0.0671	0.0005509	1.045E-03	8.207E-01	1.019E-02	8	6.5	3.30	
					6/23/2008	11:44	15	19.95	314.95	566.32	7302.86	0.0754	0.0006304	1.196E-03	8.060E-01	1.166E-02	8	6	4.58	
					6/23/2008	11:46	17	20.54	305.90	550.05	6889.35	0.0904	0.0008011	1.519E-03	7.603E-01	1.482E-02	9	6.5	5.18	
					6/23/2008	11:48	19	21.21	296.24	532.67	6460.97	0.1058	0.0009998	1.896E-03	7.131E-01	1.850E-02	7.5	5	6.45	
					6/23/2008	11:50	21	24.44	257.09	462.28	4866.05	0.1751	0.0021969	4.167E-03	5.370E-01	4.064E-02	5	3	8.13	
					6/23/2008	11:52	22.99999999	34.76	180.76	325.03	2405.58	0.276	0.0070048	1.329E-02	2.655E-01	1.296E-01	5.5	2	16.10	
					6/23/2008	11:54	25	41.06	153.02	275.16	1724.01	0.388	0.0137403	2.606E-02	1.903E-01	2.542E-01	4.5	1.5	17.48	
					6/23/2008	11:57	28	19.51	322.05	579.09	7635.97	0.0138	0.0001103	2.093E-04						
			4.5825757	21	6/23/2008	12:00	1	18.14	346.37	622.82	8832.92	0.0094	6.497E-05	1.232E-04						
				Taumax	6/23/2008	12:14	15	17.55	358.02	643.76	9436.80	0.0087	5.629E-05	1.068E-04	1.000E+00	1.041E-03	5	4.5	1.68	
				9.681162	6/23/2008	12:15	16	17.70	354.98	638.31	9277.53	0.0133	8.752E-05	1.660E-04	9.832E-01	1.618E-03	7	6	2.45	
				Gmax	6/23/2008	12:16	17	18.03	348.49	626.62	8941.03	0.0267	0.0001823	3.458E-04	9.475E-01	3.370E-03	14	12	2.45	
				9436	6/23/2008	12:17	18	18.47	340.18	611.69	8520.11	0.0374	0.000268	5.083E-04	9.029E-01	4.954E-03	9	7	4.00	
				Gam Ref	6/23/2008	12:18	19	18.78	334.57	601.60	8241.15	0.0443	0.0003282	6.225E-04	8.734E-01	6.067E-03	11.5	9	3.90	
				0.001026	6/23/2008	12:19	20	19.04	330.00	593.38	8017.61	0.0522	0.0003975	7.539E-04	8.497E-01	7.348E-03	14	11	3.84	
					6/23/2008	12:20	21	19.43	323.38	581.47	7698.98	0.0616	0.0004885	9.265E-04	8.159E-01	9.030E-03	8	6	4.58	
					6/23/2008	12:21	22	19.78	317.65	571.18	7428.93	0.0734	0.0006032	1.144E-03	7.873E-01	1.115E-02	8	5.5	5.96	
					6/23/2008	12:22	22.99999999	20.69	303.68	546.06	6789.81	0.0976	0.0008776	1.664E-03	7.196E-01	1.622E-02	9	6	6.45	
					6/23/2008	12:23	24	23.61	266.12	478.53	5214.19	0.1584	0.0018547	3.518E-03	5.526E-01	3.429E-02	5	2.5	11.03	
					6/23/2008	12:24	25	27.37	229.56	412.79	3879.98	0.255	0.0040125	7.610E-03	4.112E-01	7.418E-02	6	3	11.03	
					6/23/2008	12:25	26	33.85	185.62	333.77	2536.66	0.389	0.0093625	1.776E-02	2.688E-01	1.731E-01	5	1.5	19.16	
					6/23/2008	12:34	34.99999999	38.08	165.00	296.69	2004.40	0.418	0.012732	2.415E-02	2.124E-01	2.354E-01	4.5	1	23.94	
					6/23/2008	12:39	39.99999999	17.81	352.79	634.36	9163.28	0.0107	7.129E-05	1.352E-04						

Test C G and D vs. Shearing Strain

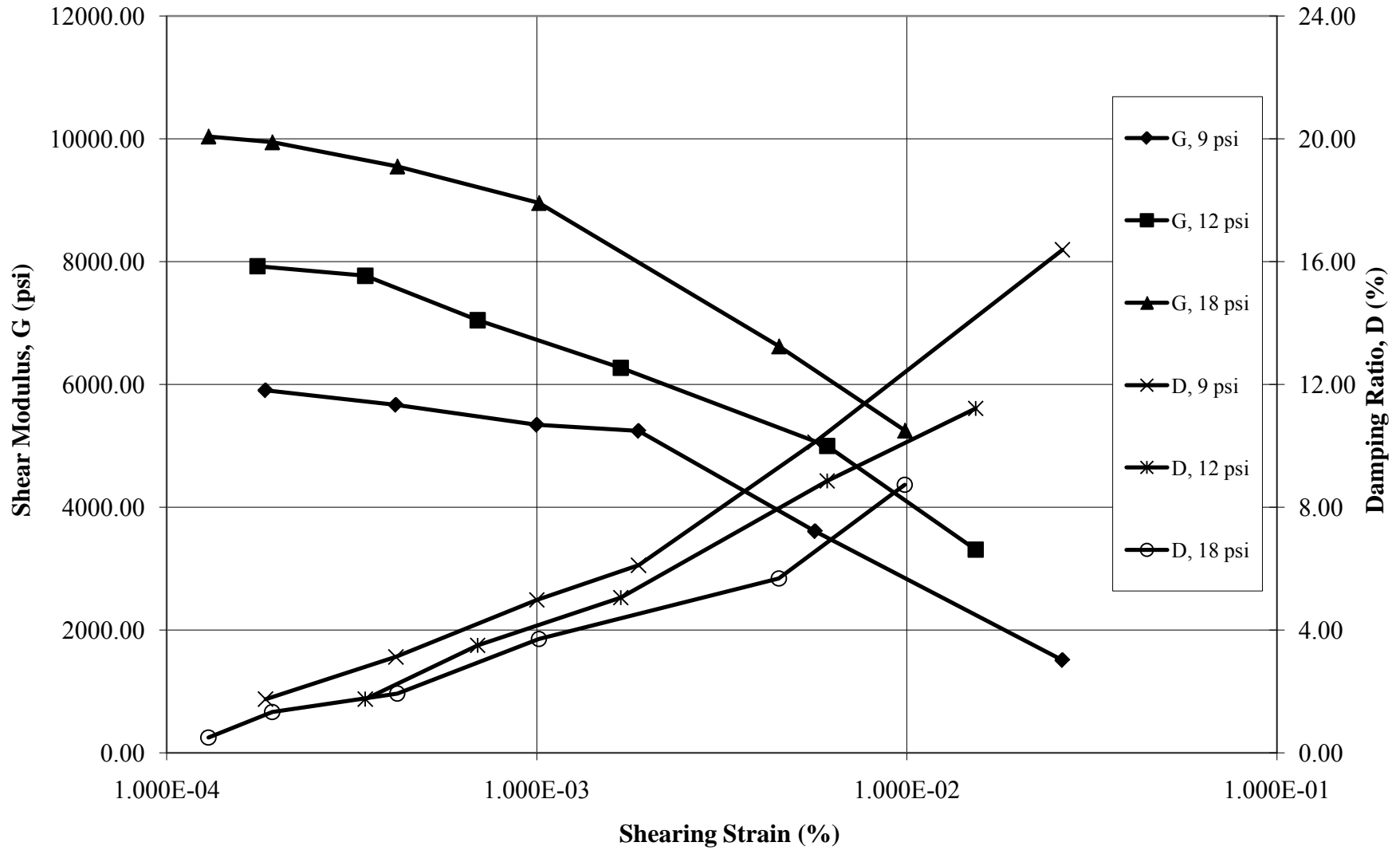


Test C G/Gmax vs. Gamma/Gamma Ref

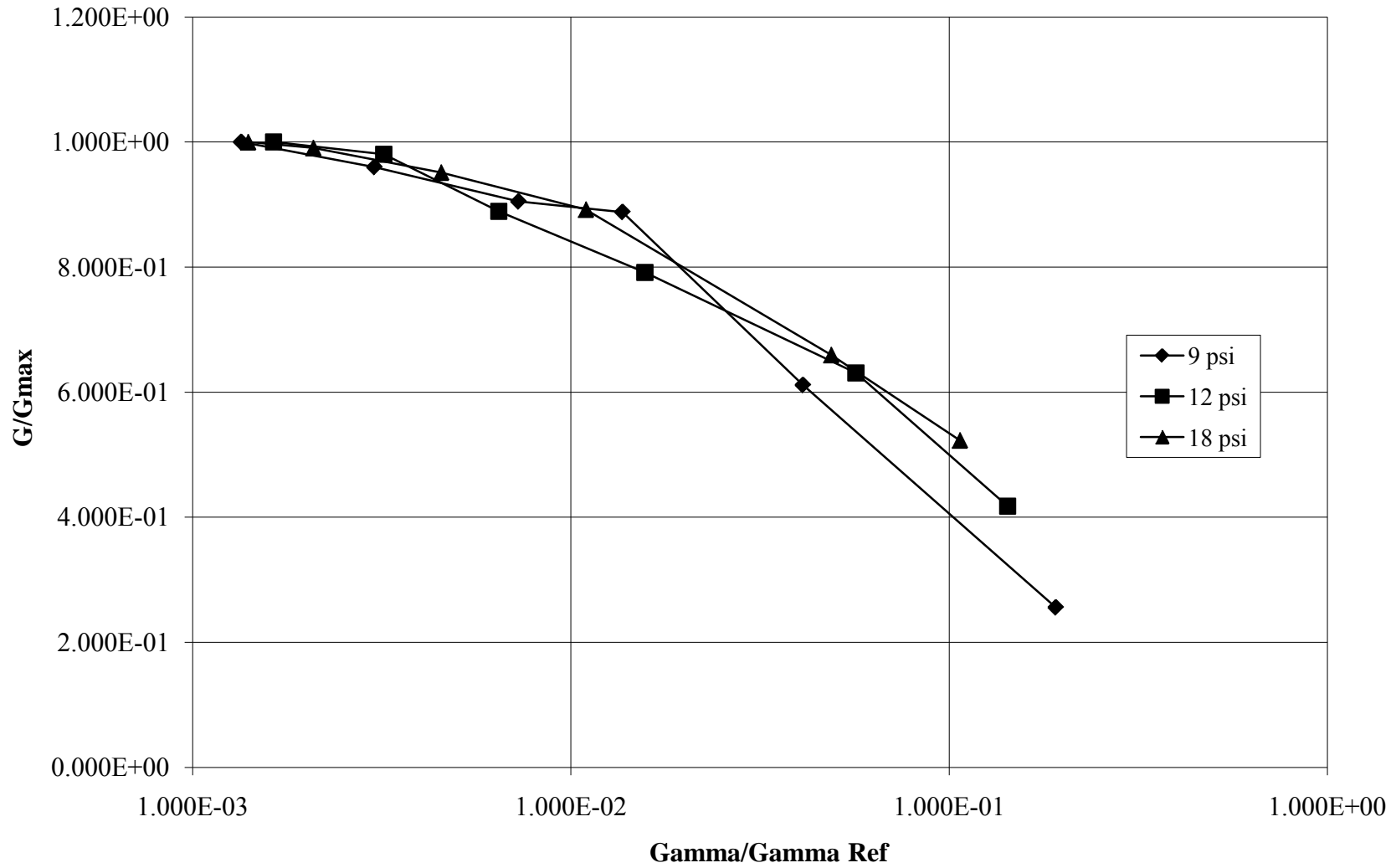


Sample																			
WB6 L-1 95-97				Conf. Pres	Date	Time	Elapsed Time	Period	Freq	Shear Wave	G	Accel Volts	Accel Disp	Strain	G/Gmax	Gam/Gam Re	Z	Z+1	Damping
Inside Dia	Outside Dia	Length		(psi)		(clock)	(min)	(msec)	(rad/sec)	(ft/sec)	(psi)	(volts rms)	(cm p-p)	(% s-a)					(%)
				9	7/7/2008	14:40	1	22.88	274.61	465.35	5568.70	0.0092	0.0001012	1.919E-04	9.432E-01	1.396E-03			
3.937	6.0452	14.25	Meas 1	Taumax	7/7/2008	20:58	378	22.22	282.77	479.17	5904.42	0.0094	9.749E-05	1.849E-04	1.000E+00	1.345E-03	12.5	11.2	1.75
			Meas 2	8.114849	7/7/2008	21:11	391	22.68	277.04	469.45	5667.34	0.0203	0.0002193	4.160E-04	9.599E-01	3.027E-03	7.3	6	3.12
			Meas 3	Gmax	7/7/2008	21:17	397	23.36	268.97	455.79	5342.20	0.046	0.0005273	1.000E-03	9.048E-01	7.276E-03	13.4	9.8	4.98
3.937	6.0452	14.25	Average	5904	7/7/2008	21:18	398	23.58	266.46	451.53	5242.98	0.085	0.0009927	1.883E-03	8.880E-01	1.370E-02	9.1	6.2	6.11
		C est (psi)	Phi est (deg)	Gam Ref	7/7/2008	21:19	399	28.42	221.08	374.64	3609.25	0.1755	0.0029775	5.647E-03	6.113E-01	4.109E-02	8.5	4.5	10.12
Sample X-sec	Sample Volume	7	7.5	0.001374	7/7/2008	21:20	400	43.95	142.96	242.26	1509.20	0.342	0.0138762	2.632E-02	2.556E-01	1.915E-01	7	2.5	16.39
(mm^2)	(mm^3)	Ko est		12															
16.528	235.528	1		Taumax															
Sample Wet Wt	Sample Dry Wt	Water Content	Wet Unit wt	8.506427	7/8/2008	8:01	1	22.58	278.26	471.53	5717.65	0.058	0.0006212	1.178E-03					
(gms)	(gms)	(%)	(gm/cm^3)	Gmax	7/8/2008	10:56	176	19.18	327.59	555.12	7924.44	0.012	9.273E-05	1.759E-04	1.000E+00	1.638E-03			
449.7	350.1	28.45	1.909	7924	7/8/2008	10:57	177	19.37	324.38	549.67	7769.74	0.023	0.0001813	3.438E-04	9.805E-01	3.203E-03	12.5	11.2	1.75
Mass Polar Moment of Inertia, J				Gam Ref	7/8/2008	10:56	176	20.34	308.91	523.46	7046.34	0.042	0.000365	6.922E-04	8.892E-01	6.449E-03	7.6	6.1	3.50
(gm-cm^2)				0.001074	7/8/2008	10:57	177	21.56	291.43	493.84	6271.45	0.091	0.0008885	1.685E-03	7.915E-01	1.570E-02	12.5	9.1	5.05
2925.55				18	7/8/2008	10:58	178	24.15	260.17	440.88	4998.40	0.262	0.0032097	6.088E-03	6.308E-01	5.671E-02	7.5	4.3	8.85
Drive Head Mass Polar Moment of Intertia, Jo				Taumax	7/8/2008	10:59	179	29.68	211.70	358.73	3309.31	0.437	0.008086	1.534E-02	4.176E-01	1.429E-01	8.5	4.2	11.22
(gm-cm^2)				9.289584															
37467.00				Gmax															
Beta				10039	7/8/2008	11:00	1	20.69	303.68	514.60	6809.96	0.076	0.0006834	1.296E-03					
0.27590				Gam Ref	7/8/2008	18:08	429	18.03	348.49	590.53	8967.56	0.0088	6.009E-05	1.140E-04					
				0.000925	7/9/2008	13:54	1615	17.04	368.73	624.83	10039.83	0.0112	6.831E-05	1.296E-04	1.000E+00	1.400E-03	6.5	6.3	0.50

Test D G and D vs. Shearing Strain

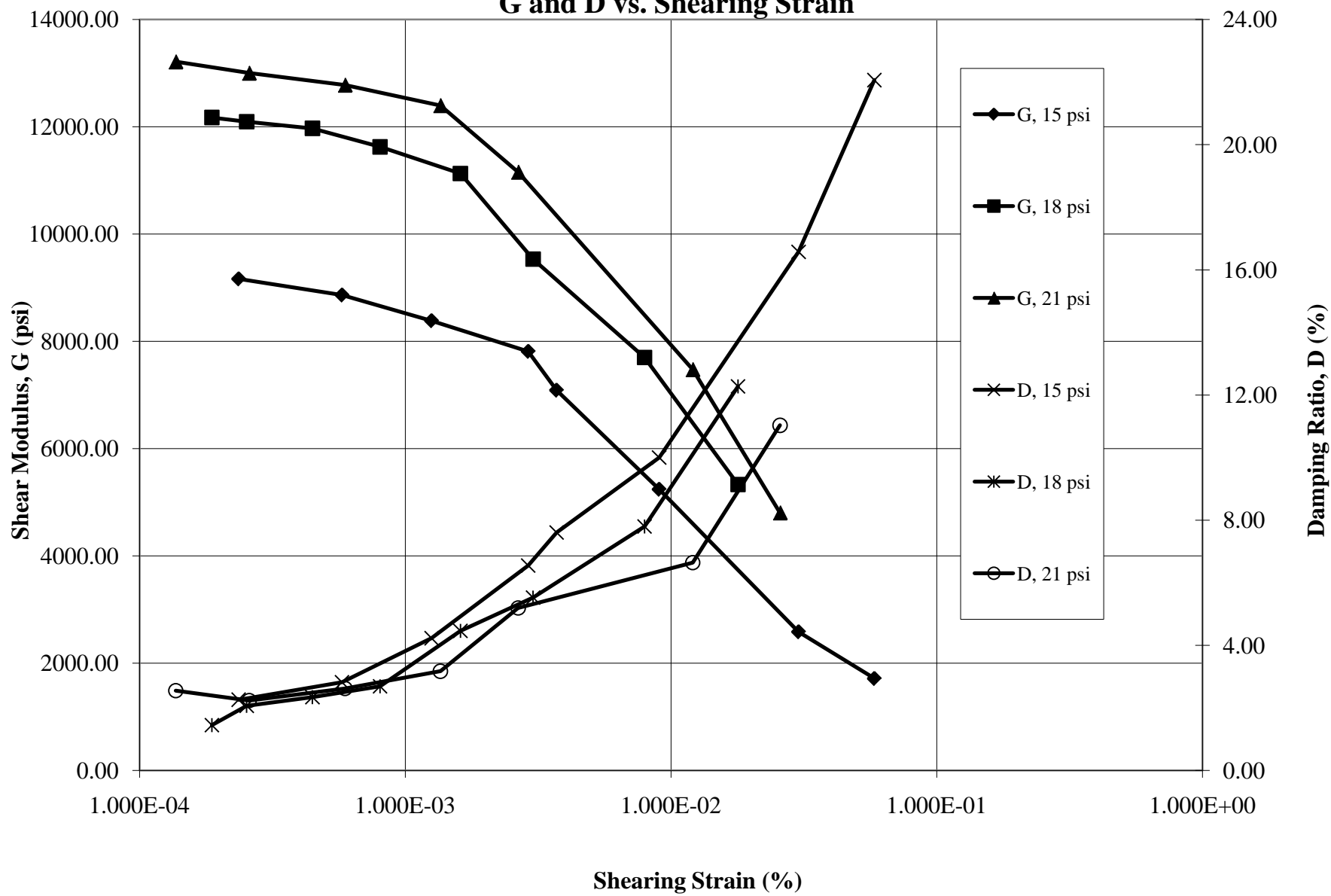


WB-6-95-97
G/Gmax vs. Gamma/Gamma Ref



Sample	Test E	Inside Dia	Outside Dia	Length	Conf. Press	Date	Time	Elapsed Time	Period	Freq	Shear Wave	G	Accel Volts	Accel Disp	Strain	G/Gmax	Gam/Gam Ref	Z	Z+1	Damping
		(cm)	(cm)	(cm)	(psi)		(clock)	(min)	(msec)	(rad/sec)	(ft/sec)	(psi)	(volts rms)	(cm p-p)	(% p-p)					(%)
		3.937	6.0452	14.25	15	2/24/2009	17:01	1	30.04	209.16	373.68	3224.32	0.0638	1.2093E-03	4.587E-03	3.519E-01	2.362E-02			
					Meas 1	Taumax	2/24/2009	18:57	117	21.34	294.43	6389.24	0.0838	8.0160E-04	3.041E-03	6.973E-01	1.566E-02			
					Meas 2	8.8980054	2/25/2009	10:51	1071	17.82	352.59	629.93	0.00933	6.2233E-05	2.361E-04	1.000E+00	1.215E-03	8.3	7.2	2.26
					Meas 3	Gmax	2/25/2009	10:52	1072	18.12	346.75	619.50	0.0221	1.5242E-04	5.782E-04	9.672E-01	2.977E-03	8	6.7	2.82
		3.937	6.0452	14.25	Average	9162.68	2/25/2009	10:52	1072	18.63	337.26	602.54	0.0454	3.3099E-04	1.256E-03	9.149E-01	6.464E-03	9	6.9	4.23
				C est (psi)	Phi est (deg)	Gam Ref	2/25/2009	10:53	1073	19.30	325.55	581.62	0.0978	7.6521E-04	2.903E-03	8.525E-01	1.494E-02	8	5.3	6.55
Sample X-sec	Sample Volume	7	7.5	0.0009711	2/25/2009	10:59	1079	20.26	310.13	554.06	7088.58	0.1134	9.7773E-04	3.709E-03	7.736E-01	1.910E-02	10	6.2	7.61	
(mm^2)	(mm^3)	Ko est			2/25/2009	11:04	1084	23.56	266.69	476.46	5241.89	0.204	2.3785E-03	9.022E-03	5.721E-01	4.645E-02	9	4.8	10.00	
16.528	235.528	1			2/25/2009	11:09	1089	33.54	187.33	334.68	2586.50	0.337	7.9631E-03	3.021E-02	2.823E-01	1.555E-01	8.5	3	16.58	
Sample Wet Wt	Sample Dry Wt	Water Content	Wet Unit wt			2/25/2009	11:25	1105	41.18	152.58	272.59	0.431	1.5352E-02	5.824E-02	1.873E-01	2.998E-01	10	2.5	22.06	
(gms)	(gms)	(%)	(gm/cm^3)			2/25/2009	11:26	1106	22.12	284.05	507.47	0.0597	6.1358E-04	2.327E-03						
403.8	290.6	38.95	1.714		18	2/25/2009	11:37	1	19.16	327.93	585.87	0.00743	5.7294E-05	2.173E-04	6.511E-01	1.424E-03				
Mass Polar Moment of Inertia, J				Taumax	2/25/2009	16:00	264	16.28	385.95	689.52	10978.15	0.00918	5.1107E-05	1.939E-04	9.018E-01	1.270E-03				
(gm-cm^2)				9.2895836	2/26/2009	12:38	1502	15.46	406.42	726.09	12173.60	0.00983	4.9351E-05	1.872E-04	1.000E+00	1.227E-03	9.2	8.4	1.45	
2626.94				Gmax	2/26/2009	12:39	1503	15.51	405.11	723.75	12095.24	0.0132	6.6700E-05	2.530E-04	9.936E-01	1.658E-03	12.3	10.8	2.07	
Drive Head Mass Polar Moment of Intertia, Jo				12173.60	2/26/2009	12:40	1504	15.59	403.03	720.03	11971.43	0.0231	1.1793E-04	4.473E-04	9.834E-01	2.931E-03	9.5	8.2	2.34	
(gm-cm^2)				Gam Ref	2/26/2009	12:41	1505	15.82	397.17	709.57	11625.86	0.0403	2.1186E-04	8.036E-04	9.550E-01	5.266E-03	13.5	11.4	2.69	
37467.00				0.0007631	2/26/2009	12:42	1506	16.17	388.57	694.21	11128.02	0.0774	4.2510E-04	1.613E-03	9.141E-01	1.057E-02	9	6.8	4.46	
Beta					2/26/2009	12:43	1507	17.47	359.66	642.55	9533.50	0.1245	7.9815E-04	3.028E-03	7.831E-01	1.984E-02	7.5	5.3	5.53	
0.26169					2/26/2009	12:44	1508	19.44	323.21	577.43	7699.20	0.264	2.0957E-03	7.949E-03	6.325E-01	5.209E-02	11.1	6.8	7.80	
					2/26/2009	12:45	1509	23.36	268.97	480.54	5332.03	0.411	4.7110E-03	1.787E-02	4.380E-01	1.171E-01	9.3	4.3	12.28	
					2/26/2009	12:56	1520	18.19	345.42	617.11	8793.72	0.0711	4.9415E-04	1.874E-03	7.224E-01	1.228E-02				
					21	2/26/2009	12:58	1	15.43	407.21	727.50	12220.99	0.0076	3.8008E-05	1.442E-04	9.250E-01	9.838E-04			
				Taumax	2/26/2009	13:14	17	14.91	421.41	752.87	13088.29	0.0086	4.0159E-05	1.523E-04	9.906E-01	1.039E-03				

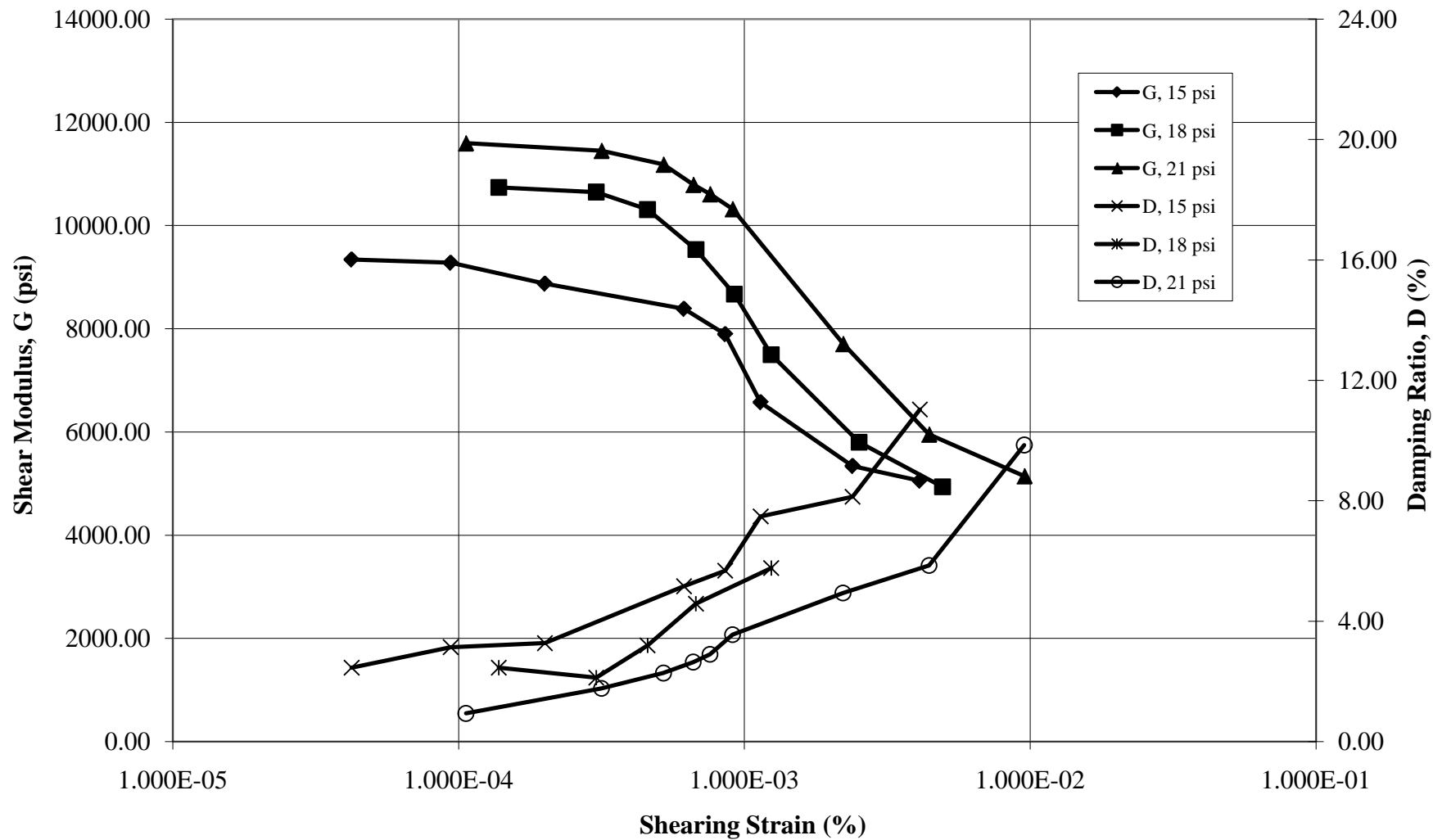
Test E G and D vs. Shearing Strain



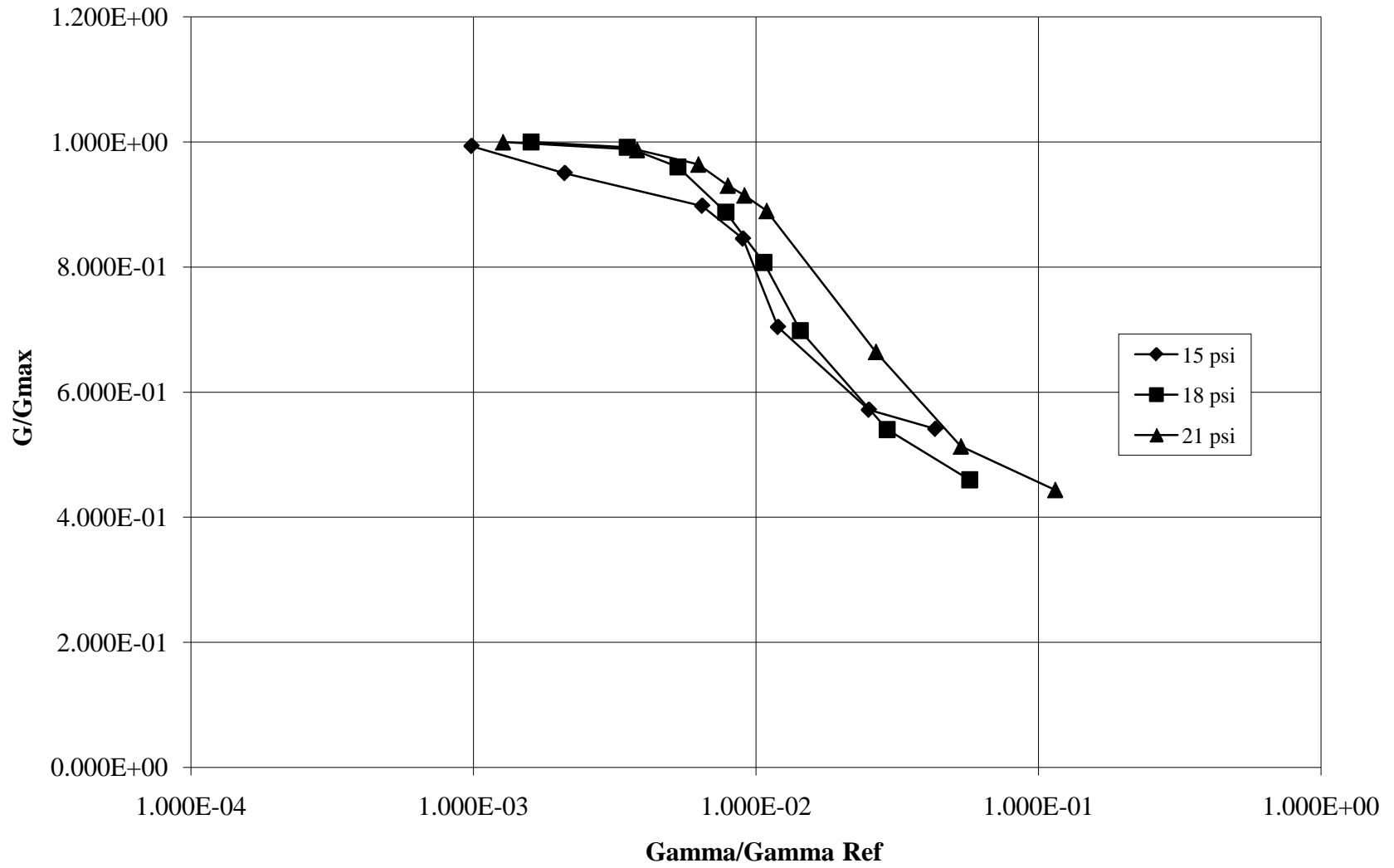
Sample	Test F	Inside Dia	Outside Dia	Length	Conf. Pres	Date	Time	Elapsed Tim	Period	Freq	Shear Wave	G	Accel Volts	Accel Displ	Strain	G/Gmax	Gam/Gam Re	Z	Z+1	Damping
(cm)	(cm)	(cm)	(cm)	(psi)	(clock)	(min)	(msec)	(rad/sec)	(ft/sec)	(psi)	(volts rms)	(cm p-p)	(% s-a)							(%)
				15	7/12/2008	17:28	1	21.99	285.73	497.88	6024.33	0.0027	2.7E-05	5.201E-05	6.450E-01	5.460E-04				
3.937	6.0452	14.25	Meas 1	Taumax	7/13/2008	9:43	976	17.66	355.79	619.95	9340.67	0.0034	2.2E-05	4.224E-05	1.000E+00	4.434E-04	3.5	3	2.45	
			Meas 2	8.898005	7/13/2008	9:44	977	17.72	354.58	617.85	9277.52	0.0075	4.9E-05	9.382E-05	9.933E-01	9.848E-04	9.5	7.8	3.14	
			Meas 3	Gmax	7/13/2008	9:45	978	18.12	346.75	604.21	8872.44	0.01533	0.00011	2.005E-04	9.499E-01	2.105E-03	7	5.7	3.27	
3.937	6.0452	14.25	Average	9340	7/13/2008	9:46	979	18.64	337.08	587.36	8384.32	0.0444	0.00032	6.146E-04	8.977E-01	6.451E-03	13	9.4	5.16	
		C est (psi)	Phi est (deg)	Gam Ref	7/13/2008	9:47	980	19.21	327.08	569.93	7894.14	0.0583	0.00045	8.571E-04	8.452E-01	8.997E-03	6	4.2	5.68	
Sample X-sec	Sample Volume	7	7.5	0.000953	7/13/2008	9:48	981	21.05	298.49	520.11	6574.39	0.0646	0.0006	1.140E-03	7.039E-01	1.197E-02	8	5	7.48	
(mm^2)	(mm^3)	Ko est			7/13/2008	9:49	982	23.36	268.97	468.68	5338.43	0.11	0.00126	2.391E-03	5.716E-01	2.510E-02	5	3	8.13	
16.528	235.528	1			7/13/2008	9:50	983	24.01	261.69	455.99	5053.30	0.179	0.00217	4.111E-03	5.410E-01	4.315E-02	5	2.5	11.03	
Sample Wet Wt	Sample Dry Wt	Water Content	Wet Unit wt		7/13/2008	9:51	984	27.7	226.83	395.25	3796.64	0.0036	5.8E-05	1.100E-04						
(gms)	(gms)	(%)	(gm/cm^3)	18	7/13/2008	10:49	1	16.47	381.49	664.74	10739.21	0.0128	7.3E-05	1.383E-04	1.000E+00	1.599E-03	7	6	2.45	
425	280.1	51.73	1.804	Taumax	7/13/2008	10:50	2	16.54	379.88	661.93	10648.50	0.0278	0.00016	3.030E-04	9.916E-01	3.503E-03	8	7	2.13	
Mass Polar Moment of Inertia, J				9.289584	7/13/2008	10:51	3	16.81	373.78	651.30	10309.18	0.0407	0.00024	4.582E-04	9.600E-01	5.297E-03	11	9	3.19	
(gm-cm^2)				Gmax	7/13/2008	10:52	4	17.48	359.45	626.34	9534.03	0.0556	0.00036	6.768E-04	8.878E-01	7.824E-03	6	4.5	4.58	
2764.86				10739.21	7/13/2008	10:53	5	18.33	342.78	597.29	8670.31	0.0689	0.00049	9.223E-04	8.074E-01	1.066E-02	8.2	5.8	5.51	
Drive Head Mass Polar Moment of Intertia, Jo				Gam Ref	7/13/2008	10:54	6	19.71	318.78	555.47	7498.70	0.0802	0.00065	1.241E-03	6.983E-01	1.435E-02	10.2	7.1	5.77	
(gm-cm^2)				0.000865	7/13/2008	10:55	7	22.41	280.37	488.55	5800.64	0.126	0.00133	2.521E-03	5.401E-01	2.914E-02	6.6	4.2	7.19	
37467.00					7/13/2008	10:56	8	24.29	258.67	450.73	4937.47	0.21	0.0026	4.936E-03	4.598E-01	5.706E-02	8.3	4.5	9.74	
Beta					7/13/2008	10:57	9	27.25	230.58	401.77	3923.07	0.0039	6.1E-05	1.154E-04						10000.0
0.26831					7/13/2008	11:07	19	24.73	254.07	442.71	4763.34	0.0151	0.00019	3.679E-04						
				21	7/13/2008	11:14	1	15.85	396.42	690.75	11595.81	0.0106	5.6E-05	1.061E-04	1.000E+00	1.271E-03	3.5	3	0.94	
				Taumax	7/13/2008	11:15	2	15.95	393.93	686.42	11450.86	0.0312	0.00017	3.162E-04	9.876E-01	3.787E-03	9.5	8	1.77	
				9.681162	7/13/2008	11:16	3	16.14	389.29	678.34	11182.85	0.0502	0.00027	5.210E-04	9.645E-01	6.240E-03	15	13	2.28	
				Gmax	7/13/2008	11:17	4	16.43	382.42	666.36	10791.56	0.0616	0.00035	6.625E-04	9.307E-01	7.934E-03	8.5	7	2.64	
				11595	7/13/2008	11:18	5	16.57	379.19	660.73	10609.98	0.0693	0.0004	7.580E-04	9.150E-01	9.079E-03	9	7	2.90	
				Gam Ref	7/13/2008	11:19	6	16.80	374.00	651.69	10321.45	0.0808	0.00048	9.085E-04	8.902E-01	1.088E-02	10	8	3.55	
				0.000835	7/13/2008	11:20	7	19.44	323.21	563.19	7708.45	0.147	0.00117	2.213E-03	6.648E-01	2.651E-02	7.5	5	4.94	
					7/13/2008	11:21	8	22.12	284.05	494.95	5953.73	0.227	0.00233	4.425E-03	5.135E-01	5.300E-02	6.5	4.5	5.85	
					7/13/2008	11:22	9	23.79	264.11	460.21	5147.19	0.423	0.00503	9.538E-03	4.439E-01	1.142E-01	6.5	3.5	9.85	

Shear Modulus, G (psi)

Test F G and D vs. Shearing Strain

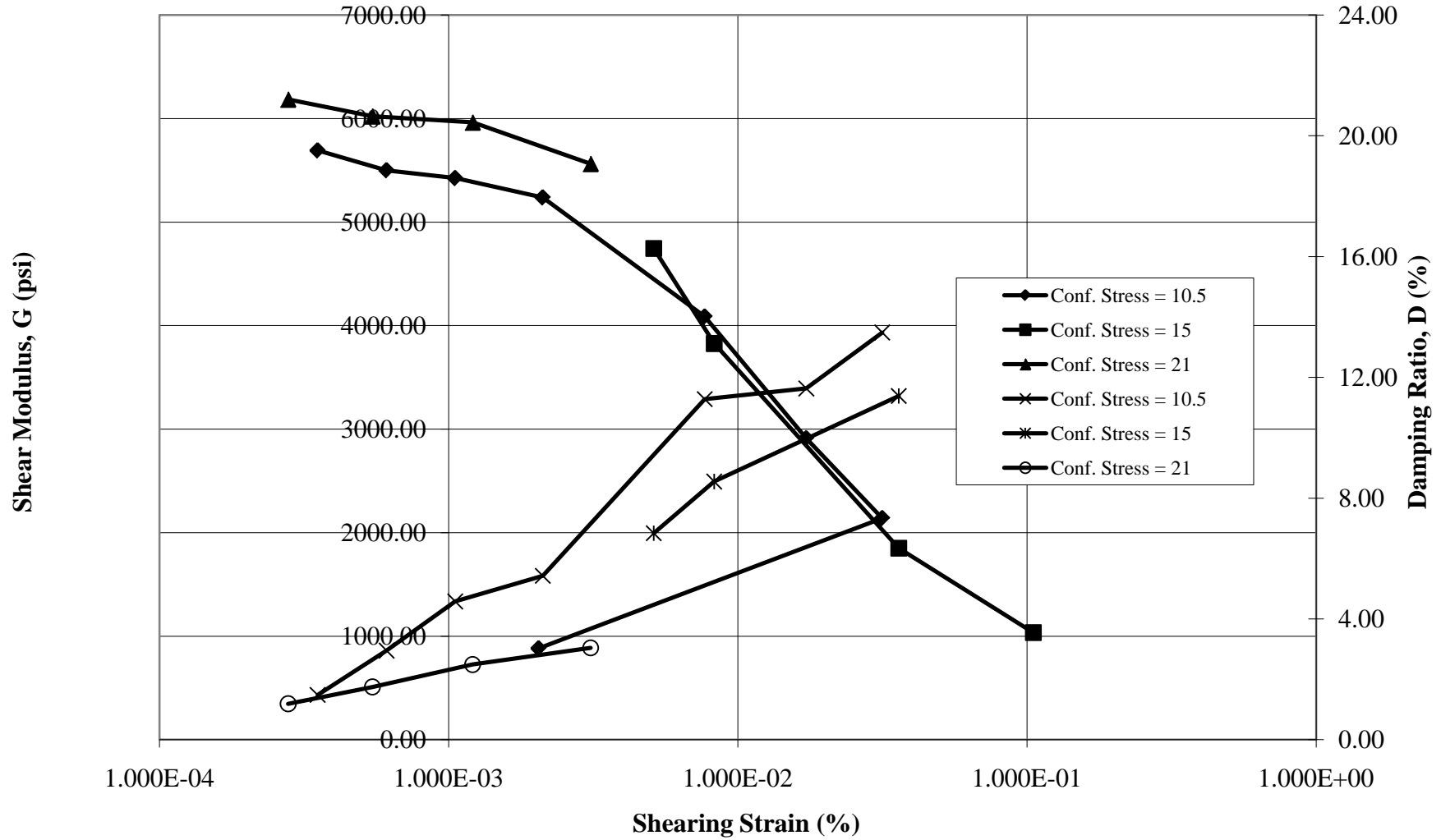


Test F
G/Gmax vs. Gamma/Gamma Ref



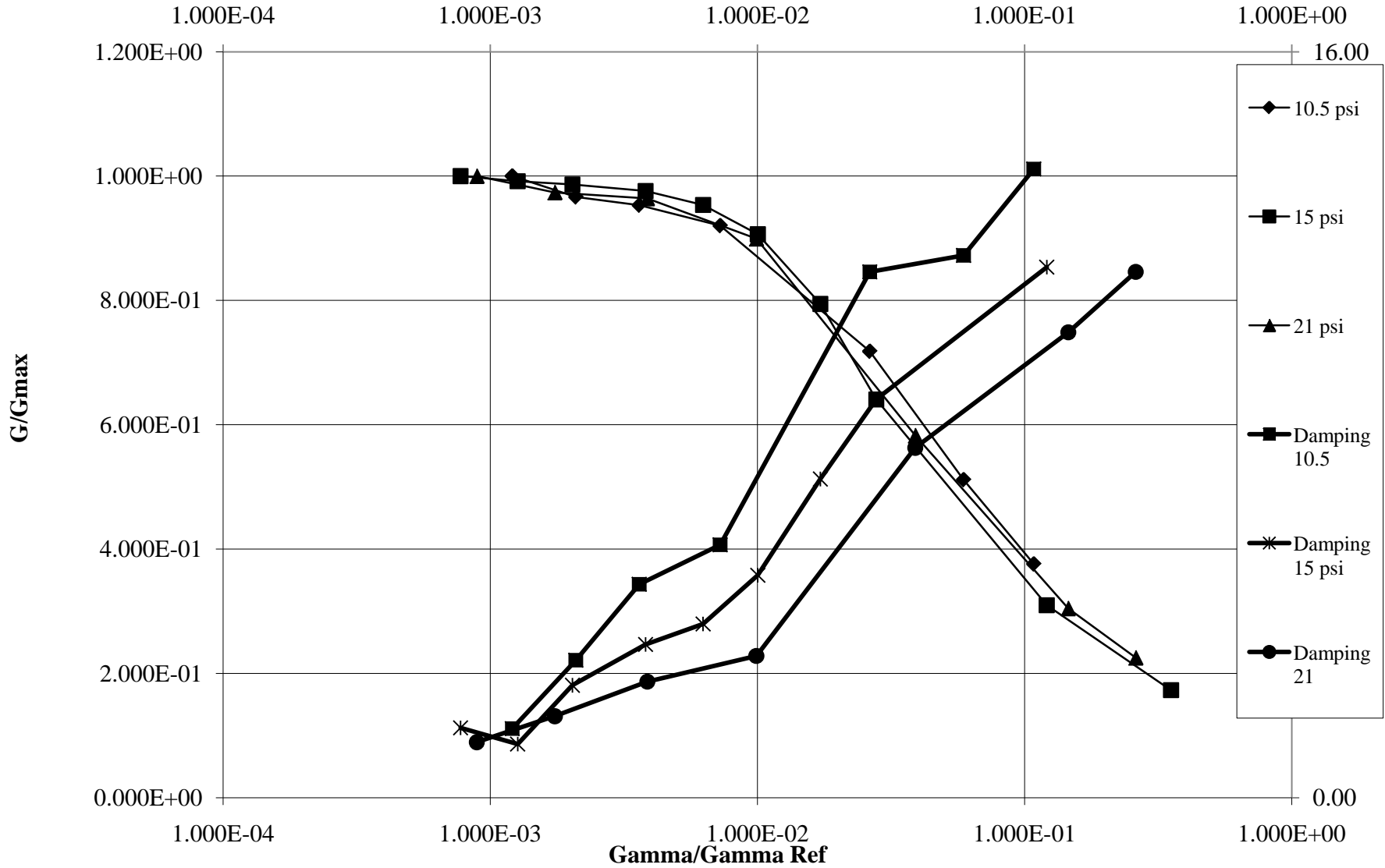
Sample	Test G	Inside Diameter (cm)	Outside Diameter (cm)	Length (cm)	Conf. Pres (psi)	Date	Time (clock)	Elapsed Time (min)	Period (msec)	Freq (rad/sec)	Shear Wave (ft/sec)	G (psi)	Accel Volts (volts rms)	Accel Disp (cm p-p)	Strain (% p-p)	G/Gmax	Gam/Gam Re	Z	Z+1	Damping (%)	
		3.937	6.0452	14.25	10.5	8/3/2008	18:28	1	29.47	213.21	389.15	3344.41	0.0068	0.000124	4.706E-04			7.5	7	1.10	
					Meas 1	Taumax	8/4/2008	10:51	984	22.59	278.14	507.67	5691.77	0.00867	9.293E-05	3.525E-04	1.000E+00	1.207E-03	9	8.2	1.48
					Meas 2	8.310638	8/4/2008	10:52	985	22.98	273.42	499.05	5500.22	0.0145	0.0001608	6.101E-04	9.663E-01	2.089E-03	6.5	5.4	2.95
					Meas 3	Gmax	8/4/2008	10:53	986	23.14	271.53	495.60	5424.42	0.0247	0.0002778	1.054E-03	9.530E-01	3.609E-03	10.8	8.1	4.58
		3.937	6.0452	14.25	Average	5691.77	8/4/2008	10:55	988	23.55	266.80	486.97	5237.19	0.0479	0.000558	2.117E-03	9.201E-01	7.248E-03	9	6.4	5.43
					Gam Ref		8/4/2008	10:58	991	26.66	235.68	430.17	4086.58	0.1357	0.0020259	7.685E-03	7.180E-01	2.632E-02	6.5	3.2	11.28
						0.00146	8/4/2008	11:01	994	31.59	198.90	363.03	2910.59	0.217	0.0045487	1.725E-02	5.114E-01	5.909E-02	10.8	5.2	11.63
							8/4/2008	11:02	995	36.85	170.51	311.21	2138.97	0.292	0.0083288	3.159E-02	3.758E-01	1.082E-01	10.5	4.5	13.49
					C est (psi)	Phi est (deg)	8/4/2008	11:03	996	57.41	109.44	199.76	881.26	0.0078	0.00054	2.048E-03					
Sample X-sec (mm^2)	Sample Volume (mm^3)	7	7.5				8/4/2008	11:04	997	28.93	217.19	396.41	3470.43	0.0065	0.0001143	4.335E-04					
					Ko est	15	8/4/2008	11:05	1	22.05	284.95	520.10	5973.96	0.00595	6.077E-05	2.305E-04	1.000E+00	7.738E-04	7.8	7.1	1.50
16.5282913	235.52815	1			Taumax		8/4/2008	11:10	6	22.14	283.79	517.99	5925.49	0.00965	9.936E-05	3.769E-04	9.919E-01	1.265E-03	8.6	8	1.15
Sample Wet (gms)	Sample Dry (gms)	Water Content (%)	Wet Unit (gm/cm^3)	8.898005			8/4/2008	11:28	24	22.2	283.03	516.59	5893.51	0.0154	0.0001594	6.047E-04	9.865E-01	2.030E-03	6.4	5.5	2.41
				Gmax			8/4/2008	11:37	33	22.32	281.50	513.81	5830.31	0.0286	0.0002993	1.135E-03	9.760E-01	3.811E-03	7.5	6.1	3.29
386.2	273	41.47	1.639719	5973.964			8/4/2008	11:38	34	22.58	278.26	507.89	5696.81	0.0459	0.0004916	1.865E-03	9.536E-01	6.260E-03	9.1	7.2	3.73
Mass Polar Moment of Inertia, J				Gam Ref			8/4/2008	11:39	35	23.16	271.29	495.17	5415.05	0.0699	0.0007876	2.987E-03	9.064E-01	1.003E-02	11.2	8.3	4.77
							8/4/2008	11:40	36	24.74	253.97	463.55	4745.48	0.105	0.0013499	5.121E-03	7.944E-01	1.719E-02	6.3	4.1	6.84
							8/4/2008	11:41	37	27.55	228.06	416.27	3826.81	0.1371	0.0021858	8.291E-03	6.406E-01	2.783E-02	7.7	4.5	8.55
							8/4/2008	11:42	38	39.63	158.55	289.38	1849.40	0.288	0.009501	3.604E-02	3.096E-01	1.210E-01	9.2	4.5	11.38
(gm-cm^2)							8/4/2008	11:42	38	53.01	118.53	216.34	1033.63	0.47	0.0277422	1.052E-01	1.730E-01	3.533E-01			
2512.44399																					
							8/4/2008	11:45	1	22.13	283.92	518.22	5930.85	0.00647	6.656E-05	2.525E-04					
Drive Head Mass Polar Moment of Intertia, Jo (gm-cm^2)					Taumax		8/4/2008	12:05	21	21.67	289.95	529.22	6185.32	0.00745	7.349E-05	2.787E-04	1.000E+00	8.905E-04	11.1	10.3	1.19
							8/4/2008	12:06	22	21.96	286.12	522.23	6023.03	0.0142	0.0001438	5.456E-04	9.738E-01	1.743E-03	12.5	11.2	1.75
37467					Gmax		8/4/2008	12:07	23	22.07	284.69	519.63	5963.14	0.0312	0.0003192	1.211E-03	9.641E-01	3.868E-03	7.6	6.5	2.49
Beta							8/4/2008	12:05	21	22.85	274.98	501.89	5562.98	0.0745	0.0008171	3.099E-03	8.994E-01	9.901E-03	9.2	7.6	3.04
0.25614337					Gam Ref		8/4/2008	12:06	22	28.39	221.32	403.95	3603.70	0.19	0.0032167	1.220E-02	5.826E-01	3.898E-02	12.5	7.8	7.51
							8/4/2008	12:07	23	39.27	160.00	292.04	1883.47	0.371	0.0120177	4.559E-02	3.045E-01	1.456E-01	8.8	4.7	9.98

LB-28A-92-93 G and D vs. Shearing Strain



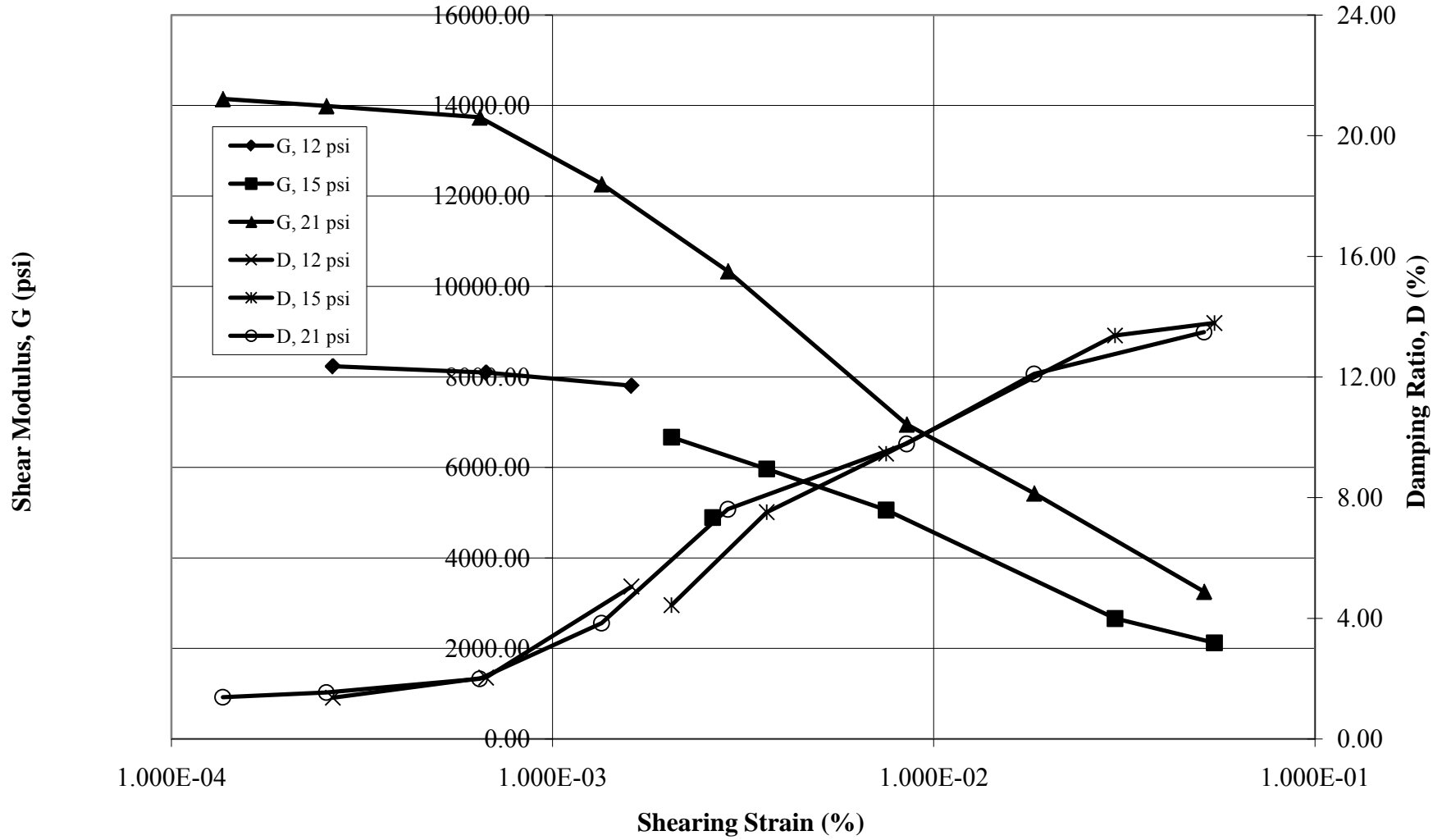
Test G

G/Gmax vs. Gamma/Gamma Ref



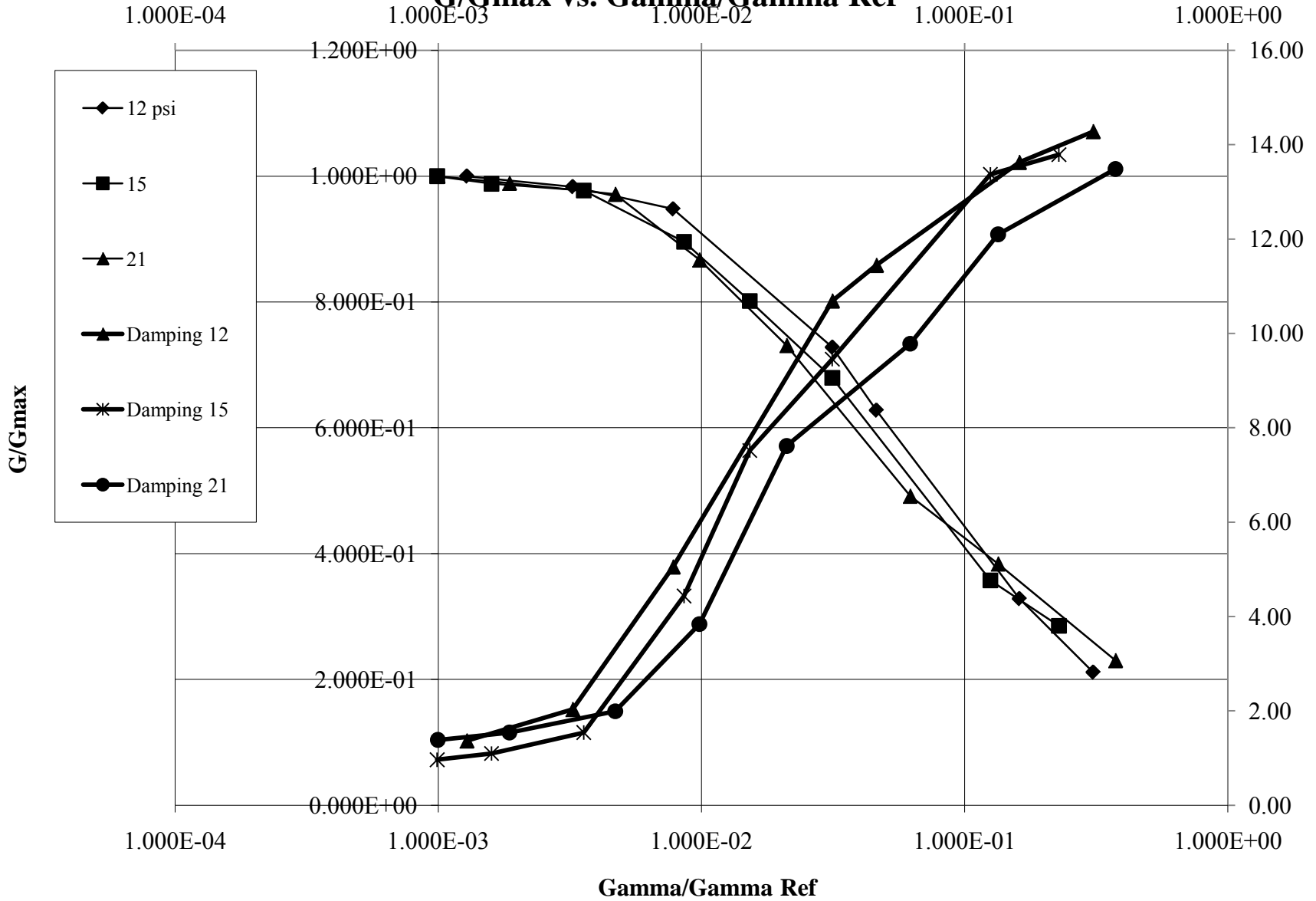
Sample	Test H	Inside Dia	Outside Dia	Length	Conf. Pres	Date	Time	Elapsed Tim	Period	Freq	Shear Wave	G	Accel Volts	Accel Disp	Strain	G/Gmax	Gam/Gam Re	Z	Z+1	Damping
(cm)	(cm)	(cm)	(cm)	(psi)	(clock)	(min)	(msec)	(rad/sec)	(ft/sec)	(psi)	(volts rms)	(cm p-p)	(% p-p)							(%)
				12	8/14/2008	18:54	1	19.74	318.30	580.96	7453.93	0.00745	6.09786E-05	2.313E-04						
3.937	6.0452	14.25	Meas 1	Taumax	8/15/2008	10:27	934	18.78	334.57	610.66	8235.47	0.00943	6.98602E-05	2.650E-04	1.000E+00	1.283E-03	8.5	7.8	1.37	
			Meas 2	8.506427	8/15/2008	10:28	935	18.94	331.74	605.50	8096.92	0.0234	0.000176321	6.688E-04	9.832E-01	3.238E-03	7.5	6.6	2.03	
			Meas 3	Gmax	8/15/2008	10:29	936	19.29	325.72	594.52	7805.76	0.0543	0.000424416	1.610E-03	9.478E-01	7.793E-03	13.6	9.9	5.05	
				8235.474	8/15/2008	10:30	937	22.01	285.47	521.05	5995.70	0.168	0.001709529	6.485E-03	7.280E-01	3.139E-02	9.2	4.7	10.69	
					8/15/2008	10:31	938	23.70	265.11	483.89	5171.10	0.213	0.002513063	9.533E-03	6.279E-01	4.615E-02	7.8	3.8	11.45	
					8/15/2008	10:32	939	32.77	191.74	349.96	2704.75	0.389	0.008774644	3.328E-02	3.284E-01	1.611E-01	11.3	4.8	13.63	
					8/15/2008	10:34	941	40.83	153.89	280.88	1742.29	0.478	0.01673839	6.349E-02	2.116E-01	3.074E-01	13	5.3	14.28	
3.937	6.0452	14.25	Average		8/15/2008	10:36	943	24.35	258.04	470.97	4898.71	0.014	0.000174362	6.614E-04						
		C est (psi)	Phi est (deg)	Gam Ref																
		7	7.5	0.001033																
		Ko est		15	8/15/2008	10:35	1	20.56	305.60	557.79	6871.22	0.00953	8.46187E-05	3.210E-04						
Sample X-sec	Sample Volume	1		Taumax	8/16/2008	10:55	1461	19.88	316.06	576.87	7349.32	0.00667	5.53714E-05	2.100E-04						
(mm^2)	(mm^3)			8.898005	8/16/2008	11:06	1472	19.75	318.14	580.67	7446.39	0.00761	6.23514E-05	2.365E-04	1.000E+00	9.897E-04	8.5	8	0.96	
16.528	235.528			Gmax	8/16/2008	11:18	1484	19.87	316.21	577.16	7356.72	0.0121	0.000100348	3.806E-04	9.880E-01	1.593E-03	7.5	7	1.10	
Sample Wet Wt	Sample Dry Wt	Water Content	Wet Unit wt	7446.39	8/16/2008	11:28	1494	19.98	314.47	573.99	7275.94	0.0268	0.000224726	8.524E-04	9.771E-01	3.567E-03	13	11.8	1.54	
(gms)	(gms)	(%)	(gm/cm^3)	Gam Ref	8/16/2008	11:38	1504	20.87	301.06	549.51	6668.60	0.0591	0.000540704	2.051E-03	8.955E-01	8.582E-03	7.4	5.6	4.44	
386.2	273	41.47	1.640	0.001195	8/16/2008	11:39	1505	22.06	284.82	519.87	5968.55	0.094	0.000960873	3.645E-03	8.015E-01	1.525E-02	8.5	5.3	7.52	
Mass Polar Moment of Inertia, J					8/16/2008	11:40	1506	23.96	262.24	478.64	5059.48	0.164	0.001977628	7.502E-03	6.795E-01	3.139E-02	9.6	5.3	9.45	
					8/16/2008	11:43	1509	33.03	190.23	347.21	2662.33	0.344	0.007883201	2.990E-02	3.575E-01	1.251E-01	9.5	4.1	13.37	
					8/16/2008	11:45	1511	36.98	169.91	310.12	2123.96	0.5	0.014362527	5.448E-02	2.852E-01	2.280E-01	8.8	3.7	13.79	
					8/16/2008	12:04		24.36	257.93	470.78	4894.69	0.0556	0.000693037	2.629E-03						
(gm-cm^2)																				
2512.44																				
Drive Head Mass Polar Moment of Intertia, Jo				21	8/16/2008	12:15	1	18.72	335.64	612.62	8288.35	0.00746	5.49133E-05	2.083E-04						
(gm-cm^2)				Taumax	8/16/2008	13:25	71	14.87	422.54	771.23	13135.84	0.00845	3.92469E-05	1.489E-04						
37467.00				9.681162	8/16/2008	16:55	281	14.55	431.83	788.19	13719.99	0.0098	4.35792E-05	1.653E-04	9.700E-01	1.208E-03				
Beta				Gmax	8/17/2008	15:05	1611	14.33	438.46	800.30	14144.49	0.00833	3.59306E-05	1.363E-04	1.000E+00	9.957E-04	12	11	1.38	
0.25614				14144.49	8/17/2008	15:06	1612	14.41	436.03	795.85	13987.88	0.0154	6.71701E-05	2.548E-04	9.889E-01	1.861E-03	6.5	5.9	1.54	
				Gam Ref	8/17/2008	15:07	1613	14.54	432.13	788.74	13738.87	0.0382	0.000169636	6.435E-04	9.713E-01	4.701E-03	6.8	6	1.99	
				0.000684	8/17/2008	15:18	1624	15.39	408.26	745.17	12263.16	0.0712	0.000354229	1.344E-03	8.670E-01	9.816E-03	11.2	8.8	3.84	
					8/17/2008	15:18	1624	16.76	374.89	684.26	10340.27	0.1288	0.00075996	2.883E-03	7.310E-01	2.106E-02	7.1	4.4	7.62	
					8/17/2008	15:18	1624	20.44	307.40	561.07	6952.13	0.255	0.00223784	8.489E-03	4.915E-01	6.201E-02	9.8	5.3	9.78	
					8/17/2008	15:18	1624	23.13	271.65	495.82	5429.11	0.43	0.004832221	1.833E-02	3.838E-01	1.339E-01	7.7	3.6	12.10	
					8/17/2008	15:25	1631	29.87	210.35	383.94	3255.44	0.72	0.013493667	5.119E-02	2.302E-01	3.739E-01	7	3	13.49	
					8/17/2008	15:30	1636	18.04	348.29	635.71	8924.97	0.0739	0.000505178	1.916E-03						
					8/17/2008	15:40	1646	17.52	358.63	654.58	9462.62	0.0785	0.000506133	1.920E-03						

Test H G and D vs. Shearing Strain



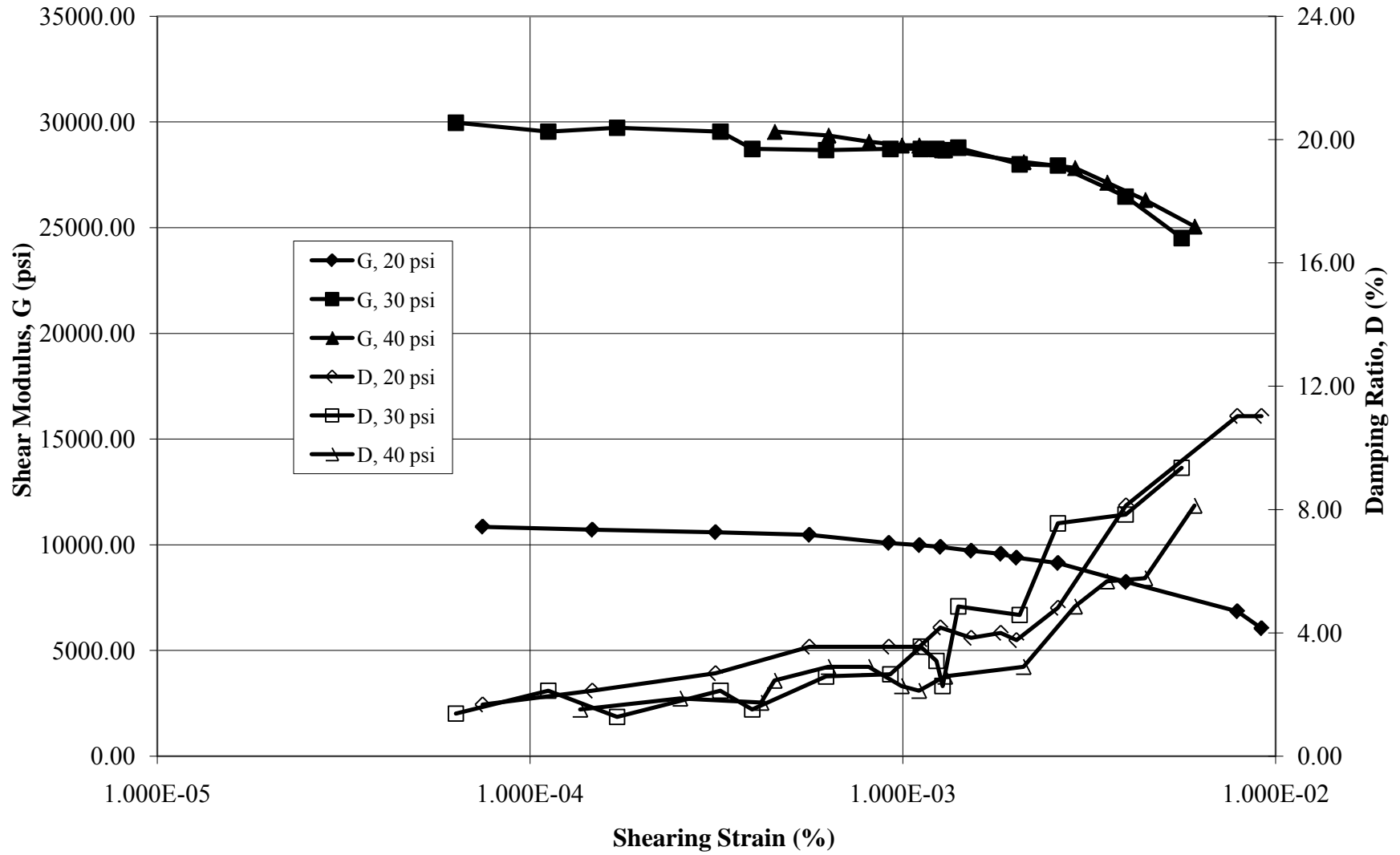
Test H

G/Gmax vs. Gamma/Gamma Ref

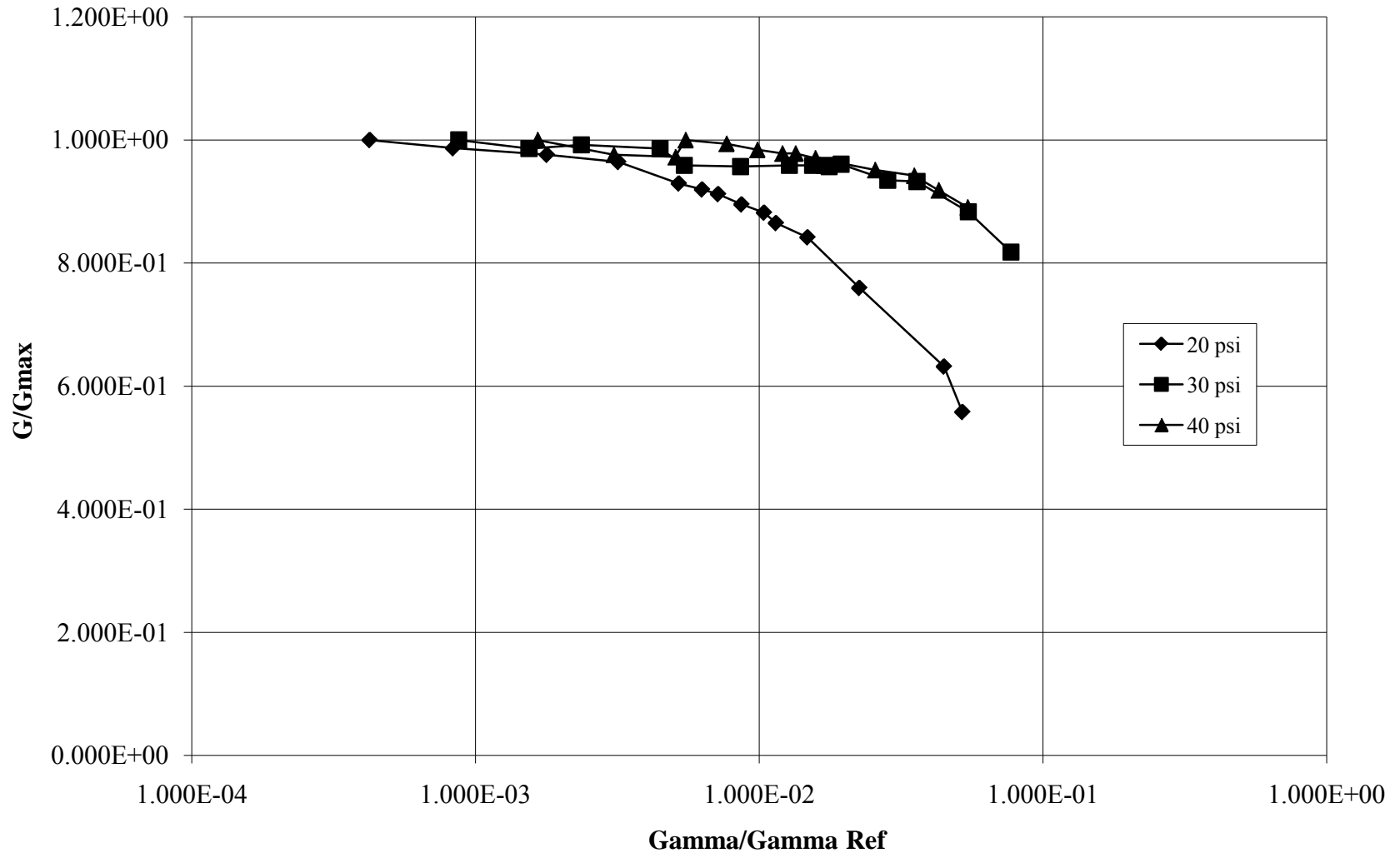


Sample				Conf. Pres	Date	Time	Lapsed Tim	Period	Freq	Shear Wav	G	Accel Volts	Accel Dis	Strain	G/Gmax	Gam/Gam Re	Z	Z+1	Damping
Test I	Inside Dia	Outside Dia	Length	(psi)		(clock)	(min)	(msec)	(rad/sec)	(ft/sec)	(psi)	(volts rms)	(cm p-p)	(% p-p)					(%)
	(cm)	(cm)	(cm)	20	3/19/2009	11:53	1	19.95	314.95	601.02	7289.54	0.0036	3E-05	1.142E-04	6.717E-01	6.487E-04			
3.937	6.0452	14.25	Meas 1	Taumax	3/19/2009	11:56	4	19.55	321.39	613.31	7590.89	0.0036	2.9E-05	1.096E-04	6.994E-01	6.229E-04			
			Meas 2	9.550636	3/19/2009	14:53	181	17.22	364.88	696.30	9784.07	0.0031	1.9E-05	7.324E-05					
			Meas 3	Gmax	3/19/2009	15:02	190	16.91	371.57	709.07	10146.09	0.0035	2.1E-05	7.974E-05					
3.937	6.0452	14.25	Average	10853	3/19/2009	15:06	194	16.78	374.44	714.56	10303.91	0.0035	2.1E-05	7.852E-05					
		C est (psi)	Phi est (deg)	Gam Ref	3/19/2009	15:52	240	16.35	384.29	733.35	10853.02	0.0035	2E-05	7.455E-05	1.000E+00	4.236E-04	5	4.5	1.68
		7	7.5	0.00088	3/19/2009	15:53	241	16.46	381.72	728.45	10708.44	0.0068	3.9E-05	1.468E-04	9.867E-01	8.341E-04	4	3.5	2.13
		Ko est			3/19/2009	15:54	242	16.55	379.65	724.49	10592.29	0.0144	8.3E-05	3.143E-04	9.760E-01	1.786E-03	4.5	3.8	2.69
Sample X-sec	Sample Volume	1			3/19/2009	15:55	243	16.65	377.37	720.14	10465.44	0.0254	0.00015	5.611E-04	9.643E-01	3.188E-03	7.5	6	3.55
(mm^2)	(mm^3)				3/19/2009	15:56	244	16.96	370.47	706.98	10086.36	0.0400	0.00024	9.168E-04	9.294E-01	5.209E-03	10	8	3.55
16.528	235.528				3/19/2009	15:57	245	17.05	368.52	703.24	9980.16	0.0478	0.00029	1.107E-03	9.196E-01	6.291E-03	12.5	10	3.55
Sample Wet Wt	Sample Dry Wt	Water Content	Wet Unit wt		3/19/2009	15:58	246	17.12	367.01	700.37	9898.71	0.0540	0.00033	1.261E-03	9.121E-01	7.165E-03	6.5	5	4.18
(gms)	(gms)	(%)	(gm/cm^3)		3/19/2009	15:59	247	17.28	363.61	693.88	9716.25	0.0641	0.0004	1.525E-03	8.953E-01	8.665E-03	7	5.5	3.84
352.9	277.2	27.31	1.498		3/19/2009	16:00	248	17.41	360.90	688.70	9571.69	0.0758	0.00048	1.831E-03	8.819E-01	1.040E-02	9	7	4.00
Mass Polar Moment of Inertia, J					3/19/2009	16:01	249	17.58	357.41	682.04	9387.46	0.0819	0.00053	2.017E-03	8.650E-01	1.146E-02	9.5	7.5	3.76
(gm-cm^2)					3/19/2009	16:02	250	17.82	352.59	672.86	9136.31	0.1030	0.00069	2.606E-03	8.418E-01	1.481E-02	11.5	8.5	4.81
2295.81					3/19/2009	16:03	251	18.76	334.92	639.14	8243.67	0.1415	0.00105	3.968E-03	7.596E-01	2.254E-02	5	3	8.13
Drive Head Mass Polar Moment of Intertia, Jo					3/19/2009	16:04	252	20.57	305.45	582.90	6856.74	0.2340	0.00208	7.889E-03	6.318E-01	4.482E-02	6	3	11.03
(gm-cm^2)					3/19/2009	16:05	253	21.89	287.03	547.75	6054.73	0.2400	0.00242	9.163E-03	5.579E-01	5.206E-02	5	2.5	11.03
37467.00					3/19/2009	16:06	254	16.38	383.59	732.01	10813.30	0.0032	1.8E-05	6.841E-05					
Beta				30	3/19/2009	16:20	1	15.98	393.19	750.33	11361.42	0.0035	1.9E-05	7.121E-05					
0.24499				Taumax	3/25/2009	13:43	8484	9.84	638.54	1218.53	29963.73	0.0082	1.7E-05	6.326E-05	1.000E+00	8.730E-04	6	5.5	1.38
				10.8559	3/25/2009	13:44	8485	9.91	634.02	1209.92	29541.92	0.0143	2.9E-05	1.119E-04	9.859E-01	1.544E-03	8	7	2.13
				Gmax	3/25/2009	13:45	8486	9.88	635.95	1213.59	29721.60	0.0220	4.5E-05	1.711E-04	9.919E-01	2.361E-03	13	12	1.27
				29963	3/25/2009	13:46	8487	9.91	634.02	1209.92	29541.92	0.0414	8.5E-05	3.240E-04	9.859E-01	4.471E-03	12	10.5	2.13
				Gam Ref	3/25/2009	13:47	8488	10.05	625.19	1193.06	28724.60	0.0490	0.0001	3.943E-04	9.587E-01	5.442E-03	5.5	5	1.52
				0.000362	3/25/2009	13:48	8489	10.06	624.57	1191.88	28667.52	0.0772	0.00016	6.225E-04	9.568E-01	8.591E-03	10	8.5	2.59
					3/25/2009	13:50	8491	10.05	625.19	1193.06	28724.60	0.1150	0.00024	9.255E-04	9.587E-01	1.277E-02	6.5	5.5	2.66
					3/25/2009	13:51	8492	10.05	625.19	1193.06	28724.60	0.1388	0.00029	1.117E-03	9.587E-01	1.542E-02	7.5	6	3.55
					3/25/2009	13:52	8493	10.05	625.19	1193.06	28724.60	0.1529	0.00032	1.230E-03	9.587E-01	1.698E-02	8.5	7	3.09
					3/25/2009	13:53	8494	10.06	624.57	1191.88	28667.52	0.1584	0.00034	1.277E-03	9.568E-01	1.763E-02	7.5	6.5	2.28
					3/25/2009	13:54	8495	10.04	625.82	1194.25	28781.84	0.1754	0.00037	1.409E-03	9.606E-01	1.944E-02	9.5	7	4.86
					3/25/2009	13:55	8496	10.18	617.21	1177.83	27995.65	0.2490	0.00054	2.056E-03	9.343E-01	2.837E-02	12	9	4.58
					3/25/2009	13:56	8497	10.19	616.60	1176.67	27940.73	0.3150	0.00069	2.606E-03	9.325E-01	3.597E-02	4.5	2.8	7.55
					3/25/2009	13:57	8498	10.47	600.11	1145.21	26466.27	0.4530	0.00104	3.957E-03	8.833E-01	5.460E-02	9	5.5	7.84
					3/25/2009	13:58	8499	10.88	577.50	1102.05	24509.15	0.5930	0.00147	5.593E-03	8.180E-01	7.719E-02	4.5	2.5	9.35
					3/25/2009	13:59	8500	10.08	623.33	1189.51	28553.87	0.0189	4E-05	1.530E-04					
					3/25/2009	14:13	1	10.00	628.32	1199.03	29012.56	0.0178	3.7E-05	1.418E-04					
				40	3/25/2009	14:46	34	9.91	634.02	1209.92	29541.92	0.0174	3.6E-05	1.362E-04	1.000E+00	1.654E-03	5.5	5	1.52
				Taumax	3/25/2009	14:47	35	10.03	626.44	1195.44	28839.27	0.0315	6.7E-05	2.525E-04	9.762E-01	3.067E-03	9	8	1.87
				12.16116	3/25/2009	14:48	36	10.05	625.19	1193.06	28724.60	0.0518	0.00011	4.169E-04	9.724E-01	5.063E-03	14.5	13	1.74
				Gmax	3/25/2009	14:49	37	9.91	634.02	1209.92	29541.92	0.0578	0.00012	4.523E-04	1.000E+00	5.493E-03	7	6	2.45
				29541	3/25/2009	14:50	38	9.94	632.11	1206.27	29363.87	0.0801	0.00017	6.306E-04	9.940E-01	7.659E-03	9	7.5	2.90
				Gam Ref	3/25/2009	14:51	39	9.99	628.95	1200.23	29070.67	0.1018	0.00021	8.095E-04	9.841E-01	9.832E-03	12	10	2.90
				0.000412	3/25/2009	14:52	40	10.02	627.06	1196.64	28896.86	0.1240	0.00026	9.920E-04	9.782E-01	1.205E-02	15	13	2.28
					3/25/2009	14:53	41	10.02	627.06	1196.64	28896.86	0.1380	0.00029	1.104E-03	9.782E-01	1.341E-02	8	7	2.13
					3/25/2009	14:54	42	10.06	624.57	1191.88	28667.52	0.1608	0.00034	1.297E-03	9.704E-01	1.575E-02	10	8.5	2.59
					3/25/2009	14:55	43	10.16	618.42	1180.15	28105.97	0.2560	0.00056	2.106E-03	9.514E-01	2.557E-02	6	5	2.90
					3/25/2009	14:56	44	10.21	615.40	1174.37	27831.37	0.3480	0.00076	2.890E-03	9.421E-01	3.511E-02	9.5	7	4.86
					3/25/2009	14:57	45	10.34	607.66	1159.60	27135.95	0.4140	0.00093	3.527E-03	9.186E-01	4.284E-02	10	7	5.68
					3/25/2009	14:58	46	10.50	598.40	1141.93	26315.25	0.5080	0.00118	4.463E-03	8.908E-01	5.420E-02	11.5	8	5.78
					3/25/2009	14:59	47	10.76	583.94	1114.34	25058.87	0.6560	0.0016	6.052E-03	8.483E-01	7.350E-02	5	3	8.13
					3/25/2009	15:00	48	10.05	625.19	1193.06	28724.60	0.0181	3.8E-05	1.457E-04					

Test I G and D vs. Shearing Strain



Test I
G/Gmax vs. Gamma/Gamma Ref



USGS Cannon Park Core																			
Charleston, 777-ft depth				Conf. Press	Date	Time	Elapsed Time	Period	Freq	Shear Wave	G	Accel Volts	Accel Disp	Strain	G/Gmax	Gam/Gam Ref	Z	Z+1	Damping
Inside Dia	Outside Dia	Length		(psi)		(clock)	(min)	(msec)	(rad/sec)	(ft/sec)	(psi)	(volts rms)	(cm/sec^2 p-p)	(% p-p)					(%)
(cm)	(cm)	(cm)		15	6/7/2008	0:12	1	12.46	504.27	843.26	19480.35	0.0216	7.04396E-05	2.582E-04	4.924E-01	8.058E-03			
3.937	6.0452	14.7447	Meas 1	Taumax	6/7/2008	0:23	12	9.49	662.43	1107.75	33616.94	0.031	5.85819E-05	2.148E-04	8.497E-01	6.702E-03	9	7	4.00
			Meas 2	6.339268916	6/7/2008	0:37	26	9.34	673.01	1125.43	34698.54	0.0113	2.06884E-05	7.584E-05	8.770E-01	2.367E-03	8.5	6.5	4.27
			Meas 3	Gmax	6/7/2008	10:24	613	8.94	702.66	1175.02	37823.66	0.0113	1.89791E-05	6.958E-05	9.560E-01	2.171E-03	7.5	6	3.55
3.937	6.0452	14.7447	Average	39565.06	6/7/2008	12:42	751	8.74	718.65	1201.77	39565.06	0.0113	1.81437E-05	6.651E-05	1.000E+00	2.076E-03	7.5	6	3.55
			C est (psi)	Phi est (deg)	Gam Ref	6/7/2008	12:47	756	8.98	700.00	1170.57	0.027	4.56937E-05	1.675E-04	9.488E-01	5.227E-03	8.5	6.5	4.27
Sample X-sec	Sample Volume	0	25	0.000160224	6/7/2008	12:47	756	8.97	700.70	1171.75	37613.05	0.0553	9.33999E-05	3.424E-04	9.507E-01	1.069E-02	6.5	5	4.18
(mm^2)	(mm^3)	Ko est		Sqrt. Sigma	6/7/2008	12:50	759	8.99	699.30	1169.40	37462.49	0.0762	0.000129217	4.737E-04	9.469E-01	1.478E-02	7.5	5.5	4.94
		1		3.872983346	6/7/2008	13:03	772	9.25	679.26	1135.90	35346.74	0.1183	0.000212616	7.794E-04	8.934E-01	2.432E-02	6	4.2	5.68
					6/7/2008	13:05	774	9.78	642.19	1073.90	31593.66	0.1965	0.000395114	1.448E-03	7.985E-01	4.520E-02	5	3.5	5.68
					6/7/2008	13:08	777	10.29	610.61	1021.09	28562.89	0.322	0.000716166	2.625E-03	7.219E-01	8.193E-02	8	4.5	9.16
					6/7/2008	13:10	779	12.53	501.61	838.82	19275.61	0.542	0.001786287	6.549E-03	4.872E-01	2.044E-01	4.7	2	13.60
					6/7/2008	13:17	786	8.75	717.91	1200.53	39483.73	0.542	0.000872049	3.197E-03	9.979E-01	9.976E-02	0	0	0.00
16.528	243.705			30	6/7/2008	13:21	1	8.43	745.07	1245.94	42527.38	0.0083	1.23985E-05	4.545E-05	9.699E-01	7.860E-04			
Sample Wet Wt	Sample Dry Wt	Water Content	Wet Unit wt	Taumax	6/7/2008	13:32	12	8.38	749.78	1253.82	43067.02	0.009	1.32757E-05	4.867E-05	9.822E-01	8.416E-04			
(gms)	(gms)	(%)	(gm/cm^3)	12.67853783	6/7/2008	14:12	52	8.36	751.58	1256.82	43273.33	0.00983	1.44309E-05	5.290E-05	9.869E-01	9.148E-04			
495.7	480.5	3.16	2.034	Gmax	6/7/2008	15:23	123	8.31	756.55	1265.15	43848.38	0.0093	1.34738E-05	4.939E-05	1.000E+00	8.542E-04	11	9	3.19
w/c wt wet	w/c wt dry		Dry Unit	43848.38	6/7/2008	15:27	127	8.38	749.78	1253.82	43067.02	0.0226	3.33368E-05	1.222E-04	9.822E-01	2.113E-03	5.5	4.5	3.19
479.6	383.1	25.19	1.572	Gam Ref	6/7/2008	15:30	130	8.45	743.66	1243.58	42366.46	0.0393	5.89292E-05	2.160E-04	9.662E-01	3.736E-03	12	8.7	5.12
			98.092	0.000289145	6/7/2008	15:34	134	8.46	742.69	1241.97	42256.36	0.0893	0.000134252	4.922E-04	9.637E-01	8.511E-03	9.5	7	4.86
Mass Polar Moment of Inertia, J				Sqrt. Sigma	6/7/2008	15:41	141	8.73	719.72	1203.56	39682.99	0.196	0.00031377	1.150E-03	9.050E-01	1.989E-02	12.5	9.5	4.37
(gm-cm^2)				5.477225575	6/7/2008	15:46	146	9.31	674.74	1128.33	34877.62	0.418	0.000761359	2.791E-03	7.954E-01	4.827E-02	12.5	8	7.10
3224.80					6/7/2008	15:49	149	10.21	615.21	1028.79	28995.20	0.74	0.001621308	5.944E-03	6.613E-01	1.028E-01	10	5	11.03
					6/7/2008	15:52	152	11.44	549.23	918.45	23108.98	0.966	0.002655561	9.735E-03	5.270E-01	1.683E-01	12.5	5	14.58
Drive Head Mass Polar Moment of Intertia, Jo					6/7/2008	15:55	155	8.30	757.01	1265.91	43901.23	0.004	5.7882E-06	2.122E-05	1.001E+00	3.669E-04			
(gm-cm^2)				45	6/7/2008	15:59	1	8.15	770.66	1288.73	45498.59	0.0034	4.74724E-06	1.740E-05	9.720E-01	2.142E-04			
37467.00				Taumax	6/7/2008	16:04	6	8.18	768.12	1284.48	45198.73	0.0035	4.91928E-06	1.803E-05	9.656E-01	2.219E-04			
Beta				19.01780675	6/7/2008	16:40	42	8.10	776.18	1297.97	46152.91	0.0034	4.67993E-06	1.716E-05	9.860E-01	2.111E-04			
0.28928				Gmax	6/7/2008	17:09	71	8.10	775.51	1296.85	46073.20	0.0036	4.9638E-06	1.820E-05	9.843E-01	2.240E-04			
				46809.80	6/7/2008	17:10	72	8.04	781.69	1307.17	46809.80	0.0093	1.26214E-05	4.627E-05	1.000E+00	5.694E-04	14	12.5	1.80
				Gam Ref	6/7/2008	17:13	75	8.08	778.10	1301.18	46381.82	0.0223	3.05434E-05	1.120E-04	9.909E-01	1.378E-03	14	11.5	3.13
				0.000406278	6/7/2008	17:15	77	8.08	777.81	1300.70	46347.37	0.0421	5.77054E-05	2.115E-04	9.901E-01	2.603E-03	12.5	10	3.55
				Sqrt. Sigma	6/7/2008	17:17	79	8.19	767.18	1282.91	45088.42	0.0922	0.000129905	4.762E-04	9.632E-01	5.861E-03	11	9	3.19

**Figure 3. G and D vs. Shearing Strain
Cannon Park 777**

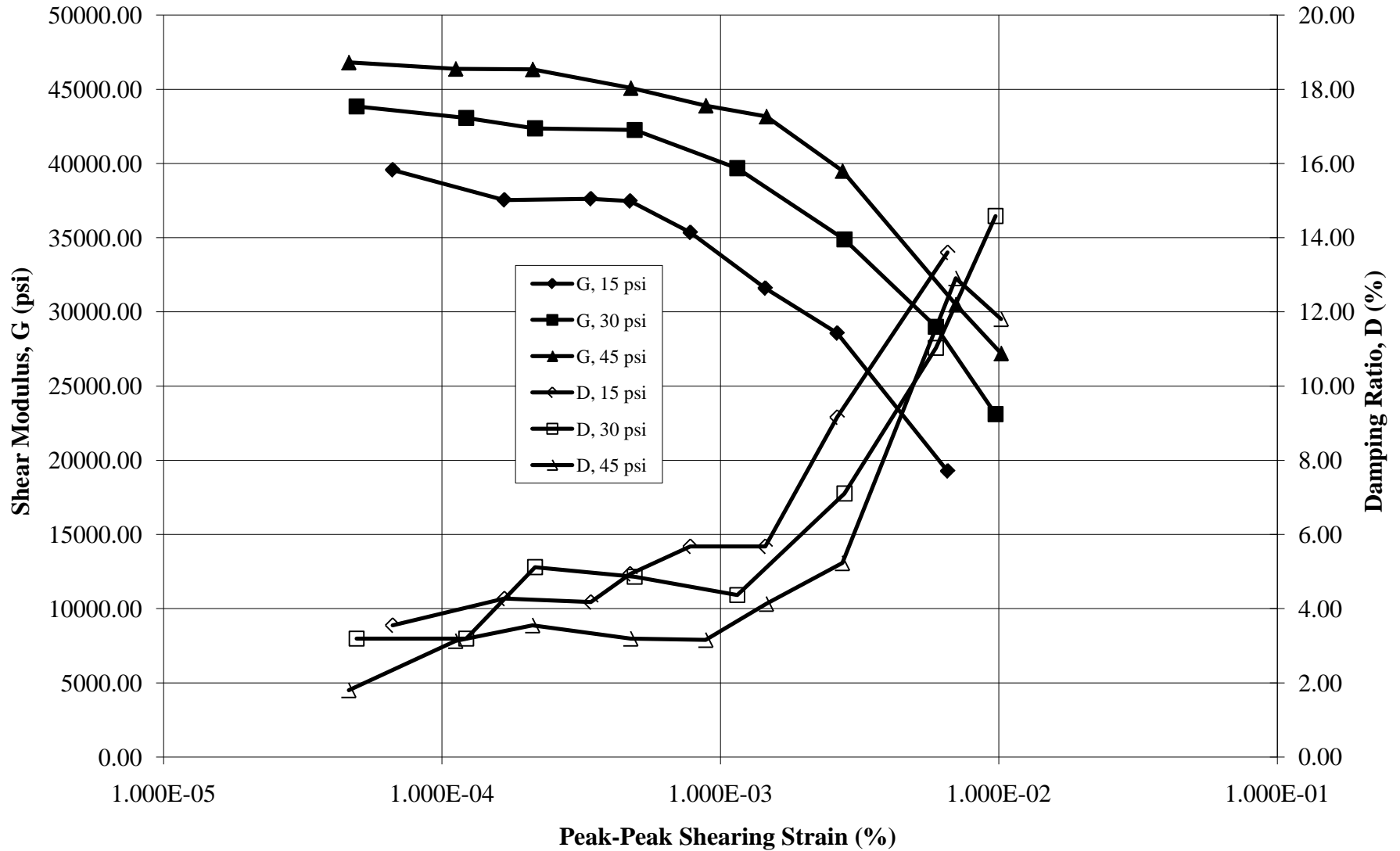
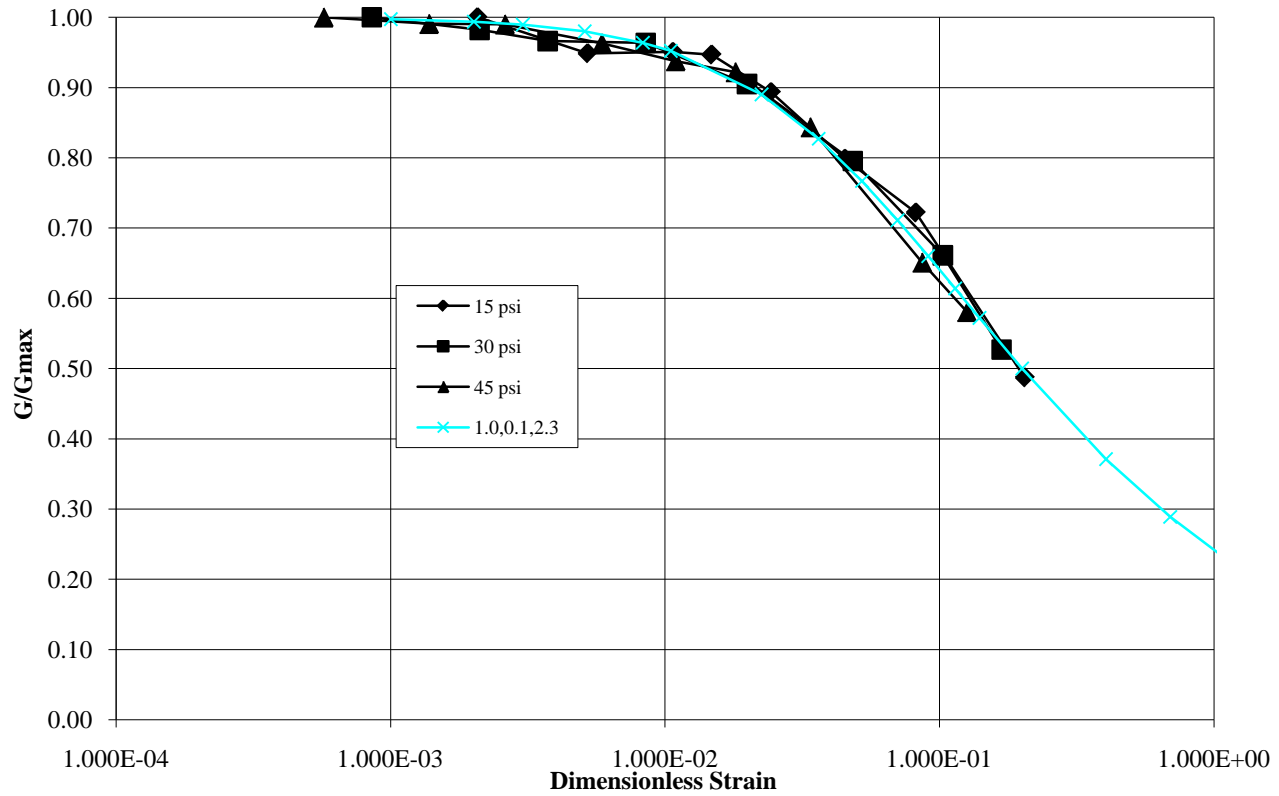


**Figure 4. G/Gmax vs. Gamma/GamRef
Cannon Park 777**



Appendix D. Summary of Ramberg Osgood Equation and Its Application to Soils

Introduction

The Ramberg-Osgood model was initially developed to represent the non-linear behavior of metals (Ramberg and Osgood, 1948?). It is a convenient and compact empirical formulation for nonlinear stress-strain behavior. As it is applied to soil mechanics, the reader is referred to Richart (1977) or Ray and Woods (1987). However, one may find all the necessary equations below.

Formulation

The stress-strain formulation is straightforward, however it is very difficult to invert. First, the basic equation and its parameters are presented, then the derived (and somewhat more useful) equations. Finally, a method for computing the best-fit parameters is discussed. The basic formula for stress-strain behavior is shown below;

$$\gamma = \frac{\tau}{G} \left[1 + \alpha \left| \frac{\tau}{C\tau_{max}} \right|^{R-1} \right] \quad Eq. 1$$

where

γ = shearing strain

τ = shearing stress

G = shear modulus at very low amplitudes (typically $\gamma \leq 10^{-4}$ %)

τ_{max} = maximum shear strength, usually from triaxial test results

α, C, R = curve-fitting constants

A typical stress-strain curve for soils is shown in figure 1 below. Note that the two curves are slightly different due to the choice of different C-values. The values of G and τ_{max} are equal for both curves and represent typical values

The use of Ramberg-Osgood parameters are also applied through the definitions of secant and tangent modulus as well as through the use of reference strain; yielding dimensionless curves

that are readily applied to response analyses and allow for comparison of test results performed at different confining stresses.

Definitions for secant and tangent modulus follow directly from their definitions such that

$$G_{sec} = \frac{\tau}{\gamma} = \frac{G}{\left[1 + \left|\frac{\tau}{C\tau_{max}}\right|^{R-1}\right]} \quad Eq. 2$$

and for tangent modulus

$$G_{tan} = \frac{\partial\tau}{\partial\gamma} = \frac{G}{\left[1 + R\left|\frac{\tau}{C\tau_{max}}\right|^{R-1}\right]} \quad Eq. 3$$

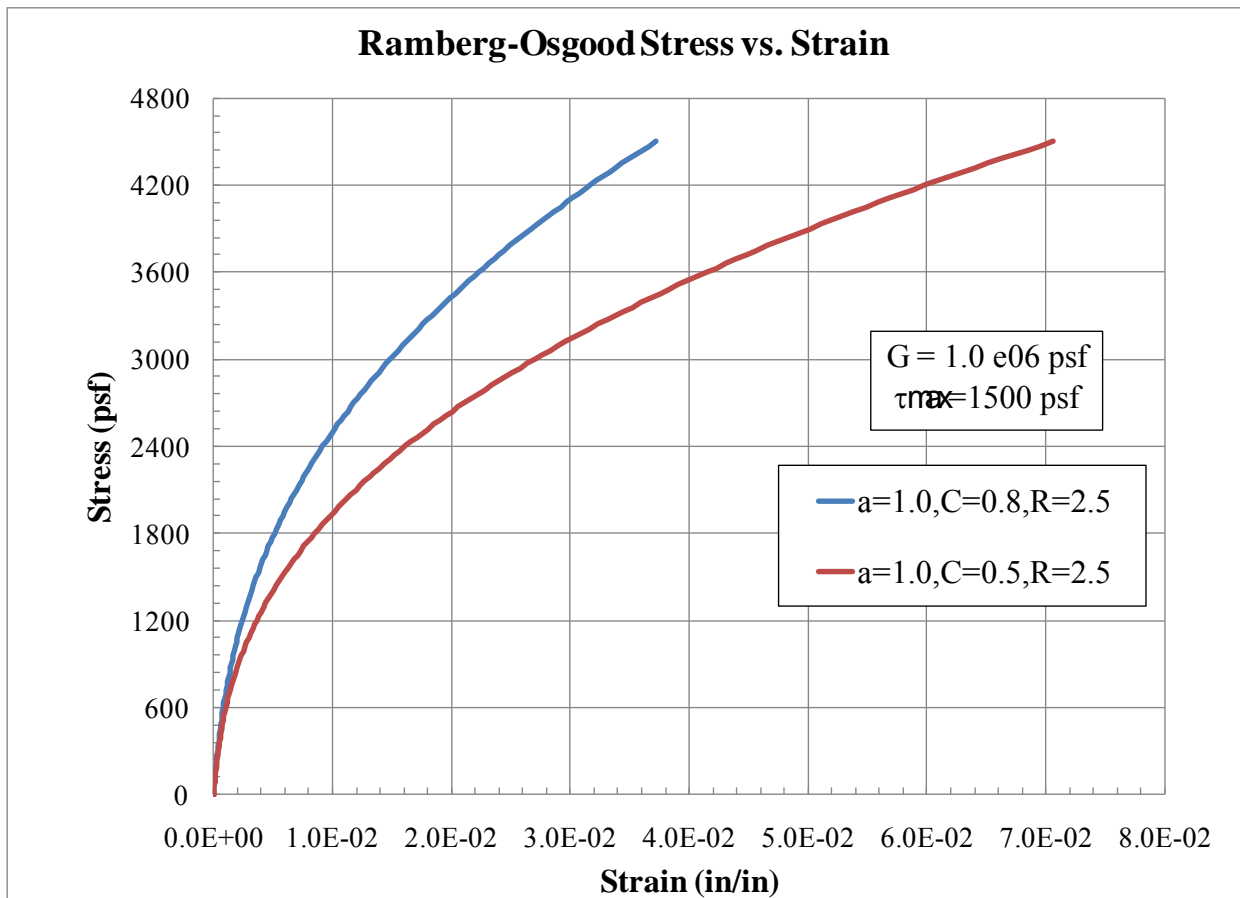


Figure 1. Stress vs. Strain for Two Ramberg-Osgood Models

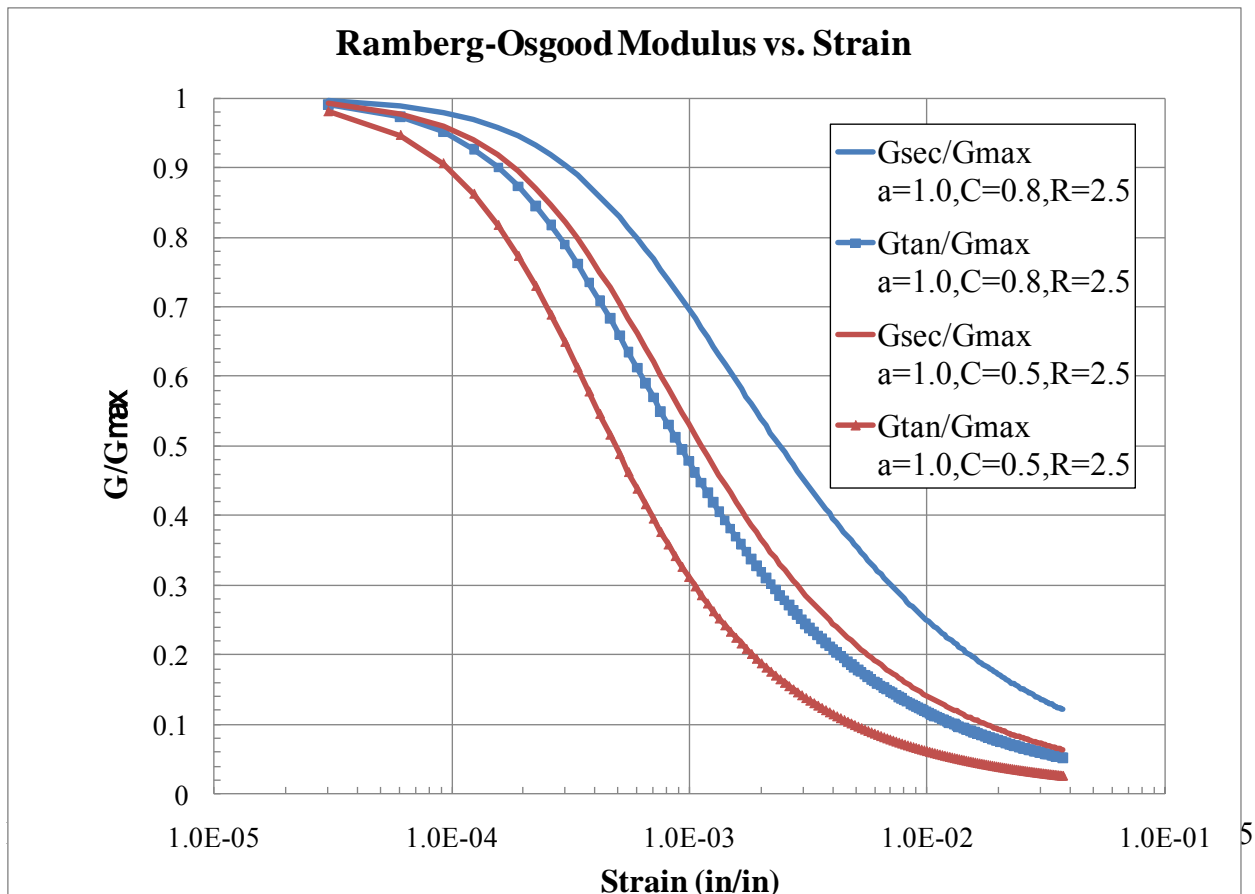
Secant modulus is often used for equivalent linear analyses like SHAKE, while tangent modulus is used in time-stepping analyses such as MOC. The use of a non-dimensional formulation allows for comparing test data for the same soil at different confining stresses. These data can then be applied to the entire soil layer (of the same soil) while considering the effects of confining stress (i.e. depth). The dimensionless form of the R-O equation follows as

$$\frac{\gamma}{\gamma_{ref}} = \frac{\tau}{\tau_{max}} \left[1 + \alpha \left| \frac{\tau}{C\tau_{max}} \right|^{R-1} \right] \quad Eq. 4$$

where $\gamma_{ref} = \tau_{max}/G$

The dimensionless form will produce different curves at different depths if τ_{max} is a function of confining stress. Note also that the low-amplitude shear modulus, G , will also be a function of depth and is usually measured by field seismic testing. Generally, field tests satisfy the low amplitude criteria quite easily.

Plots of secant and tangent modulus vs. strain are given below. Note that the computation of moduli vs. strain is not a straightforward process since strain does not appear in the formulation. However, one may choose a value of τ , then compute both moduli via equations 3 and 4, then



compute strain via equation 1. This is a simple exercise with spreadsheets.

Figure 2. Secant and Tangent Modulus Reduction vs. Strain for Two R-O models

Some obvious behavior from the figure is worth noting. First; strain is plotted on the horizontal axis using a logarithmic scale. This shows typical soil behavior more clearly than a linear scale would (try it and see for yourself). Keep in mind that strain is often expressed in percent (%) instead of (in/in). This is a very common blunder in transposing various authors' data from one graph to another. Second; tangent modulus will always be less than secant modulus at any given strain. Third; modulus ratios become significantly less than 1.0 at fairly low strain levels ($\gamma \leq 0.1\%$). Finally; soils can behave significantly different from what is shown here. These curves can slide horizontally by an order of magnitude in either direction.

Using dimensionless values is not difficult; however, some agreement must be made about the evaluation of τ_{max} for each specific soil layer. A typical assumption is Mohr-Coulomb failure envelope strength with effective stress properties. Such an envelope is shown below in figure 3.

Based on the diagram the maximum shear strength is

$$\tau_{max} = \left(\frac{c'}{\tan \phi'} + \sigma'_0 \right) \sin \phi' \cos \phi' \tag{Eq. 5}$$

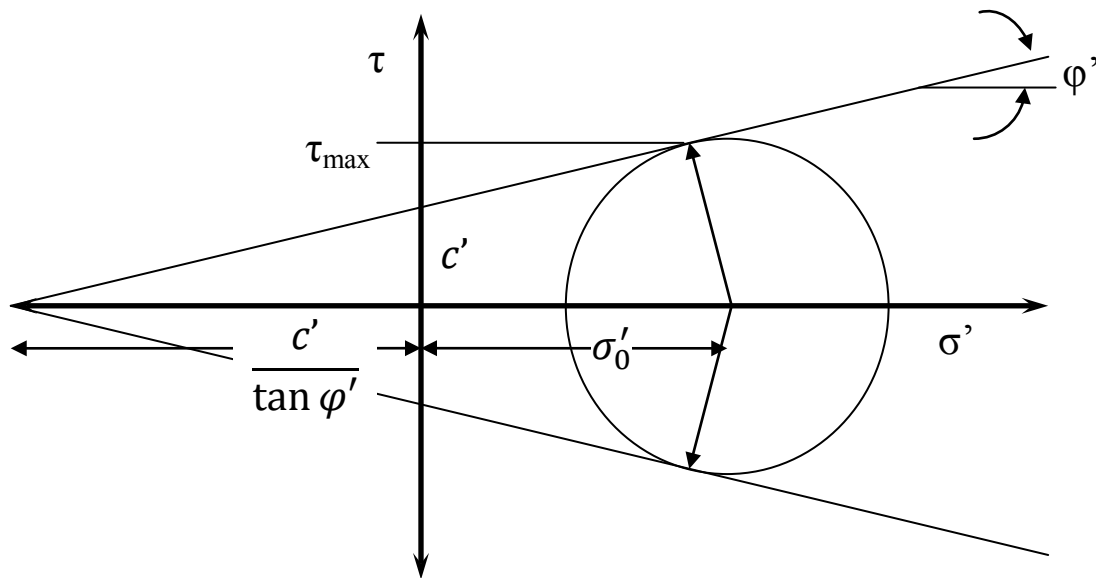


Figure 3. Mohr Diagram for Maximum Shear Strength

Shear modulus, G , in the field will be whatever is measured or may be estimated by a variety of empirical equations (Harding and Black, 1979; Kramer, 1996; Das 1999). Dimensionless stress-

strain curves can be generated in the same manner as the curves in figure 1 by simply substituting values as shown below.

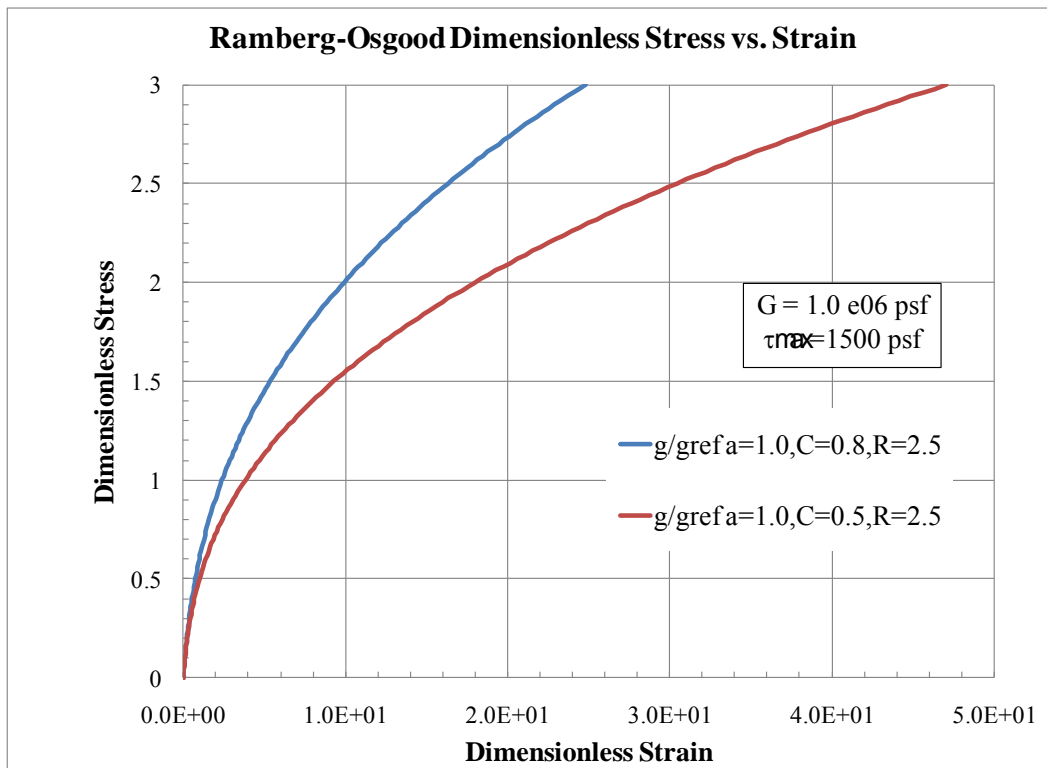
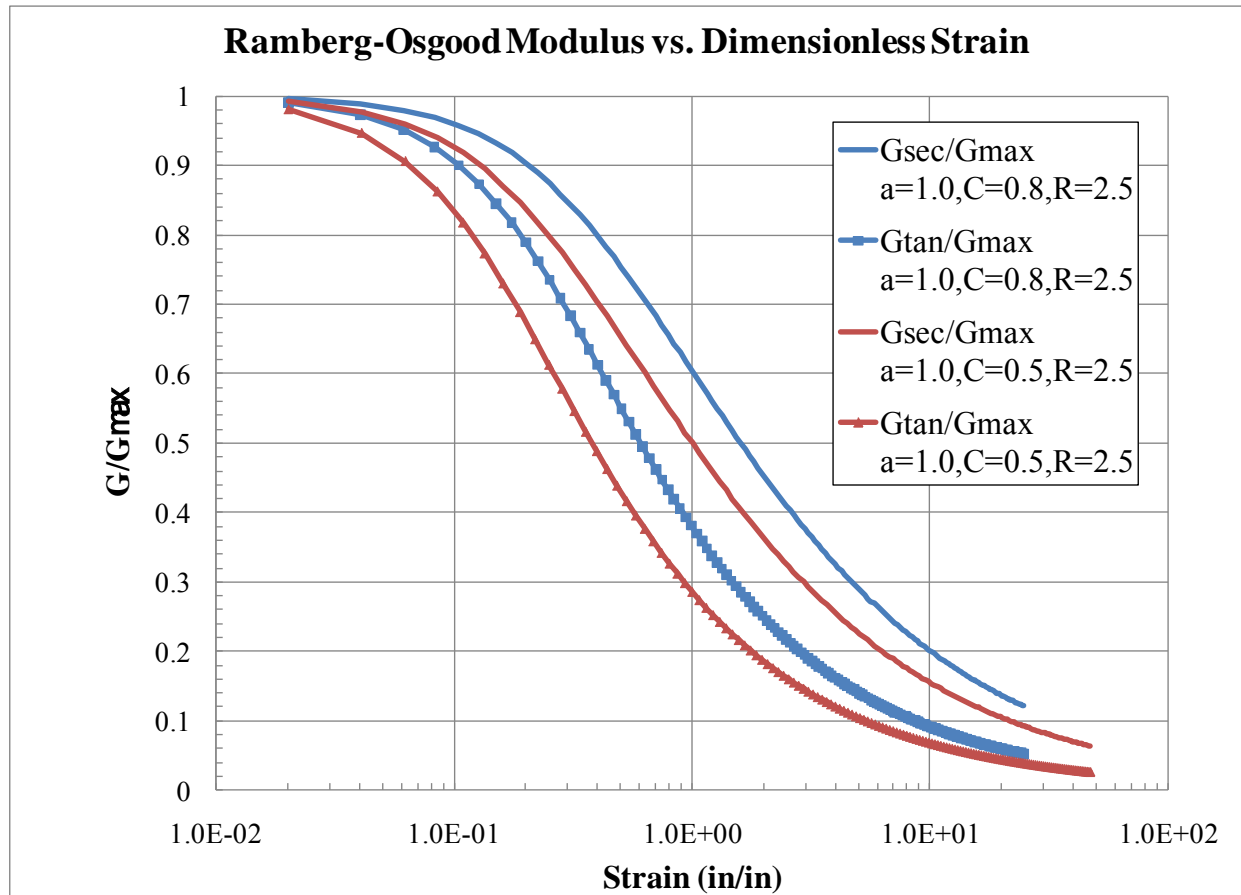


Figure 4. Dimensionless Stress-Strain for Two R-O Models

The plots for secant and tangent modulus are exactly the same equations (2, 3). The corresponding value of dimensionless strain is now used as the abscissa. The dimensionless strain values are different than “regular” strain values shown in figure 2 by a factor of about



1000. While this may first seem to be a waste of effort, when viewed from the laboratory data, it is very valuable.

One difficulty with the Ramberg-Osgood model persists: its inability to be inverted so that either stress or strain can be the independent variable. This is not too great a problem, however, and there are ways to compute one’s way around the problem. The approach uses a Newton-Raphson method to solve the problem. One need only to grasp the idea that all the equations so far can be cast as $f(x) = 0$ and then can be solved with a little guesswork. Equation 1 is re-cast as such below

$$f(\tau) = \frac{\tau}{G} \left[1 + \left| \frac{\tau}{C \tau_{max}} \right|^{R-1} \right] - \gamma = 0 \quad \text{Eq. 1b}$$

Figure 5. Modulus Reduction vs. Dimensionless Shear Strain for Two R-O Models

so given values for everything but τ , one should be able to compute τ . The derivative of the function above reduces to

$$f'(\tau) = \frac{1}{G} \left(1 + R \left(\frac{\tau}{C\tau_{max}} \right)^{R-1} \right) \quad Eq. 6$$

Equations 1b and 6 are then used in the typical Newton-Raphson algorithm where an initial guess for τ is made and successive calculations converge quickly to a solution. The astute reader will notice that this is the same expression as for tangent modulus G_{tan} as it should be since the tangent modulus is the derivative of the stress-strain curve.

$$\tau_{new} = \tau_{old} - \frac{f(\tau_{old})}{f'(\tau_{old})} \quad Eq. 7$$

A solution is reached when $f(\tau_{old})$ is sufficiently close to zero (say, 10^{-12}). Once the value for stress is found, computation of secant or tangent modulus follows according to the equations above. For 1-D site response analysis where modulus must be computed very often due to changes in stress-strain, a better method is to pre-compute a table of values (say, 256 values of stress, strain, and modulus) over a reasonably large range and use a binary table look-up routine with a final interpolation step. This eliminates any unintended computational crashes and reduces the computing effort to seven comparisons and a simple division problem. I have used this approach extensively with success. Of course the table look-up approach can be applied to any equation or data set used for soil properties (eg soil-water characteristic curves).

Application to Laboratory Test Data

Ramberg-Osgood parameters are generated from laboratory test data. Typical tests would be resonant column or torsional simple shear. Resonant column data is usually presented as G_{sec} versus γ similar to figure 2. Parameters can be fit to the data by trial and error using visual inspection to decide when it is good enough. Alternatively, a least-squares regression fit can be performed by “brute-force” method.

Brute-force regression Regression methods seek to minimize the error between a fitting function and the data it is try to fit. Recall that the sum of the square of the residuals is the target for minimization.

$$Minimize \sum_{i=1}^{Ndata} \omega_i (y_i func - y_i meas)^2 \quad Eq. 8$$

where ω_i = weighing factor = 1.0 unless specified otherwise

$y_{i \text{ func}} = y$ calculated from the fitting function for a given x

$y_{i \text{ meas}} = y$ measured for the same x value

Ndata = number of data pairs used in analysis

Normally the function used to fit the data is a line, polynomial, power function, or other fairly simple equation that can be placed in equation 8, its derivative taken, set to zero and function parameters determined by solving a series of linear equations. However, the Ramberg-Osgood formulation is not so easily manipulated, so the engineer is left to systematically guess parameters, determine the sum of residuals (equation 8) and compare the newly computed sum to the best candidate (smallest sum of residuals) so far. This is performed systematically until all reasonable combinations of parameters are exhausted.

Weighing factors can be used for each data pair to give “extra credit” to those who are perhaps more representative of the data set (factor > 1.0) and prevent problematical data pairs from skewing the fit (factor < 1.0). This may especially be necessary when a group of data pairs is closely bunched together.

The systematic method, or computational algorithm is a series of nested loops where each loop is a progression of R-O values. Such a code is shown schematically below

```
! Code for programming brute force regression
! Some code before this is necessary to read in the
! Ndata—number of data pairs
! x(i),y(i) pairs and w(i) weights
! Additional code is necessary for the R-O computation
! for Gsec, Gtan, or Tau, depending on what you want to fit
! it would reside in a separate function, here called RamOs()
! x-values would be strain or dimensionless strain.
Bestalpha = 0.0          ! Set best values to zero
BestC      = 0.0          ! initially
BestR      = 0.0          !
BestResidual = 1.0e6     ! Set best residual sum to large number

For alpha = 0.1 to 2.0 step 0.01  !outer loop
  For C = 0.1 to 2.0 step 0.01    !middle loop
```

```

For R = 1.0 to 5.0 step 0.01 !inner loop
  Residual = 0.0           !zero out sum
  For i = 1 to Ndata       !take each data pair
    ycomp = RamOs(x(i), alpha, C, R) !compute y-val
    Residual = Residual + w(i)*(ycomp-y(i))^2 !take weight
                                !times sum of square of residual
  Next i
  If (Residual < BestResidual) then !if this one is best
    Bestalpha = alpha         !save alpha
    BestC = C                 !save C
    BestR = R                 !save R
    BestResidual = Residual   !save new Residual
  End If
Next R
Next C
  Next alpha
!Continue with output code here

```

Figure 6. Code Snippet for Performing Brute Force Regression

Note that the maximum, minimum and step values can be set to any arbitrary (reasonable) value. This procedure can be made more efficient by using an optimization process such as method of steepest descent. It could be used to further narrow the parameter loop limits and reduce the stepping distance. However, when programmed in a compiled language (Fortran, C) the process takes about 3 minutes to produce a very satisfactory result. The results can be confirmed visually by plotting the computed values with the measured ones.

Resonant Column Example

A computational example is given below for resonant column data generated on Ottawa Sand. The blue columns represent data entered by the operator, white columns are computed values. Initial values are for typical specimen dimensions and weight. Specimen wet weight is used to compute mass density, dry weight is used for computing void ratio, etc. References